Gfat1 and *Gfat2* encode functionally equivalent enzymes in *Drosophila melanogaster*: a molecular, genetic, and evolutionary analysis

by

Shawn Eric Polnik Cotsworth

B.Sc., Simon Fraser University, 2010

Thesis Submitted in Partial Fulfillment of the
Requirements for the Degree of
Master of Science

in the
Department of Molecular Biology and Biochemistry
Faculty of Science

© Shawn Eric Polnik Cotsworth 2018
SIMON FRASER UNIVERSITY
Fall 2018

Copyright in this work rests with the author. Please ensure that any reproduction or re-use is done in accordance with the relevant national copyright legislation.

Approval

Name:	**Shawn Eric Polnik Cotsworth**
Degree:	**Master of Science**
Title:	***Gfat1* and *Gfat2* encode functionally equivalent enzymes in *Drosophila melanogaster*: a molecular, genetic, and evolutionary analysis**
Examining Committee:	**Chair:** Ryan Morin Assistant Professor
	Barry Honda Senior Supervisor Professor
	Nicholas Harden Supervisor Professor
	Kathleen Fitzpatrick Supervisor Senior Lecturer Department of Biological Sciences
	Gratien Prefontaine Internal Examiner Associate Professor Faculty of Health Sciences
Date Defended/Approved:	October 26th, 2018

Abstract

The hexosamine biosynthesis pathway (HBP) diverts 2-5% of glucose from glycolysis, ultimately producing uridine diphosphate *N*-acetylglucosamine (UDP-GlcNAc), an important substrate in protein glycosylation. This pathway is of particular importance in *Drosophila melanogaster* because chitin, the primary component of insect cuticle, is composed of *N*-acetylglucosamine polymers. I report that the rate-limiting enzymes of the HBP, GFAT1 and GFAT2 (glutamine:fructose-6-phosphate aminotransferase), are functionally equivalent by genetic rescue using cDNA transgenes of both genes. I also report that neither transgenically upregulating the enzymes of the HBP, nor those of the hexosamine signalling pathway (HexSP), extends the lifespan of *D. melanogaster*. Evolutionary analyses using fluorescence *in situ* hybridization in six species of *Drosophila* support a model that would place the *Gfat1* relocalization event from euchromatin to heterochromatin after the *melanogaster* group diverged from the rest of *Drosophila*.

Keywords: *Gfat*; hexosamine; UDP-GlcNAc; paralogue; *Drosophila melanogaster*; heterochromatin

To my darling Maeve–

may this dedication

never go the way of so many deeply

regretted tattoos

Acknowledgements

I would first like to express my sincere appreciation for the wonderful administrative and technical staff we have in MBB – particularly Deirdre de Jong-Wong who was incredibly helpful when we moved our lab from SSB7166 to SSB7124 in the summer of 2016.

I would also like to thank members of the Harden, Verheyen and Vocadlo labs for their assistance over the years; in particular Xi Chen, for her help with looking at 'dorsal open' phenotypes in the *Gfat* mutants.

I would also like to thank all of the undergraduate volunteers and researchers I've worked with for helping me, if not with this project, one of the many others. These include (in no order of importance) Amita Kandola, Gladys Mira, Katrina Besler, Linda Yang, Mary Chan, Sara Brown, Stephanie Luongo, Danielle Thompson, Franklin Tam, April Balcita, Ivan Asmaro, Anne Lin, Chris Bonar, Reggie Samujh, Baltej Bagri, Lawrence Haiducu, Stephanie Luongo, and a special thank you to Lisa Bell for helping me make the probes for FISH of mitotic and polytene chromosomes.

I would also like to thank the former master's students I've worked with Teresa Stefanelli, Jack Yang and Jonathan Radke for their comraderie and assistance during my work as a technician. I would like to extend a special thank you to Graham Hallson whose extreme dedication and patience was incredibly valuable to me as an impressionable, nascent scientist.

It would be remiss of me to not also acknowledge the hard work of two former technicians: Inho Kim and Kevin Beja with whom I commiserated during some of the long nights working in the lab running western blots for Graham, or collecting salivary glands for Graham, or dissecting wing discs for Graham.

I would also like to thank my committee members Dr. Nicholas Harden and Dr. Kathleen Fitzpatrick. Thank you, Nick, for the excellent comments during my committee meetings and for sharing with me a predilection for one-liner comedians. Thank you, Kathleen, for laying the ground upon which this body of work stands, the detailed edits you provided as I was writing, and for directing me to the lab in the first place.

I would also like to express a deep appreciation for Dr. Donald Sinclair. Thank you so much for listening to all of my ideas, no matter how outlandish, and for your incredible feedback on my thesis. Your deep commitment to your work and to science has shown me that to be a *Drosophila* geneticist isn't a profession but a lifestyle choice.

I would also like to thank my partner Maeve for looking over my thesis, sifting through all the "AKATAKAGAKA" and providing useful edits where they were needed. Thank you for being so patient as you've watched me tearing my hair out over the computer and not properly enjoying the summer.

I would also like to thank my sister, parents and grandparents. Together, you laid the foundation down for who I am as a person and I was more grateful for the support you gave me while I was working on this thesis than you knew.

And lastly, I would like to thank my supervisor Dr. Barry Honda. Thank you for taking a chance on me as a technician and graduate student. You have been so helpful throughout this process with your insightful edits, helpful advice and keeping me to task with the paperwork. It was incredibly wonderful that you encouraged me to TA and allowed me to lecture during a few of your classes. You have been a wonderful mentor on a personal and professional level and I owe you the deepest thanks.

Table of Contents

List of Tables

List of Figures

List of Acronyms

ChIP-seq	Chromatin Immunoprecipitation Sequencing
ESTs	Expressed Sequence Tags
FISH	Fluorescence *In Situ* Hybridization
gof	Gain of Function
GFAT	Glutamine:fructose-6-phosphate aminotransferase
GFPT	Glutamine-fructose-6-phosphate transaminase
Gln	Glucosamine
Gln-6P	Glucosamine-6-phosphate
GlcNAc	*N*-acetylglucosamine
GlcNAc-6P	*N*-acetylglucosamine-6-phosphate
GlcNAcylated	O-linked β-*N*-acetylglucosamine Modified Protein
Grh	Grainy head
HP1	Heterochromatin Protein 1
HBP	Hexosamine Biosynthesis Pathway
HexSP	Hexosamine Signalling Pathway
L1	*Drosophila melanogaster* first instar larvae
mmy	*mummy*
OGT	O-linked β-*N*-acetylglucosamine transferase
OGA	O-linked β-*N*-acetylglucosaminidase
PEV	Position Effect Variegation
RNAi	RNA Interference
seDNA	Single Embryo Genomic DNA
sePCR	Single Embryo PCR
UBC NAPS	University of British Columbia Nucleic Acid and Protein Service
UDP-GlcNAc	Uridine diphosphate *N*-acetylglucosamine
zep	*zeppelin*

Executive Summary

The hexosamine biosynthesis pathway (HBP) diverts 2-5% of glucose from glycolysis ultimately producing UDP-GlcNAc, an important substrate in protein glycosylation and GlcNAcylation. Dysregulation of this pathway is associated with a host of human diseases, including cancer, diabetes, and neurodegenerative disorders such as Alzheimer's. This pathway is of particular importance in arthropods such as *Drosophila melanogaster*, as chitin, the primary component of the insect cuticle, is the product of *N*-acetylglucosamine polymerization.

In this work, I describe the characterization of putative *Gfat2* mutants, previously isolated using P-element excision, and while lethal phase analysis of these mutants shows that though the majority are embryonic lethal, some persist to the first larval instar. Using genetic rescue by constitutively expressing cDNAs for each of these genes, I demonstrate that the rate-limiting enzymes of the HBP, GFAT1 and GFAT2, are functionally equivalent. I also report that conducting RT-qPCR on wild type flies during discrete stages of embryogenesis demonstrates drastic changes in expression between the two paralogues and these results have strong functional implications for both genes. I also explore the impact of upregulating the HBP by *Gfat1* cDNA expression, or by effecting an increase in global protein GlcNAcylation by exogenous expression of *Ogt* cDNA and *Oga* RNAi, on lifespan.

Additionally, an exploration of the evolutionary history of the *Gfat* paralogues using fluorescence in situ hybridization revealed that while *Gfat1* is in heterochromatin in *D. melanogaster* and other species of the melanogaster group, it is in euchromatin in all other drosophilid species examined. These data support a model that would place the *Gfat1* relocalization event from euchromatin to heterochromatin after the *melanogaster* subgenus group diverged from the rest of Drosophila 25 million years ago.

As *D. melanogaster* has become an increasingly important model organism in the study of diabetes, cancer, and neurodegenerative disorders, the genetic reagents developed in this research, along with the observations regarding their function and transcriptional regulation, will be valuable to researchers who seek to understand the HBP and its role in human diseases.

Chapter 1. Introduction

1.1. The hexosamine biosynthesis pathway (HBP)

The hexosamine biosynthesis pathway involves a series of enzymes that divert 2-5% of glucose from glycolysis to ultimately produce uridine diphosphate *N*-acetylglucosamine (UDP-GlcNAc), an important substrate for the synthesis of glycoproteins, glycolipids, and other important macromolecules (Marshal, Bacote & Traxinger, 1991; Traxinger & Marshal, 1991; reviewed in Denzel & Antebi, 2015) (Figure 1). In humans, *de novo* synthesis of UDP-GlcNAc is regulated by the rate-limiting enzymes Glutamine-fructose-6-phosphate transaminase 1 (GFPT1) and Glutamine-fructose-6-phosphate transaminase 2 (GFPT2), which convert fructose-6-phophate and glutamine to glucosamine-6-phosphate (GlcN-6P) (Figure 1). Although these enzymes control the first step of the pathway, not all of the UDP-GlcNAc generated by the HBP goes through GFPT1 and GFPT2 as they can be bypassed by one of the 'salvage pathways'. Extensive research has demonstrated that Glucosamine (GlcN) can be phosphorylated by hexokinase (HEXK), also producing GlcN-6P (Harpur & Quastel, 1949; Brown, 1951; Masson, Wiernsperger, Lagarde & El Bawab, 2005), and *N*-acetylglucosamine kinase (NAGK) can phosphorylate *N*-acetylglucosamine producing *N*-acetylglucosamine-6-phosphate (GlcNAc-6P) (Hinderlich, Berger, Schwarzkopf, Effertz, & Reutter, 2000; Weihofen, Berger, Chen, Saenger, & Hinderlich, 2006; Ryczko et al., 2016) (Figure 1). A nexus of glucose metabolism and protein glycosylation, the HBP acts as a nutrient sensor (reviewed in Hanover, Krause & Love, 2010) and defects in its regulation are associated with a host of metabolic (Yki-Järvinen et al., 1996; Virkamaki & Yki-Jarvinen, 1999; Srinivasan et al., 2009; reviewed in Qin et al., 2017), neurological (Senderek et al., 2011; reviewed in Willems, van Engelen & Lefeber, 2016) and oncological diseases (reviewed in Hanover, Chen, & Bond, 2018).

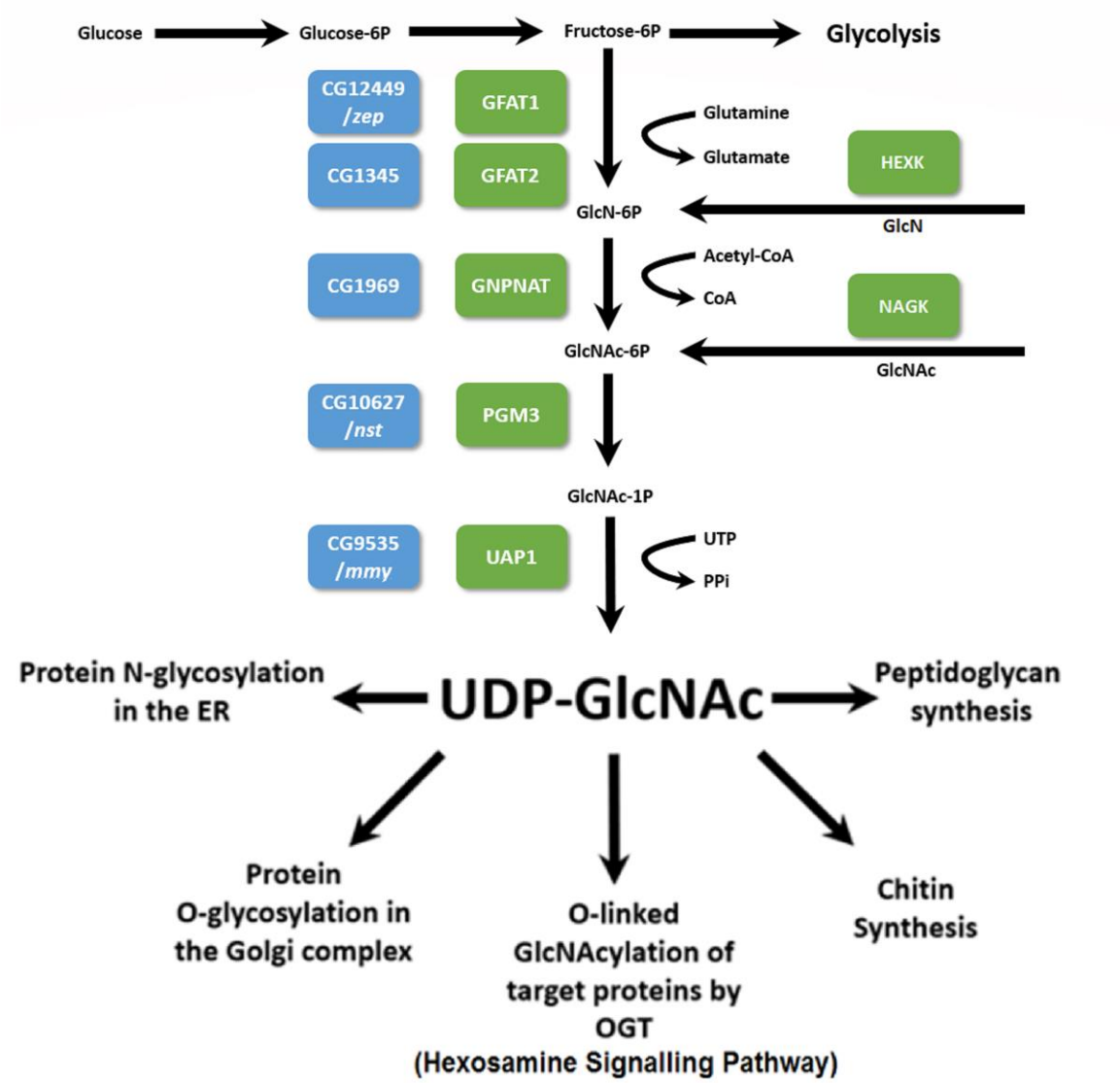

Figure 1 Depiction of the HBP and downstream pathways
Blue boxes correspond to the gene names in *Drosophila melanogaster* and the green boxes correspond to the enzymes that they encode. Note that glucosamine and *N*-acetylglucosamine can enter the HBP via a salvage pathway when they are phosphorylated by HEXK and NAGK, respectively.

1.2. The HBP in *Drosophila melanogaster*

The HBP is of particular importance to arthropods, including *Drosophila melanogaster (D. melanogaster),* because chitin, the primary component of insect cuticle, is a long-chain polymer of *N*-acetylglucosamine (GlcNAc) and is one of the most abundant macromolecules found in nature (Finke, 2007). In *D. melanogaster*, the HBP is regulated by two enzymes encoded by the paralogous genes *Glutamine:fructose-6-phosphate aminotransferase 1* (*Gfat1*) and *Glutamine:fructose-6-phosphate*

aminotransferase 2 (*Gfat2)* which share 79% transcript identity and reside in 3R heterochromatin and 3R euchromatin, respectively (Graack, Cinque & Kress, 2001; Jackson, 2007; Gramates et al., 2017; https://flybase.org, subsequently referred to as 'Flybase').

1.3. Architecture and location of the *Gfat1* gene

Gfat1 resides in 3R heterochromatin and has a typical architecture of a heterochromatic gene: it is a large gene at 11,441 base pairs (bp) in length, and some transcripts can have as many as 10 introns according to Flybase. A TATA box is present 40 bp 5' to the transcription start site of the smaller reported *Gfat1* transcripts (Graack, Cinque & Kress, 2001); however, there is no TATA box in the first 250 bp 5' to the larger *Gfat1* transcripts (Flybase). No expressed sequence tags (ESTs) corresponding to the larger *Gfat1* transcripts have been reported, so their inclusion on Flybase may not be valid, and it may therefore be more accurate to regard the gene as being 7362 bp long. Four cDNAs, each derived from unique splicing events have thus far been reported for *Gfat1,* so it is unlikely there are additional splice variants (Flybase).

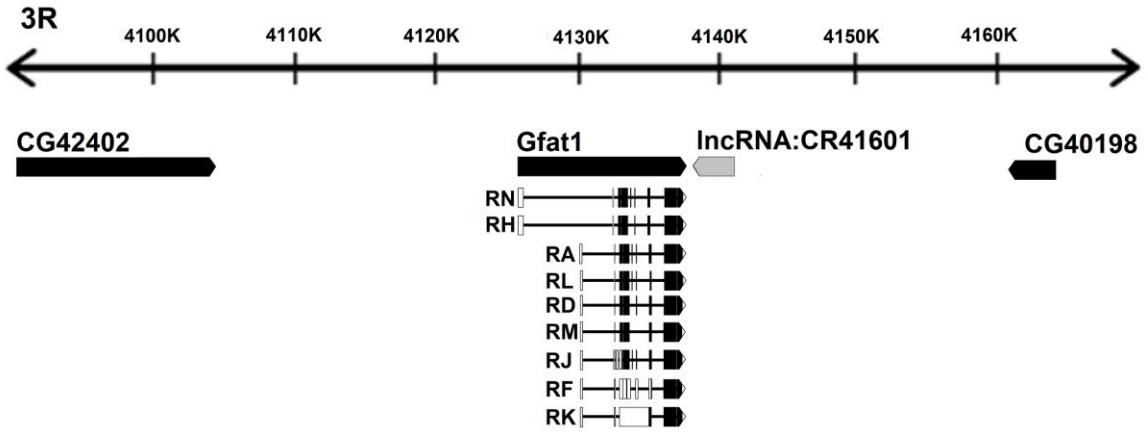

Figure 2 Gfat1 location, architecture, and neighbouring genes
Gfat1 transcripts depicted with white boxes representing UTR, black boxes representing translated exons, and solid lines representing introns.

Gfat1 is flanked by the genes *CG42402* and *CG40198* (Flybase) (Figure 2). *CG42402,* which maps 5' to *Gfat1*, encodes a protein with a molecular function of carbohydrate binding and possesses a SUEL lectin domain. *CG40198,* which maps 3' to *Gfat1*, encodes a protein with no known molecular or biological function. Between

CG40198 and *Gfat1* is the long non-coding RNA *CR41601,* which also has no known molecular or biological function (Flybase).

1.4. Architecture and location of the *Gfat2* gene

Gfat2 resides in 3R euchromatin, is far smaller than *Gfat1* at 2747 bp, has only one transcript with a single intron and has no TATA box within the first 100 bp 5' of the transcription start site (Graack, Cinque & Kress, 2001; Flybase). It is flanked by the *Moca-cyp* and *larp* genes (Flybase) (Figure 3). *Moca-cyp,* which maps 569 bp 5' of *Gfat2* and is transcribed in the opposite direction, encodes a Peptidyl-prolyl cis-trans isomerase. *Larp,* which maps 3' of *Gfat2*, encodes the "La related protein" and is implicated in mitotic and meiotic cell division although a precise molecular function has not yet been described. Beginning immediately 3' of *Gfat2* and nested within the *Gfat2* 3' untranslated region (UTR) and second exon is the non-coding gene *CR46104,* which has unknown molecular and biological functions (Flybase).

Figure 3 Gfat2 location, architecture, and neighbouring genes
Gfat2-RA transcript depicted with UTR represented by white boxes, translated exons by black boxes, and the single intron represented by a solid line.

1.5. Transcriptional regulation of *Gfat1* and *Gfat2*

Large scale genome and transcriptome analyses have identified Grainy head (Grh), a transcription factor that controls epithelial morphogenesis (Bray & Kafatos 1991; Mace, Pearson, & McGinnis, 2005), as potentially regulating both the *Gfat1* and *Gfat2* genes (Nevil, Bondra, Schulz, Kaplan, & Harrison, 2017; Yao et al., 2017). ChIP-seq of Grh in *D. melanogaster embryos* identified both *Gfat1* and *Gfat2* as potential targets of the transcription factor but found neither to be activated or repressed when they followed up with microarray analysis using grh^{B37} mutants and epithelially overexpressed *grh* cDNA (Yao et al., 2017). In a similar study using RNA-seq, the expression of *Gfat1* and

Gfat2 were found to be down- and upregulated, respectively, in embryos in which *grh* expression was both maternally and zygotically depleted; however, ChIP-seq using a Grh antibody only identified the *Gfat1* locus as a potential binding site (Nevil, Bondra, Schulz, Kaplan, & Harrison, 2017).

1.6. Protein domains and regulation of the GFAT enzymes

The GFAT enzymes share 81% amino acid identities (Jackson, 2007; Flybase) and each have 3 major protein domains: 2 sugar isomerase (SIS) domains and a glutamine amidotransferase type 2 (GATT2) domain (Interproscan, Appendix A). In GFAT1, the GATT2 domain, extends from amino acids (a.a.) 2-300, and the SIS domains extend from a.a. 372-512 and a.a. 539-692. In GFAT2, the GATT2 domain extends from a.a. 2-288, and the SIS domains extend from a.a. 361-501 and a.a. 528-681. In humans, a crystal structure of the GFPT1 enzyme has been determined and revealed a dimer bound to UDP-GlcNAc and, presumably, this dimerization is necessary for its enzymatic activity (Chou, 2004).

Research has shown that UDP-GlcNAc inhibits GFAT enzymatic activity in humans and *D. melanogaster,* thus serving as a means of feedback inhibition. (McKnight, 1992; Graack, Cinque & Kress, 2001). *In vitro* analyses of the human GFPT1 and the *D. melanogaster* GFAT1 have demonstrated that these are regulated by the cAMP-dependent Protein Kinase A (PKA); however, whereas PKA negatively regulates GFPT enzymatic activity in humans (Chang et al., 2000), it stimulates activity in *Drosophila* (Graack, Cinque & Kress, 2001). Interestingly, while human GFPT1 and GFPT2 have two and one PKA reactive serines, respectively, both *D. melanogaster* GFAT enzymes have just one PKA reactive serine.

1.7. Previous work identifying ‘blimp’ phenotype genes

In an earlier search to discover genes involved in cuticle production in *D. melanogaster*, the Bejsovec lab identified loci which, when homozygous mutant, exhibited an expanded and elastic embryonic cuticle when the embryos were dechorionated and devitellinized which they named the ‘blimp’ phenotype (Ostrowski, Dierick, & Bejsovec, 2002). In their study, they isolated EMS-induced embryonic lethal alleles of two different loci: four alleles of a euchromatic locus, they called the *blimp*

locus, and a single allele of a heterochromatic locus they called the *zeppelin* (*zep*) locus. Furthermore, they showed that all four alleles of the euchromatic locus were allelic to the previously identified *krotzkopf verkehrt* and via molecular analysis they were able to determine that this locus corresponds to a chitin synthase gene. Lacking the genetic tools and heterochromatic sequencing data necessary to identify the gene encoding the *zep* allele, its molecular identity remained undefined. As an extension of this work, they determined that lethal alleles of *knickkopf*, *retroactive,* as well as the abovementioned *grh,* also exhibit the embryonic blimp phenotype. Interestingly, subsequent work has shown that *knickkopf* and *retroactive* encode proteins required for proper orientation of chitin filaments (Moussian et al., 2006).

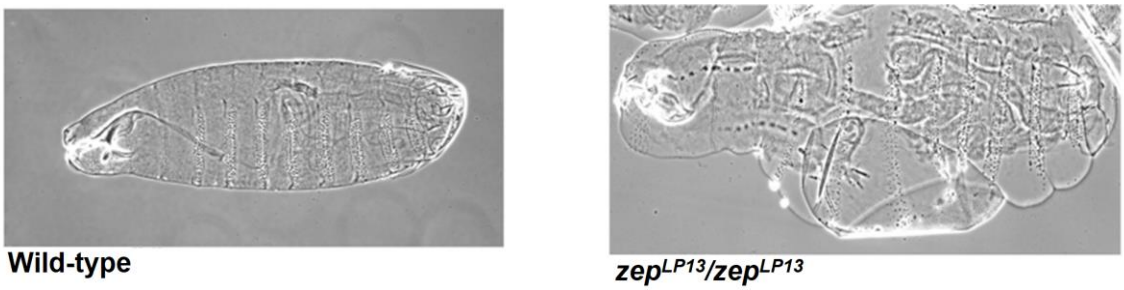

Figure 4 Image of the 'blimp' phenotype observed in homozygous zep mutants.
Image courtesy of the Bejsovec lab

1.8. Genes in heterochromatin

Studying genes in constitutive heterochromatin provides unique challenges to *Drosophila* geneticists as this region is characterized by a high number of repetitive sequence elements and low gene density (Corradini et al., 2007). Additionally, the absence of meiotic recombination and the inability to observe defined polytene banding near the chromocenter impedes characterization of genes in this region using classical genetic tools (Baker, 1958).

Interestingly, the transposition of heterochromatic segments can be responsible for the silencing of nearby euchromatic genes, an effect known as position effect variegation (PEV) (reviewed by Eissenberg & Reuter, 2009). Furthermore, when heterochromatic genes become positioned within euchromatin, their expression is also silenced (Eissenberg & Reuter, 2009). This contrast between the expression of heterochromatic and euchromatic genes and their environments has provoked an

important question: which factors govern the expression of heterochromatic genes? The notion that gene transcription in heterochromatin is affected by suppressors of variegation has now been supported by a persuasive amount of evidence. For instance, knockout of *HP1 Su(var)2-5* results in a significant level of PEV (reviewed by Vermaak & Malik, 2009). *Su(var)3-9,* a histone 3 lysine 9 methyltransferase which is homologous with HP1, is required for heterochromatin specific methylation; this modification mediates and is critical to the assembly of heterochromatin and allows HP1 binding via its chromodomain (Corradini et al., 2007). These HP1 proteins have also been shown to be necessary for various other heterochromatin maintenance functions ranging from telomere maintenance and nuclear organization to transcriptional regulation (Vermaak & Malik, 2009). Associating HP1 with the expression of heterochromatic genes exclusively is tempting as this would help resolve the paradox presented by PEV; however, HP1 appears to be necessary for the expression of some euchromatic genes as well (Vermaak & Malik, 2009).

1.9. The *zeppelin (zep)* locus corresponds to the *Gfat1* gene

Previous work by our research group has focused on the physical mapping and functional annotation of heterochromatic genes, and the Bejsovec lab generously sent us the zep^{LP13} mutant strain for analysis. A subsequent release of the *Drosophila* genome project revealed that the gene encoding GFAT1 resided at position h54-55 in heterochromatin. It was observed that this locus was affected by the *Df(3R)4-75* deficiency, which failed to complement the *zep* allele*,* and suggested it may be encoding the *Gfat1* gene.

This led to subsequent work involving genetic complementation, PCR analysis, sequencing mutant alleles, RNA interference (RNAi), and genetic rescue to confirm that the *zep* locus encodes the GFAT1 enzyme (Fitzpatrick, 2005; Jackson, 2007) (Figure 5). Additionally, if *Gfat1* expression is knocked down using RNAi targeting leg and wing imaginal discs, adult flies with a *splayed*-like phenotype were observed (Lindsley et al., 1972; Jackson, 2007). These flies also showed melanin deposits in the legs and locomotion difficulties, presumably due to weakness in the legs resulting from deficiency of chitin. Similar phenotypes were observed in certain transheterozygote *zep* allele combinations (Jackson, 2007).

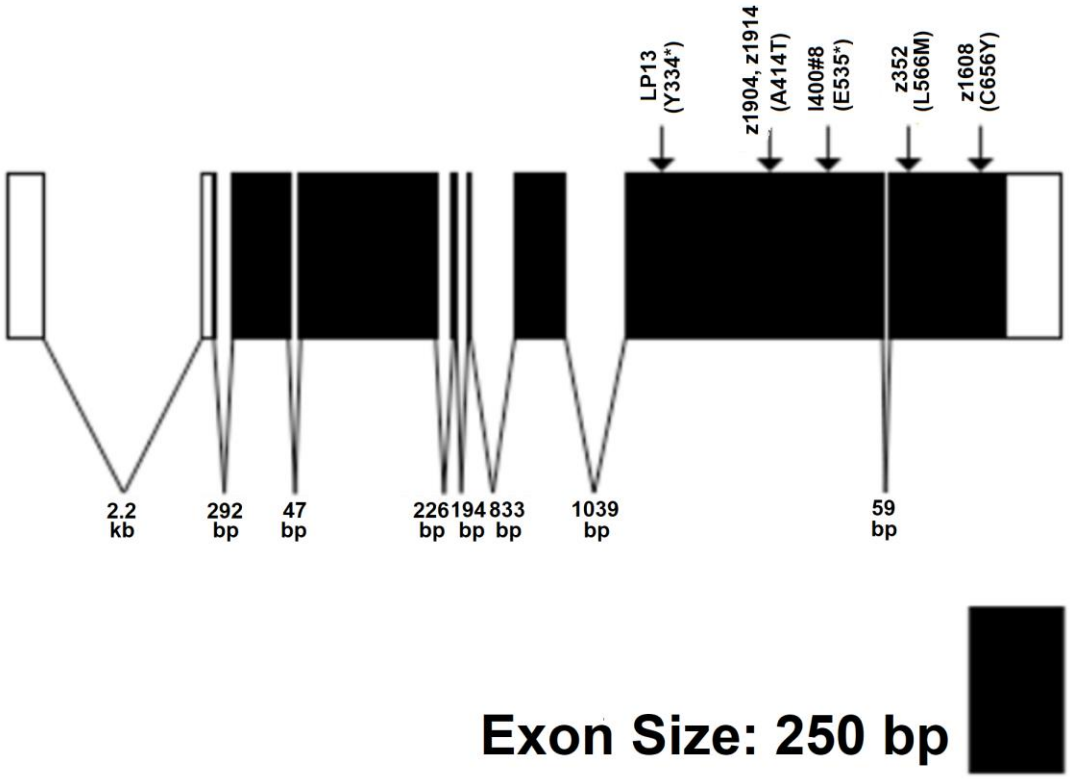

Figure 5 Gfat1 architecture and isolated mutations
Based on the work of C. Jackson (2007)

1.10. Isolation of *Gfat2* mutants by P-element excision

To further characterize the *D. melanogaster* HBP and the potential interplay between the GFAT enzymes, we undertook the generation of a series of *Gfat2* mutants using imprecise P-element excision. BL #22502 males, which possess the homozygous, non-autonomous P-element P{EPgy2}*Gfat2*^{21762} in the 5' UTR of *Gfat2*, were crossed to virgin females expressing a transposase source and rebalanced over *TM6 Tb Hu* to identify homozygous lethal mutants with the expectation that some of them would be *bona fide Gfat2* deletion mutants. These lines were crossed to a homozygous lethal *larp* mutant to confirm the integrity of the gene located 3' to *Gfat2*. Nine *Gfat2* lethal lines successfully complemented *larp* and their further characterization is described in this work.

1.11. O-linked β-*N*-acetylglucosamine transferase (OGT), O-linked β-*N*-acetylglucosaminidase (OGA) and the hexosamine signalling pathway (HexSP)

Of the many downstream enzymes that use the UDP-GlcNAc generated by the HBP, our laboratory has focused on O-linked β-*N*-acetylglucosamine transferase (OGT). We have shown that this enzyme is encoded by the Polycomb group gene *super sex combs* (*sxc*) in 2R heterochromatin of *D. melanogaster*, and mutations in this gene result in the death of pharate adults which have additional sex combs on the mesothoracic and metathoracic legs among other homeotic transformations (Sinclair, 2009). OGT, the first enzyme in the hexosamine signalling pathway (HexSP), GlcNAcylates serine and threonine residues of thousands of intracellular proteins with β-linked O-*N*-acetylglucosamine (O-GlcNAc) (reviewed in Hart, Housley & Slawson, 2007; Chatham, Nöt, Fülöp & Marchase, 2008) (Figure 6), and competes with kinases as a form of post-translational regulation by limiting the access of key regulatory amino acids (Kaasik, 2013; Bauer, 2015). Serine and threonine residues modified with this hydrophilic sugar moiety can lessen protein aggregation, and disruptions in this pathway are associated with Alzheimer's disease, which has been hypothesized to result from hyper-phosphorylated tau aggregates (Ksiezak-Reding, Liu & Yen, 1992; O'Donnell, Zachara, Hart & Marth, 2004; reviewed in Yuzwa & Vocadlo, 2014). A second enzyme, O-linked β-*N*-acetylglucosaminidase (OGA) removes O-GlcNAc residues via hydrolysis producing GlcNAc and water and, in contrast to OGT, it has not been shown to be essential in *Drosophila* (Sinclair et al., 2009; Radermacher et al., 2014) (Figure 6). GlcNAc released by OGA can be re-phosphorylated by NAGK to produce GlcNAc-6P, one of the intermediary metabolites of the HBP, allowing its reconversion to UDP-GlcNAc (Hinderlich, Berger, Schwarzkopf, Effertz, & Reutter, 2000; Weihofen, Berger, Chen, Saenger, & Hinderlich, 2006; Ryczko et al., 2016) (Figures 1, 6). The process of addition and removal of β-linked O-GlcNAc, known as O-GlcNAc cycling, plays important roles in signal transduction pathways and has also been implicated in neurodegenerative and metabolic diseases (Hanover, Krause & Love, 2010; reviewed in Vaidyanathan & Wells, 2014; Yuzwa & Vocadlo, 2014).

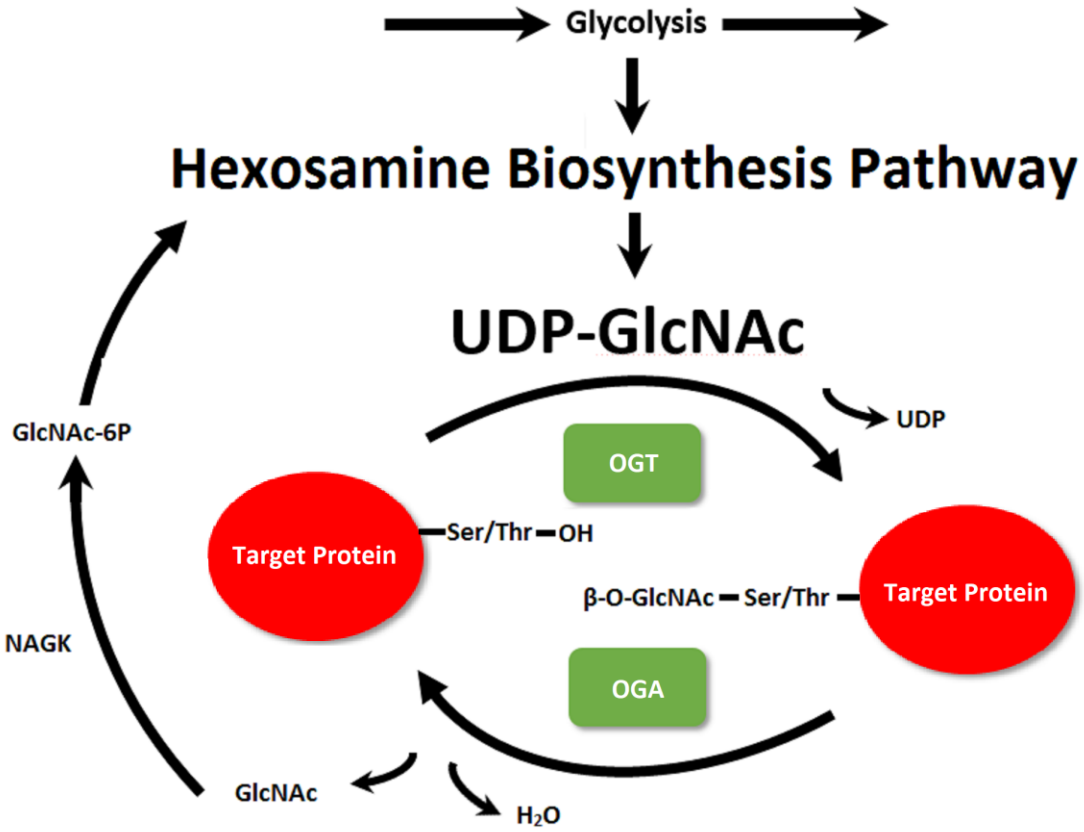

Figure 6 Depiction of the hexosamine signalling pathway.
Note that *N*-acetylglucosamine can re-enter the HBP via a salvage pathway when phosphorylated by NAGK

1.12. Potential impact of the GFAT, OGT, and OGA enzymes on *D. melanogaster* lifespan

Research has recently indicated that diets enriched with glucosamine are capable of extending the lifespan of *Caenorhabditis elegans* (*C. elegans*), as well as that of aging mice (*M. musculus),* by way of AMP-activated protein kinase (AMPK) induced mitochondrial respiration (Weimer et al., 2014). Exposure to glucosamine results in phosphorylation of AAK-2, the regulatory subunit of AMPK and induces the formation of reactive oxygen species, which are necessary by-products of mitochondrial respiration. Weimer et al. also reported that this extension of lifespan was not a result of HBP metabolism because the addition of glucosamine, which can enter the HBP when it is phosphorylated by hexokinase (Harpur & Quastel, 1949; Brown, 1951; Masson, Wiernsperger, Lagarde & El Bawab, 2005), did not result in greater concentrations of UDP-GlcNAc (Weimer et al., 2014). However, it is possible that this could be a result of

increased generation of UDP-GlcNAc via the HBP, if OGT activity has sufficiently increased to compensate for the increase in UDP-GlcNAc by diverting it to the HexSP, since research has demonstrated that GlcNAcylation by OGT correlates with HBP activity (Virkamaki, & Yki-Jarvinen, 1999; Hamiel, Pinto, Hau & Wischmeyer, 2009). However, neither assays of OGT activity nor assays of total protein GlcNAcylation were carried out in this study; therefore, the possibility remains that the HBP and HexSP may be playing a role in the increases in lifespan observed. It has also been demonstrated that increased lifespan by way of HBP upregulation is dependent on enhanced ER-associated protein degradation and proteasomal activity in *C. elegans* using gain of function (gof) *Gfat1* mutants and *Gfat1* cDNA transgenes (Denzel et al., 2014). *Oga* mutants in *C. elegans* likewise demonstrate an increase in lifespan (Rahman et al., 2010); however, when the gof *Gfat1* mutants were observed in an *Ogt* mutant background, no reduction in the extended lifespan was observed relative to the control (Denzel et al., 2014).

1.13. Evolutionary analyses of heterochromatic genes in *Drosophila*

As part of an ongoing project to understand the processes by which genes become relocated within heterochromatin, our lab previously studied two adjacent genes in *D. melanogaster* 3L heterochromatin, *Dbp80* and *RpL15*, and compared their location and architecture in two other drosophilid species: *Drosophila pseudoobscura* and *Drosophila virilis* (Schulze et al., 2006). Schulze et al. conducted fluorescence *in situ* hybridization (FISH) on polytene and mitotic chromosomes using labelled probes derived from species specific cDNAs of both genes. This allowed them to identify which of the genes were located to the chromocenter, indicating a heterochromatic localization, and also within which Muller element, a standardized nomenclature that ascribes synteny based on homology to each of the *D. melanogaster* chromosomal arms (Muller, 1940). In *D. melanogaster, Dmel*/*Dbp80* is a large gene in 3L heterochromatin (Muller element D), spread over 140kb with 10 introns and encodes a DEAD box RNA helicase (Schulze et al., 2006). On the other hand, *Dmel/RpL15,* is atypically small for a heterochromatic gene, contains two introns and encodes an essential component of the ribosome (Schulze et al., 2006).

In *D. virilis*, the two genes reside on separate Muller elements. *Dvir*/*Dbp80* is located within the same Muller element as it is for *D. melanogaster,* but is in euchromatin and is much smaller as it has only 1 intron. *Dvir/RpL15* is also a small gene but is located within heterochromatin in element E (Schulze et al., 2006). In *D. pseudoobscura*, both genes are located in Muller element D but possess a euchromatic localization. Despite being structurally similar in terms of intron number, the introns in *Dpse/Dbp80* are much smaller than its *D. melanogaster* orthologue and has approximately one seventh of its euchromatic paralogue's total length. By comparing two genes in multiple drosophilid species, Schulze et al. revealed major changes in gene architecture when genes are relocated to heterochromatin but there are exceptions to the contention that heterochromatic genes tend to have longer introns (Schulze et al., 2006).

The approach of examining two paralogues in distinct chromosomal environments in a wider variety of drosophilids may be informative in terms of understanding the evolution of gene architecture and examining functional significance. There are several other gene pairs that have the same heterochromatin/euchromatin localization as *Gfat1* and *Gfat2* including *spookier* and *spook*, and *Snap25* and *Snap24* so investigating their localization may have additional relevance (Ono H et al., 2002; Vilinsky, Stewart, Drummond, Robinson, & Deitcher, 2002; Syrzycka, 2009).

1.14. Research Goals

As mentioned, the *zeppelin* locus is now known to correspond to the *Gfat1* gene, which encodes an enzyme with a critical role in chitin synthesis as demonstrated by the *blimp* and *splayed* phenotypes. However, no such characterization has been conducted for *Gfat2.*

The objectives of this research were as follows:

1. identify and characterize the putative *Gfat2* mutants that were generated by imprecise P-element excision;

2. use the *Gfat1* and *Gfat2* mutants, the *UAS-Gfat1*-cDNA and the available *UAS-Gfat2-cDNA* transgenes, and other genetic reagents to determine if the two genes encode functionally equivalent enzymes;

3. use RT-qPCR on embryos collected at distinct stages of embryogenesis in order to characterize the transcriptional profiles of these paralogues, since heterochromatin and euchromatin are expected to be regulated in different ways;

4. test the effects of increased global protein GlcNAcylation by individually expressing *Gfat1 cDNA, Ogt* cDNA and *Oga* RNAi and then observe the effects on *D. melanogaster* lifespans;

5. do an evolutionary comparison of the genome locations for the *Gfat* paralogues in five other drosophilid species using fluorescence *in situ* hybridization on polytene and mitotic chromosomes.

Chapter 2. Materials and Methods

2.1. Fly Cultures

All fly cultures were maintained at 18°C on a medium of agar, yeast, cornmeal, molasses laced with 0.15% tegosept, and either tetracycline, or penicillin and streptomycin. Embryo lay plates consisted of a mixture of fruit juice, sucrose, agar, and 4-methyl-paraben poured into a 9 X 50 mm petri dish. All genetic crosses were conducted at 25°C unless otherwise stated. Scoring and isolation of flies was accomplished using a Leica MZ6 stereomicroscope while flies were immobilized with CO_2. A complete list of *D. melanogaster* mutants, deficiencies, transgenes and other genetic lines can be viewed in Appendix B.

2.2. Identification of *Gfat2* mutants generated by P-element excision

2.2.1. GFP diagnostics of putative *Gfat2* homozygous mutants using single embryo PCR

As the putative *Gfat2* mutants died before reaching adulthood, I employed single embryo PCR (sePCR) to isolate DNA from homozygous individuals. This involved caging mature putative *Gfat2* mutant flies that have an *enhanced green fluorescent protein* (*eGFP*) transgene on the balancer chromosome (for example: $Gfat2^{18A\text{-}14}$*/TM3 Sb Ser eGFP)* over embryo lay plates for 6 hours at 25°C to collect eggs from mature females. After this period, the adults were removed and the embryo lay plates were returned to the incubator where they remained overnight. Next, I used a GFP microscope to identify and collect non-fluorescent embryos that were homozygous for the putative *Gfat2* mutant. eGFP negative embryos must be homozygous for the P-element mutated chromosome, since any other allele combination on the third chromosome would contain at least one copy of the balancer with the e*GFP* transgene. Next these embryos were collected, dechorionated, and individually lysed in 10 mM Tris pH 8.2, 1 mM EDTA, 25 mM NaCl and 2.7 mg/mL proteinase K. These single embryo genomic DNA (seDNA) samples were further scrutinized for the presence of *eGFP* using PCR with the eGPFfwd and eGFPrev primers and for the presence of genomic DNA using the Grip84Fwd and Grip84Rev primers (Appendix C). The 20 ul PCR reactions run

for 33 cycles with an annealing temperature of 60°C and subsequently run on a 2% agarose gel. sePCR of embryos observed to fluoresce under the GFP microscope served as a positive control.

2.2.2. Assessing the integrity of the 5' end of *Moca-cyp* in putative *Gfat2* mutants using PCR

To determine that the P-element excision did not extend into *Moca-cyp*, the gene directly 5' of *Gfat2*, I employed a PCR diagnostic testing its integrity. This PCR approach was necessary because we were unable to test for the integrity of the *Moca-cyp* gene by complementation testing, due to the lack of available mutant strains. The *Moca*-cyp 5' end PCR diagnostic employed primers Mocacypfwd and Mocacyprev, as well as the Grip84 primer set for additional confirmation that we had successfully isolated seDNA in each of the tested samples (Appendix C). Embryo samples that tested positive for homozygous mutant DNA based on sePCR were set up in 20 ul PCR reactions which were run for 35 cycles with an annealing temperature of 65°C and subsequently run on a 0.5X TBE 1% agarose gel.

2.2.3. Complete gene PCR amplification and purification from putative *Gfat2* mutants

In order to pinpoint the nature of the lesion in the putative *Gfat2* P-element mutant alleles, I designed a strategy to PCR amplify the entire *Gfat2* gene for the three putative mutant lines, ligate them into a vector, then clone and sequence the plasmids. This was done only using seDNA samples that tested positive for the 5' end of *Moca-cyp,* suggesting that whatever mutation generated by P-element excision was restricted to *Gfat2*. Putative mutants $Gfat2^{10A-2}$, $Gfat2^{18A-14}$ and $Gfat2^{1C-25}$ were PCR amplified with Gfat2CompleteGeneFwd2 and Gfat2CompleteGeneRev primers (Appendix C). I used the Fermentas™ High fidelity Taq Polymerase kit, and the reaction conditions consisted of cycling 35 times with an annealing temperature of 65ºC for 40 seconds, and an initial extension temperature of 68 ºC for 4 minutes that increased 10 seconds/cycle after the tenth cycle. The PCR reaction was subsequently run on a 0.5X TBE 0.5% agarose gel, observed using high wavelength UV, cut from the agarose, and purified using the Illustra™ GFX™ PCR DNA and Gel Band Purification Kit.

2.2.4. Cloning, sequencing and analysis of the *Gfat2* mutant deletions

The *Gfat2* complete gene PCR amplicons from putative mutant seDNA samples were ligated into the pJET1.2 vector using the Fermentas™ Clonejet PCR cloning kit, transformed into DH5α cells via heat shock, and spread over ampicillin plates. Plasmid DNA was isolated from positive clones that were candidates for possessing the putative mutant *Gfat2* insert using the Fermentas™ GeneJet™ Plasmid Miniprep kit and digested in React™ 2 buffer with one or two of XbaI, PvuI, NotI and BamHI for restriction digestion analysis. The digested fragments were electrophoresed on a 0.5X TBE 0.5% agarose gel and observed using low-wavelength UV light in order to visualize the size of the insert. The entirety of the *Gfat2* gene for the plasmids containing the $Gfat2^{10A-2}$, $Gfat2^{18A-14}$, and $Gfat2^{1C-25}$ cloned inserts were sequenced by the University of British Columbia Nucleic Acid and Protein Service (UBC NAPS) laboratory using the primers which can be viewed in Appendix C.

2.3. Lethal phase analysis of *Gfat2* mutants

$Gfat2^{10A-2}$*/TM3 Sb Ser eGFP* virgin females were crossed to *Df(3R)BSC460/TM3 Sb Ser eGFP* males and incubated at 25ºC for 5 days. The cross was then caged over an embryo lay plate for 6 hours at 25ºC, after which adult flies were removed and the plate was returned to the incubator where it remained overnight. $Gfat2^{10A-2}$*/Df(3R)BSC460* hemizygous mutants, which do not fluoresce under examination by GFP microscopy, were placed on a new plate and examined the following day. The number of unhatched embryos and first instar larvae (L1) remaining on the plate was used to determine the number of organisms that died during embryogenesis. The plate was checked again the following day to check for any surviving larvae.

2.4. Genetic rescue of *Gfat1* and *Gfat2* double mutants

2.4.1. Generation of lines for genetic rescue of *Gfat2* hemizygous mutants by constitutive expression of *Gfat1* cDNA

To determine whether or not *Gfat1* and *Gfat2* encoded functionally equivalent enzymes via genetic rescue, I generated two stocks that, when crossed, would express *Gfat1* cDNA constitutively under the control of the yeast UAS-GAL4 system in a *Gfat2*

hemizygous mutant background. The first possessed a heterozygous *Gfat2* mutation on the third chromosome and a copy of a constitutively active GAL4 driver on the second chromosome. The second line possessed a heterozygous genetic deficiency of *Gfat2* on the third chromosome and a copy of the *Gfat1* cDNA transgene under the control of an upstream activating sequence (UAS) on the second chromosome. In order to generate these two stocks, each of the lines containing elements necessary for determining successful genetic rescue were initially crossed to double balancer strains. A depiction of these crosses can be viewed in Appendix E. *UAS-Gfat1-cDNA/CyO* ; +/+ males were crossed to *CyRoi/sxc*^{3} *; TM3 Ser/Tub Gal4* virgin females to generate *UAS-Gfat1-cDNA /CyRoi ; TM3 Ser/*+ males. *Gfat2*$^{10A-2}$*/TM3 Sb Ser eGFP* males were crossed *to Ap*^{Xa}*/CyO ; TM3 Sb* virgin females to generate *+/CyO* ; *Gfat2*$^{10A-2}$*/ TM3 Sb* virgin females. *Actin5C-Gal4/CyO* males were crossed to *CyRoi/sxc*^{3} *; TM3 Ser/Tub-Gal4* virgin females to generate *Actin-5C Gal4/CyRoi ; TM3 Ser/*+ males. *Df(3R)BSC567/TM6 Tb* males were crossed to *Ap*^{Xa}*/CyO ; TM3 Sb* virgin females to generate *CyO/+ ; Df(3R)BSC567/TM3 Sb* virgin females. These double balancer strains containing the genetic element of interest were crossed together to generate the parental strains of the rescue cross. *UAS-Gfat1-cDNA/CyRoi ; TM3 Ser/*+ males were crossed to *CyO/*+ ; *Gfat2*$^{10A-2}$*/TM3 Sb* virgin females to generate a *UAS-Gfat1-cDNA/CyO ; Gfat2*$^{10A-2}$*/TM3 Ser* stock. *Actin5C-Gal4/ CyRoi ; TM3 Ser/*+ males were crossed to *CyO/+ ; Df(3R)BSC567/TM3* Sb virgin females to generate an *Actin5C-Gal4/CyO ; Df(3R)BSC567/TM3 Ser* stock. Genetic rescue of *Gfat2* mutants by *Gfat1* cDNA was tested by crossing *UAS-Gfat1-cDNA/CyO ; Gfat2*$^{10A-2}$*/TM3 Ser* males to *Actin5C-Gal4/CyO ; Df(3R)BSC567/TM3 Ser* virgin females.

2.4.2. Generation of lines for genetic rescue of *Gfat1 and Gfat2* mutants by constitutive expression of *Gfat2* cDNA

To confirm that the GFAT enzymes can substitute for one another, I generated stocks that would rescue *Gfat1* transheterozygous mutants and *Gfat2* hemizygous mutants in a similar manner as described above but with a copy of *Gfat2* cDNA instead of *Gfat1* cDNA and is depicted in Appendix E: *UAS-Gfat2-cDNA/CyRoi ; Df(3R)BSC460/TM6 B , Actin5C-Gal4/CyO ; Gfat2*$^{10A-2}$*/TM3 Ser, UAS-Gfat2-cDNA/CyRoi ; Gfat1*$^{z-1904}$*/TM6 B*, *Actin5C-Gal4/CyO ; Gfat1*$^{l400\#8}$*/TM3 Ser*. *UAS-Gfat2-cDNA/CyRoi ; Df(3R)BSC460/TM6 B* males were crossed to *Actin5C-Gal4/CyO ; Gfat2*$^{10A-2}$*/TM3 Ser* virgin females to ensure that that the *Gfat2* cDNA was being

accurately transcribed. *UAS-Gfat2-cDNA/CyRoi ; Gfat1$^{z\text{-}1904}$/TM6 B* males were crossed to *Actin5C-Gal4/CyO ; Gfat1$^{l400\#8}$/TM3 Ser* virgin females to test the genetic rescue of *Gfat1* mutants with *Gfat2* cDNA.

2.4.3. Generation of *Gfat1* and *Gfat2* double mutant lines

The *Gfat1*, *Gfat2* double mutant lines were generated by homologous recombination and a depiction of the crosses can be seen in Appendix E. The *XM3* (a deficiency spanning over Gfat1), *Gfat2$^{10A\text{-}2}$* double mutant was generated by crossing *p^{+} e^{+} Gfat2$^{10A\text{-}2}$/TM3 Sb Ser eGFP* males to *Df(3R)XM3 p^{p} e^{1}*/TM3, Sb virgin females. *p^{+} e^{+} Gfat2$^{10A\text{-}2}$ /XM3 p^{p} e^{1}* virgin females were crossed to *y25 e^{1}/TM3 Sb Ser p^{p} e^{1}* and the males with a phenotype indicating a successful homologous recombination event that would include copies of *XM3* and *Gfat2$^{10A\text{-}2}$*, as well as the *p^{p} and e^{+}* markers, were used to create balanced stocks by crossing them to *TM3 Sb/TM6 B Tb Hu* to create the *XM3 p^{P} Gfat2$^{10A\text{-}2}$ e^{+}/ TM3 Sb* line (henceforth referred to as *XM3, Gfat2$^{10A\text{-}2}$/TM3 Sb)*. The *Gfat1$^{l400\#8}$*, *Df(3R)BSC567* double mutant was generated by first crossing *ri^{+} Df(3R)BSC567 p^{+}/TM3 Sb Ser eGFP* males to *kni$^{ri\text{-}1}$ Gfat1$^{l400\#8}$ p^{p}/TM3 Sb* virgin females. *kni$^{ri\text{-}1}$ Gfat1$^{l400\#8}$* p^{p}/*ri^{+} Df(3R)BSC567 p^{+}* virgin females were crossed to *y25e/TM3 Sb Ser p^{p} e^{1}* males and the males with a phenotype indicating a successful homologous recombination event that included copies of *Df(3R)BSC567* and *Gfat1*$^{l400\#8}$, as well as the *kni$^{ri\text{-}1}$ p^{+}* markers, were used to create balanced stocks by crossing them to *TM3 Sb/TM6 B Hu Tb* to generate *Gfat1$^{l400\#8}$ kni$^{ri\text{-}1}$ p Df(3R)BSC567/TM3 Sb* (henceforth referred to as *Gfat1$^{l400\#8}$, Df(3R)BSC567/TM3 Sb.* Once both of these balanced stocks had been established, they were crossed to lines with either a *Gfat1* or *Gfat2* deficiency to confirm that the lines possessed the mutation of interest.

2.4.4. Generation of lines for genetic rescue of *Gfat1, Gfat2* mutants by constitutive expression of *Gfat1* cDNA

The lines for generating the *Gfat* double mutant rescue crosses were designed in the same manner as making the abovementioned rescue lines to generate the *Actin5C-Gal4/CyRoi ; Gfat1$^{l400\#8}$*, *Df(3R)BSC567/TM3 Sb* and *UAS-Gfat1-cDNA/CyRoi* ; *XM3*, *Gfat2$^{10A\text{-}2}$/TM3 Sb* stocks which can be seen in Appendix E. *Actin5C-Gal4/CyRoi ; Gfat1$^{l400\#8}$*, *Df(3R)BSC567/TM3 Sb* males and *UAS-Gfat1-cDNA/CyRoi ; Df(3R)XM3*, *Gfat2$^{10A\text{-}2}$/TM3 Sb* virgin females were crossed and resultant progeny were scored.

2.5. RT-qPCR of *Gfat1* and *Gfat2* during embryogenesis

2.5.1. Primer and probe design of *RpL32, Gfat1* and *Gfat2* for qPCR using Taqman method

The *Gfat1* and *Gfat2* mRNA levels during embryogenesis were assayed by qPCR using the Taqman method. Primers that would produce an amplicon between 91 bp and 146 bp in size that also spanned over an intron in genomic DNA were designed along with a probe possessing a 5' 6-FAM fluorophore, a 3' Iowa Black FQ quencher, and an intermediate ZEN quencher located 9 bp from the 5' end of the probe. An exon-exon junction that was conserved between all the transcripts for each gene was selected as the site for the design of each primer and probe set and can be seen in Appendix C.

2.5.2. RNA purification and cDNA synthesis

Embryos were collected by caging adult female wild type *Oregon R* (*Ore R*) flies over embryo lay plates for either 1.5, 3 or 12 hours, then allowed to develop until the embryos became 0 - 1.5 hours, 1.5 - 3 hours, 3 - 6 hours, 6 - 9 hours, 9 - 12 hours, or 12 - 24 hours staged samples. RNA from these embryos was isolated via a modified Trizol/chloroform purification protocol that includes 3 extra chloroform purification steps, isopropanol precipitation, and resuspension in DEPC-treated water. These RNA samples were spectrophotometrically quantified and 1 µg of RNA sample was digested with DNase at 37°C for 2 hours. The reaction was stopped by adding 1 ul of EDTA and heating the mixture for 15 minutes at 65°C. 4 µL (364 ng) of DNA-free RNA sample were used to create cDNAs using the BioRad™ iScript select cDNA synthesis kit using the random hexamer primers provided.

2.5.3. RT-qPCR standard curves of *RpL32, Gfat1 and Gfat2*

2 µL of adult female *Ore R* cDNA was serially diluted with ddH_20 4 times using either 1:2 or 1:4 cDNA to total volume ratios. They were used for generating the standard curves along with a negative control and a 2:5 DNase-treated adult female RNA to total volume control using either BioRad™ iTaq Supermix with Rox or BioRad™ iTaq Supermix and 1 µL of the appropriate primer/probe set. All reactions were conducted using the Applied Biosystems™ Step-One Real-Time PCR system using an

annealing temperature of either 58°C, 60°C, 62°C for the *RpL32, Gfat1* and *Gfat2* primer/probe sets, respectively, and repeated for 40 cycles. A standard curve was derived using the software supplied by the Applied Biosystems Step-One Real-Time PCR system which determined primer efficiency.

2.5.4. Relative quantification of *Gfat1* and *Gfat2* mRNA during embryogenesis using RT-qPCR

2 µL of cDNA from the 0 - 1.5 hour, 1.5 - 3 hour, 3 - 6 hour, 6 - 9 hour, 9 -12 hour, and 12 - 24 hour staged embryos were used along with the *RpL32, Gfat1* and *Gfat2* primers. 2:5 DNase-treated RNA was used in the *RpL32* assay for each of the different embryo life stages as a control and ddH_2O was used as a diluent and negative control. A relative quantification of *Gfat1* and *Gfat2* of each of these stages was conducted using the formula:

$$ratio = (Etarget)^{(control-target)}/(Ereference)^{(control-target)} (1)$$

I used this formula treating the *RpL32* assays as the reference, the *Gfat1* or *Gfat2* assays as the target and the 0 - 1.5 hour sample as the control (Pfaffl, 2001). The error between the target of interest and the reference gene was propagated using the standard deviations of the technical replicates. This was multiplied by the average ratio of expression to return a coefficient of variation for each target and is represented by the error bars (Pfaffl, 2001).

2.6. Lifespan assay of adult flies with induced expression of *Ogt* cDNA, *Oga* RNAi or *Gfat1* cDNA driven by *Actin5C-Gal4*

To examine the effects of upregulating the HBP and the HexSP, female virgin *Actin5C-Gal4/CyO* ; *Gal80^{ts}/TM3 Ser* flies were crossed to one of *UAS-Ogt-cDNA, UAS-Oga-RNAi*, *UAS-Gfat1-cDNA,* or *w^{1118}*, which was used as a control. To ensure that none of the transgenes were being expressed until the progeny reached adulthood, the crosses were kept at 18°C. Adult males from each cross with the genotype *Actin5C-Gal4/*UAS of interest*; Gal80^{ts}/+* were immobilized with CO_2, housed in vials in groups of ten individuals, and moved to a 29°C incubator. The total number of adults in each vial

was counted each day or every other day upon transfer to a new vial until there were no remaining live flies. Escapees were deducted from the total number of flies considered and removed from the analysis. The lifespan assay was visualized with a Kaplan-Meier survival curve and statistical significance was determined based on log-rank tests for equality of survivors using w^{1118}; *+/Actin5C-Gal4* ; *+/Gal80ts* as the control group and was calculated by the STATA stats software (Bonferonni adjustment = 0.01).

2.7. Evolutionary analysis of *Gfat1* and *Gfat2*

2.7.1. Probe generation for fluorescence *in situ* hybridization of polytene and mitotic chromosomes

To identify the chromatin environments in which *Gfat1* and *Gfat2* reside in the other drosophilid species, I first needed to determine their sequences. *D. melanogaster* GFAT1-PA and GFAT2-PA amino acid sequences (Appendix F) were retrieved from Flybase and input into tBLASTn (Basic Local Alignment Search Tool) to identify the orthologues in five other species: *D. erecta, D. ananassae, D. pseudoobscura, D. willistoni* and *D. virilis* (Flybase). Once these *Gfat1* and *Gfat2* orthologues had been successfully identified, Lisa Bell, an undergraduate researcher, and I designed PCR primers for each of these species, as well as *D. melanogaster,* that would amplify a segment of each gene ranging between 501-1247 bp with the least amount of sequence similarity to its respective paralogue and the other genes in the species (Appendix C). We isolated DNA from each of these species using phenol/chloroform extraction precipitated with 85% ethanol and 300 mM sodium acetate based on a method originally described by Jowett (1986). Our subsequent PCR ran for 35 cycles with specific annealing temperatures for each primer set that can be viewed in Appendix B. These amplicons were gel purified and cloned using the above-mentioned kits and digested with *EcoRI* to confirm that the correct gene fragment had been inserted, and then sent to UBC NAPS for sequencing. Once the constructs were determined to contain the correct sequences, they were sent to the Pimpinelli lab who used them for FISH on polytene and mitotic chromosomes (for materials and methods, see Appendix G)

2.7.2. Intron content analysis of *Gfat1* in 12 drosophilid species

In order to see if there were any differences in *Gfat1* architecture between these six drosophilid species, I decided to see if there were major differences in the intron length between the coding sequences. This was done by measuring the distance between the start and stop codon in the genomic sequence and subtracting the length of the coding region in the longest reported transcript. After this, I expanded my analysis to the six other fully sequenced species: *D. sechellia*, *D. simulans*, *D. yakuba*, *D. persimilis*, *D. mojavensis* and *D. grimshawi* and their respective *Gfat1* and *Gfat2* orthologues were identified in the same manner mentioned above.

Chapter 3. Results

3.1. Characterizing *Gfat2* mutants generated by P-element excision

3.1.1. sePCR diagnostics to correctly identify putative *Gfat2* homozygous mutant DNA

Figure 7 Depiction of the Gfat2 gene and adjacent genes Moca-cyp and larp
To confirm that the lesion generated by imprecise P-element excision did not extend into the *Moca-cyp* gene, a PCR diagnostic was designed to confirm the integrity of its 5' end with the primers depicted in grey. The entirety of the *Gfat2* gene was PCR amplified using the primers depicted in black to allow for complete gene sequencing.

In order to understand the importance of both *Gfat1* and *Gfat2* in *Drosophila melanogaster,* I decided to identify and characterize *bona fide Gfat2* mutant alleles. Previously, undergraduate researchers in our lab crossed a line with a tranposase source to a line containing the non-autonomous transposable element, $Gfat2^{EY21762}$ to generate imprecise excision mutants that would, hopefully, remove a fragment of *Gfat2*'s coding region but leave the adjacent genes, *larp* and *Moca-cyp*, intact. Once these putative *Gfat2* mutants were rebalanced over TM6, they were crossed to a line with a mutation in the *larp* gene, which is essential and those that failed to complement were removed from further testing. Since there were no available alleles for the 5' gene, *Moca-cyp*, I designed a PCR strategy that would allow me to determine the lines that had a P-element excision restricted to *Gfat2*. Before I could confirm that this excision did not extend into *Moca-cyp*, I first needed to isolate DNA that was homozygous for the lesion (Figure 7). This was done by sePCR the results of which can be observed in Figures 8A-H. The presence of a band at 225 bp corresponding to the *Grip84* gene indicates the presence of *D. melanogaster* seDNA. The presence of a band at 328 bp corresponding to the *eGFP* gene indicates the presence of either heterozygote DNA or DNA homozygous for the balancer chromosome which excluded it from further testing. For example, in Figure 8A, embryo samples used for PCR in lanes 1-4, 7, 10, 12, 14, and 16 contained homozygous mutant seDNA as they produced a band at 225 bp, but

no band at 328 bp. The sample 5 lane contained a band at both 225 bp and 328 bp revealing it to contain DNA with at least one balancer chromosome. Lanes 6, 8, 9, 11, 13, and 15 contained no bands suggesting a failure of the PCR, presumably due to a lack of either heterozygote or homozygote seDNA in the sample.

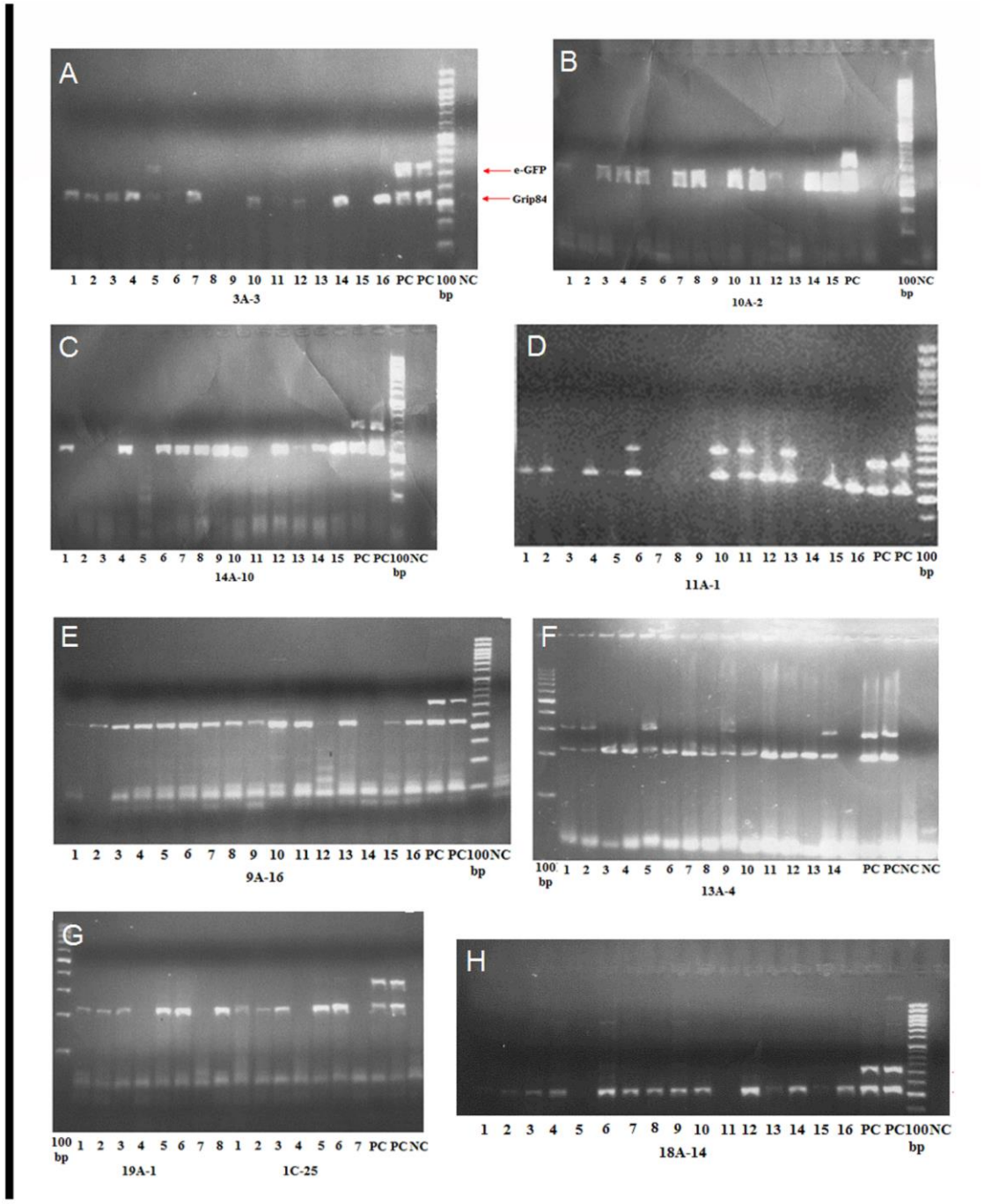

Figure 8 Single Embryo PCR diagnostics for putative Gfat2 mutants

A. 3A-3: From left to right seDNA preps 1-16, positive control 1 (PC1), PC2, 100 bp ladder, and a negative control (NC). **B. 10A-2:** From left to right: seDNA preps 1-15, PC1, PC2, empty lane , 100 bp ladder and, NC. **C. 14A-10:** From left to right: seDNA preps 1-15, PC1, PC2, 100 bp ladder, and NC. **D. 11A-1:** From left to right: seDNA preps 1-16, PC1, PC2, and 100 bp ladder **E. 9A-16:** From left to right: seDNA preps 1-16, PC1, PC2, 100 bp ladder, and NC. **F. 13A-4:** From left to right: 100 bp ladder, seDNA preps 1-14, empty well, PC1, PC2 and NC. **G. 19A-2 and 1C-25:** From left to right: 100 bp ladder, 19A-1 seDNA preps 1-8, 1C-25 seDNA preps 1-7, PC1, PC2, 100 bp ladder and NC. **H. 18A-14**: From left to right: seDNA preps 1-16, PC1, PC2, 100 bp ladder and a NC.

3.1.2. PCR assays to ensure *Moca-cyp* 5' integrity

Confirmed homozygous single embryo genomic samples were subjected to a diagnostic PCR to determine the presence or absence of the neighbouring gene, *Moca-cyp.* The PCR was performed using primers that amplified the *Moca-cyp* 5' end which is proximal to *Gfat2* (Figure 7). The presence of a band at 225 bp corresponds to the *Grip84* gene and the presence of a band at 471 bp corresponds to the 5' end of *Moca-cyp*. Out of the 9 putative *Gfat2* alleles, only three, $Gfat2^{10A-2}$, $Gfat2^{18A-14}$, and $Gfat2^{1C-25}$ had an intact copy of the *Moca-cyp* gene (Figure 9).

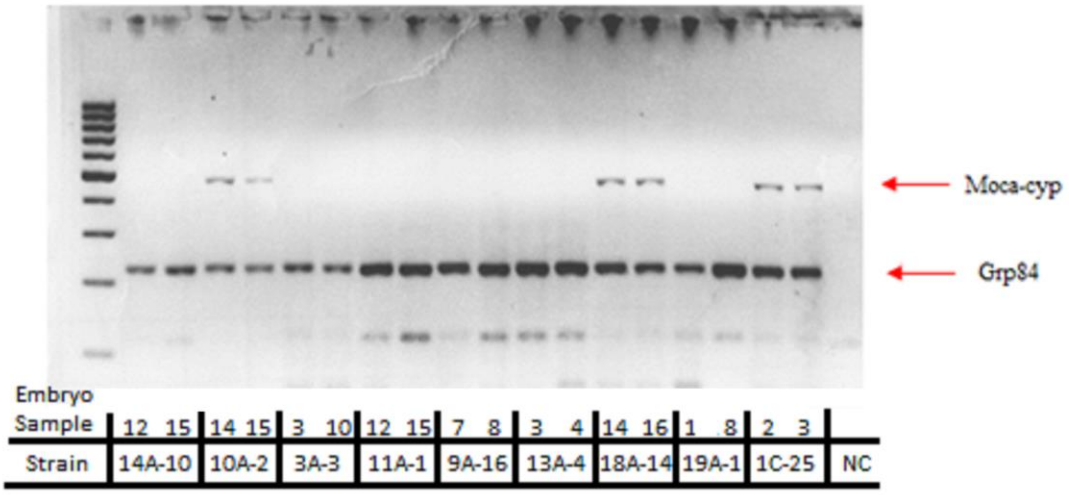

Figure 9 Moca-cyp PCR Diagnostic for Putative Gfat2 Mutants
From left to right: 100 bp ladder, strain $Gfat2^{14A-10}$ samples 12 and 15; strain $Gfat2^{10A-2}$, samples 14 and 15; strain $Gfat2^{3A-3}$, samples 3 and 10; strain $Gfat2^{11A-1}$, samples 12 and 15; strain $Gfat2^{9A-16}$, samples 7 and 8; strain $Gfat2^{13A-4}$, samples 3 and 4; strain $Gfat2^{18A-14}$, samples 14 and 16; strain $Gfat2^{19A-1}$, samples 1 and 8; strain $Gfat2^{1C-25}$, samples 2 and 3 and a negative control containing PCR master mix and ddH_2O. The diagnostic confirmed that out of the nine different *Gfat2* putative mutants tested, $Gfat2^{10A-2}$, $Gfat2^{18A-14}$ and $Gfat2^{1C-25}$ contained intact copies of *Moca-cyp.*

3.1.3. *Gfat2* complete gene amplification by PCR

The homozygous *Gfat2* mutant allele seDNA samples that tested positive for intact copies of *Moca-cyp* had the entirety of *Gfat2*, as well as part of the 5' UTRs of *Moca-cyp* and *larp,* amplified via PCR (Figure 7). The UTRs of the genes adjacent to *Gfat2* were also amplified because I did not know the extent of the lesion and I wanted to be sure that my PCR would not fail due to an absence of an annealing sequence for the primers. $Gfat2^{10A-2}$ produced an amplicon of ≈3200 bp in size, $Gfat2^{18A-14}$ produced an

amplicon ≈3900 bp in size, *Gfat2*$^{1C\text{-}25}$ produced an amplicon of ≈4300 bp in size and wild type *Ore R* genomic DNA, which served as a positive control, produced an amplicon 4298 bp in size (Figure 10). After successfully ligating the *Gfat2* complete gene fragments into a plasmid vector (confirmed by restriction mapping), the plasmids were sent to UBC NAPS for sequencing.

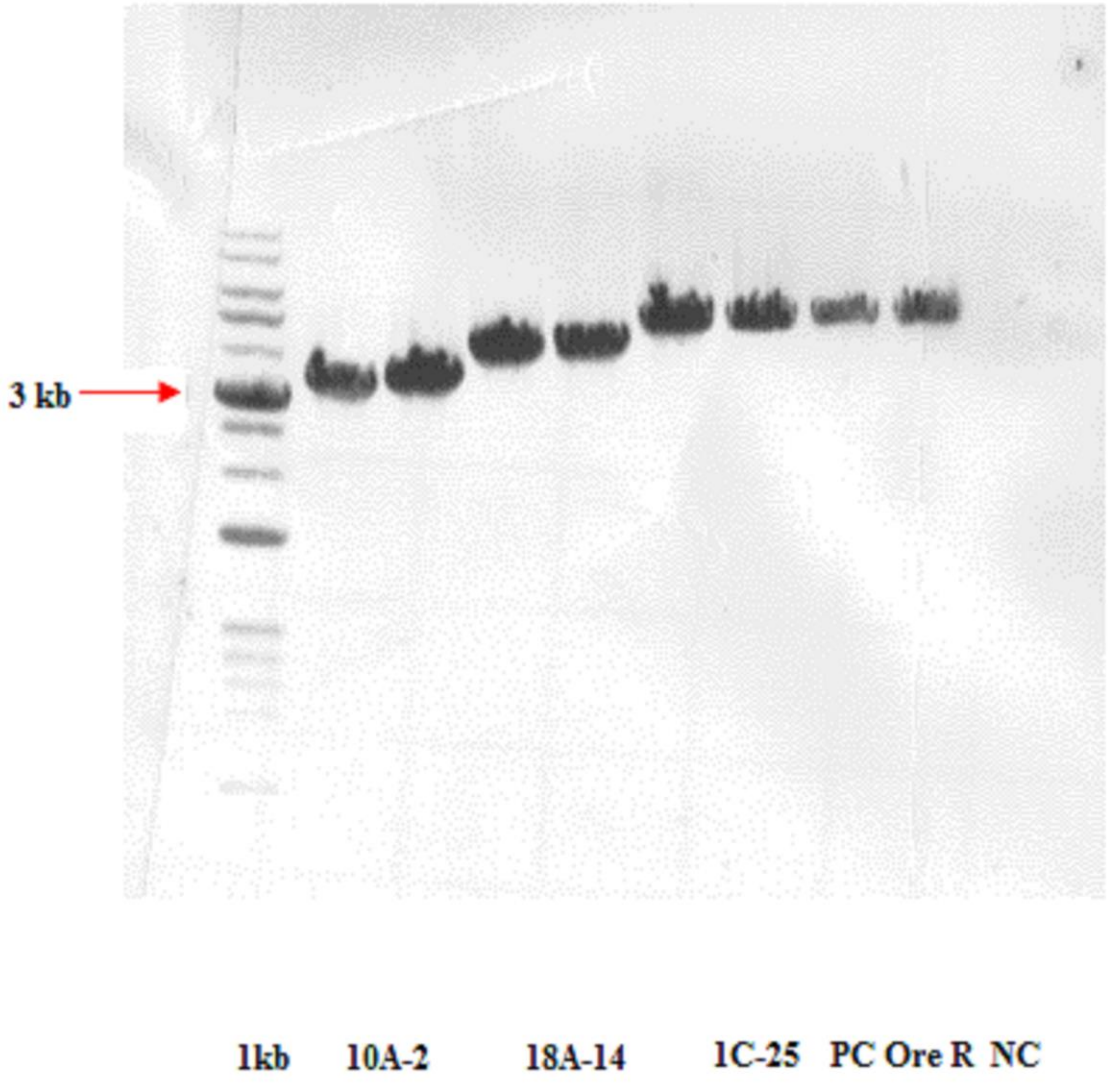

Figure 10 Gfat2 PCR complete gene amplification
From left to right: 1 kb DNA ladder, strain *Gfat2*$^{10A\text{-}2}$, samples 7 and 15; strain *Gfat2*$^{18A\text{-}14}$, samples 7 and 16; strain *Gfat2*$^{1C\text{-}25}$, samples 2 and 3, two *Ore R* genomic DNA positive controls and a negative control containing PCR master mix and ddH_2O.

3.1.4. Sequence analyses of *Gfat2* putative mutants *Gfat2^{10A-2}*, *Gfat2^{18A-14}, and Gfat2^{1C-25}*

The sequencing results of the *Gfat2^{10A-2}*, *Gfat2^{18A-14}, and Gfat2^{1C-25}* putative mutants were BLASTed against the *D. melanogaster* genome to identify potential lesions, the relevant results of which can be seen in Appendix D.

For the putative mutant *Gfat2$^{10A-2,}$* only the Gfat2Fwd206 and Gfat2CG1rev primers generated relevant results. The sequencing reaction of *Gfat2^{10A-2}* using the Gfat2-F primers failed to produce any recognizable signal. For the putative mutant *Gfat2^{10A-2}*: Gfat2Fwd206 sequencing results, BLAST returned two distinctly localized sequences along the *Gfat2* gene. The termini of these two sequences were found to be separated by 1052 nucleotides including the 13-nucleotide sequence 5'-CATGATGAAATAA-3' that is not found in the gene. The breakpoint deletes thymine 47 up to and including guanine 1085: a 1039 deletion of fragments from the 5' UTR and the first exon (Figure 11). Sequencing with the Gfat2CG1rev primer gave an identical result.

For the putative mutant *Gfat2^{18A-14}*, only the Gfat2Fwd206, Gfat2-R, Gfat2CG1rev primers generated relevant results. The sequencing reaction *Gfat2^{18A-14}* using the Gfat2-F primers failed to produce any recognizable signal. In the *Gfat2^{18A-14}*: Gfat2Fwd206 reaction, BLAST returned two distinctly localized sequences along the *Gfat2* gene. The termini of these two sequences were found to be separated by 512 nucleotides including the 13-nucleotide sequence 5'- CATGATGAAATAA-3' that is not found in the gene. The breakpoint deletes thymine 47 up to and including cytosine 545: a 499bp deletion of fragments from the 5' UTR and the first exon (Figure 11). Sequencing with the Gfat2CG1rev and Gfat2-R primers gave identical results.

No aberrations were identified in the sequencing results of *Gfat2^{1C-25}* suggesting that a human error occurred in either the genetic complementation experiments or sePCR.

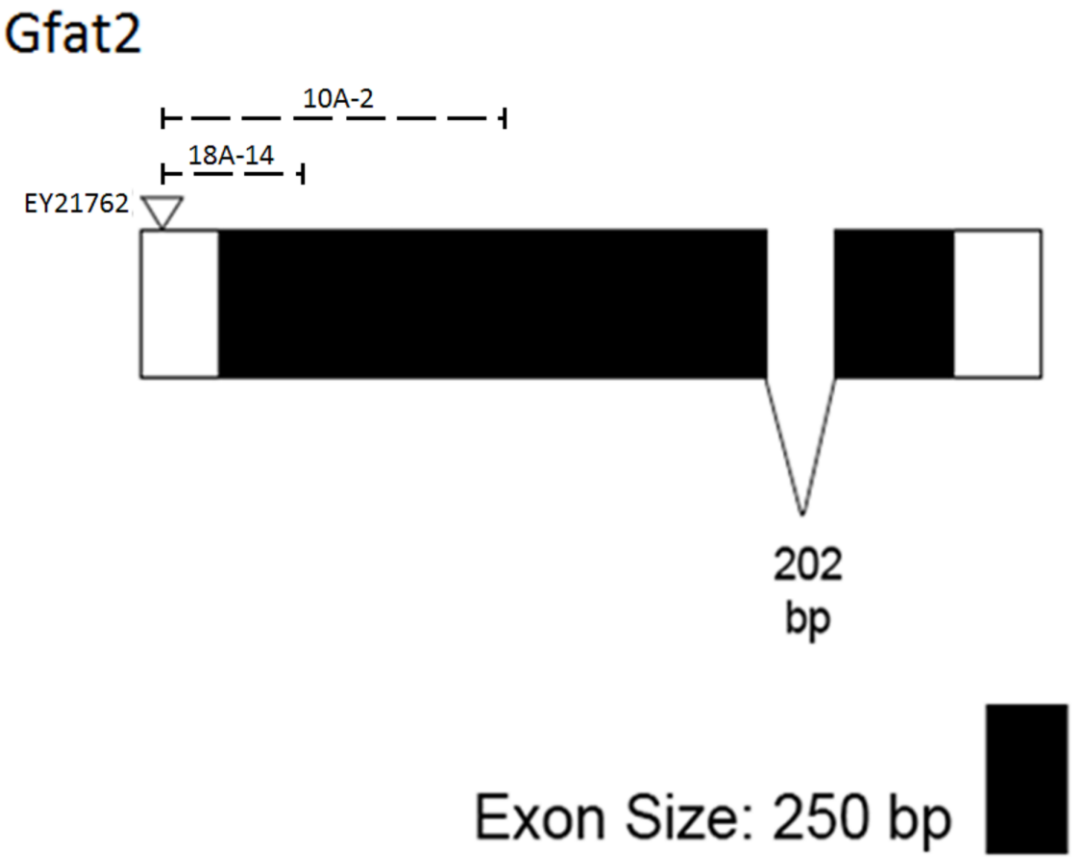

Figure 11 Depiction of Gfat2 mutants generated by P-element excision
. The *Gfat2*$^{10A-2}$ mutant has a deletion spanning 1039 bp, removing part of the 5' UTR and first exon. The *Gfat2*$^{18A-14}$ mutant has a deletion spanning 499 bp removing part of the 5' UTR and first exon.

3.2. Lethal phase analysis of *Gfat2* hemizygous mutants

As transheterozygous *Gfat1* mutants of the strongest allele combinations fail to hatch into first instar larvae and are characterized by the 'blimp' phenotype (Ostrowski, Dierick, & Bejsovec, 2002; Jackson, 2007), I decided to determine the lethal phase of *Gfat2* mutants using the newly generated *Gfat2*$^{10A-2}$ line. *Gfat2* hemizygous mutant *Gfat2*$^{10A-2}$*/Df(3R)BSC460* individuals have an early lethal phase, suggesting that *Gfat2* is an essential gene during embryogenesis, as 59 out of the 100 embryos examined died before reaching L1. The remaining L1 larvae were slower, did not grow and died before reaching the L2 stage (Figure 12).

	Gfat2 hemizygous mutant embryos		
	Unhatched	L1	L2
Gfat2^{10A-2}/*TM3 Sb Ser eGFP* X *Df(3R)BSC460/TM3 Sb Ser eGFP*	59	41	0

Figure 12 Lethal phase analysis of Gfat2 hemizygous mutants

3.3. Genetic rescue of *Gfat1* and *Gfat2*

3.3.1. Genetic rescue of *Gfat2* hemizygous mutants by constitutive expression of *Gfat1* cDNA

In order to determine if *Gfat1* and *Gfat2* encode functionally equivalent enzymes, I constitutively expressed either *Gfat1* or *Gfat2* cDNA in a *Gfat2* hemizygous mutant or *Gfat1* transheterozygous mutant background. To test if constitutive expression of *Gfat1* cDNA is capable of rescuing *Gfat2* mutants, *UAS-Gfat1-cDNA/CyO ; Gfat2*$^{10A-2}$*/TM3 Ser* males were crossed to *Actin5C-Gal4/CyO ; Df(3R)BSC567/TM3 Ser* virgin females and the progeny resulting from this cross are shown in Table 1. Of the 179 flies scored, 15 were of the *Actin5C-Gal4/UAS-Gfat1-cDNA ; Gfat2*$^{10A-2}$*/Df(3R)BSC567* genotype indicating that *Gfat1* cDNA can rescue *Gfat2* mutants and the enzymes are functionally equivalent. No *Gfat2*$^{10A-2}$*/Df(3R)BSC567* offspring were scored that didn't also have copies of both the *Actin5C-GAL4/CyO* and *UAS-Gfat1-cDNA* transgenes; demonstrating that, without the expression of the *Gfat1* cDNA, the combination of mutant alleles would be lethal (Table 1).

Table 1 ***Progeny count of constitutively expressed Gfat1 cDNA rescuing Gfat2 hemizygous mutants***

	F1 Genotype				
Cross	Cy	TM3	Cy ; TM3	mutant allele/mutant allele	Total
UAS-Gfat1-cDNA/CyRoi ; Gfat2^{10A-2}/TM3 Ser X Actin-5C-Gal4/CyO ; Df(3R)BSC567/TM3 Ser	0	49	115	15	179

3.3.2. Genetic rescue of *Gfat2* and *Gfat1* mutants by constitutive expression of *Gfat2* cDNA

I next wanted to see if constitutive expression of *Gfat2* cDNA was capable of rescuing *Gfat1* mutants; however, I first needed to confirm that the *UAS-Gfat2-cDNA* transgenic line was accurately constructed so I tested it by constitutively expressing it in a *Gfat2* hemizygous mutant background. The progeny resulting from crossing *UAS-Gfat2-cDNA/CyRoi ; Df(3R)BSC460/TM3 Ser* males to *Actin5C-Gal4/CyO ; Gfat2^{10A-2}/TM3 Ser* virgin females are shown in Table 2. Of the 177 flies scored, 32 had the *Actin5C-Gal4/UAS-Gfat2-cDNA; Gfat2^{10A-2}/Df(3R)BSC460* genotype indicating that the *Gfat2* cDNA is a reliably constructed transgene. No flies that were *Gfat2^{10A-2}/ Df(3R)BSC460* were scored that also did not have copies of both the *Actin5C-Gal4* and *UAS-Gfat2-cDNA* transgenes; demonstrating that, without the expression of the *Gfat2* cDNA, the combination of mutant alleles would be lethal (Table 2).

To confirm that the genes encode true functionally equivalent enzymes and can substitute for one another, I constitutively drove the *Gfat2 cDNA* using *Actin5C-Gal4* in *Gfat1* transheterozygous mutants. The progeny resulting from crossing *UAS-Gfat2-cDNA/CyRoi ; Gfat1^{z-1904}/TM6 B* males to *Actin5C-Gal4/CyO ; Gfat1$^{l400\#8}$/TM3 Ser* virgin females are shown in Table 2. Of the 156 flies scored, 18 had the *Actin5C-Gal4/UAS-Gfat2-cDNA ; Gfat1$^{l400\#8}$/Gfat1^{z-1904}* genotype indicating *Gfat1* and *Gfat2* encode functionally equivalent enzymes. No flies that were *Gfat1$^{l400\#8}$/Gfat1^{z-1904}* were scored that also did not have copies of both the *Actin5C-Gal4* and *UAS-Gfat2-cDNA* transgenes demonstrating that, without the expression of the *Gfat2* cDNA, the combination of mutant alleles would be lethal (Table 2).

Table 2 ***Progeny counts of constitutively expressed Gfat2 cDNA rescuing Gfat1 transheterozyougs mutants and Gfat2 hemizygous mutants***

	F1 Genotype				
Cross	**Cy**	**TM3**	**Cy ; TM3**	**mutant allele/mutant allele**	**Total**
UAS-Gfat2-cDNA/CyRoi ; Df(3R)BSC460/TM6 B X Actin5C-Gal4/CyO ; Gfat2^{10A-2}/TM3 Ser	0	50	95	32	177
UAS-Gfat2-cDNA/CyRoi ; Gfat1^{z-1904}/TM6 B X Actin5C-Gal4/CyO ; Gfat1$^{l400\#8}$/TM3 Ser	0	54	84	18	156

3.3.3. Genetic rescue of *Gfat1, Gfat2* double mutants by constitutive expression of *Gfat1* cDNA

As additional confirmation that the *Gfat* genes encode functionally equivalent enzymes, I attempted a genetic rescue of the *Gfat1, Gfat2* double mutants using *Gfat1* cDNA driven by *Actin5C-Gal4*. The progeny resulting from crossing *Actin5C-Gal4/CyRoi ; Gfat1*$^{l400\#8}$, *Df(3R)BSC567/TM3 Sb* males to *UAS-Gfat1*-cDNA/CyRoi ; *XM3*, *Gfat2*$^{10A-2}$*/TM3, Sb* virgin females cross can be seen in Table 3. Of the 127 flies scored, 18 had the *Actin5C-Gal4/UAS-Gfat1-cDNA ; Gfat1*$^{l400\#8}$, *Df(3R)BSC567/ XM3*, *Gfat2*$^{10A-2}$ *genotype* indicating that *Gfat1* cDNA can rescue *Gfat1, Gfat2* double mutants. No flies that had the genotype of *Gfat1*$^{l400\#8}$, *Df(3R)BSC567/ XM3*, *Gfat2*$^{10A-2}$ were scored that did not have a copy of both *Actin5C-Gal4* and *UAS-Gfat1-cDNA* transgenes, demonstrating that the combination of mutant alleles would otherwise be lethal (Table 3).

Table 3 Progeny count of constitutively expressed Gfat1 cDNA rescuing Gfat1, Gfat2 double mutants

	F1 Genotype				
Cross	**Cy**	**TM3**	**Cy ; TM3**	**mutant allele/mutant allele**	**Total**
UAS-Gfat1-cDNA/CyRoi ; $Gfat2^{10A-2}$, XM3/TM3 Ser X Actin5C-Gal4/CyO ; Df(3R)BSC567, $Gfat1^{l400\#8}$/TM3 Sb	0	43	66	18	127

3.4. Gfat1 and *Gfat2* have distinct expression patterns during embryogenesis

Since *Gfat1* and *Gfat2* encode functionally equivalent enzymes, I became interested in the possibility that their may be differences in their expression patterns which may account for why paralogous copies exist in *Drosophila melanogaster*. Since the developing *Drosophila* embryo undergoes many dramatic changes in morphology and gene expression, I decided to assess changes in gene expression of *Gfat1* and *Gfat2* at 6 discrete stages of embryogenesis using RT-qPCR. The relative changes in expression of *Gfat1* and *Gfat2* of the 0 - 1.5 hours, 1.5 - 3 hours, 3 - 6 hours, 6 - 9 hours, 9 - 12 hours, and 12 - 24 hours embryo staged samples using RT-qPCR primer can be seen in Figure 13. *Gfat1* expression is virtually absent in the earlier stages of embryogenesis and reaches a maximum in the last stage while *Gfat2* is expressed at moderately high levels and can change up to 2-fold.

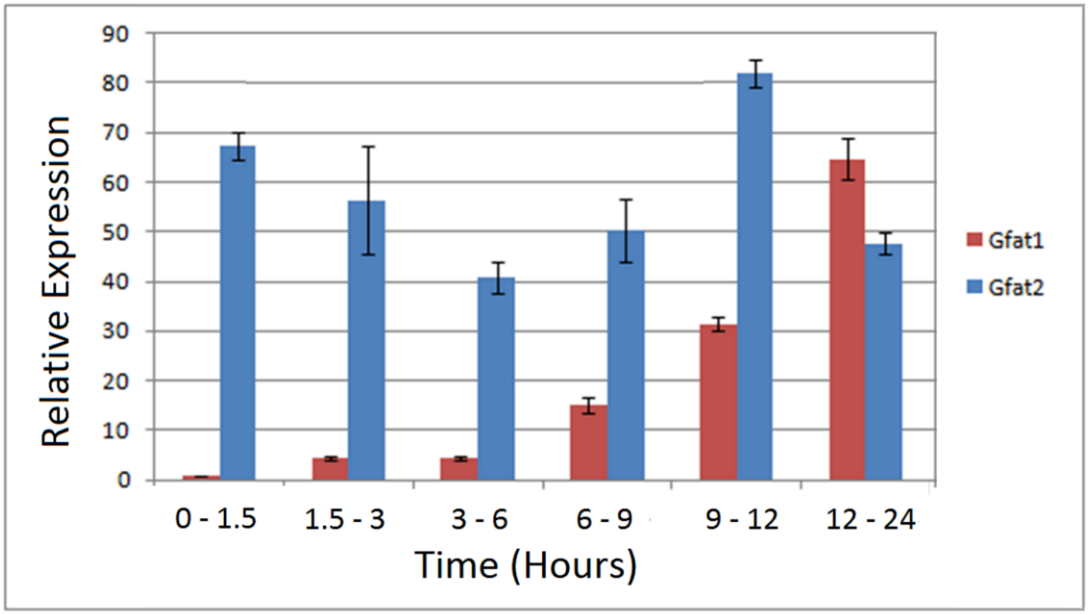

Figure 13 ***RT-qPCR of Gfat1 and Gfat2 mRNA using RpL32 as a reference gene and the Gfat1 0 – 1.5 hour min sample as the control group at different stages of embryogenesis***

3.5. Adult constitutive expression of *Ogt* cDNA and *Oga* RNAi reduces lifespan

Since previous work has demonstrated that glucosamine added to the diets of aging mice and nematodes can extend their lifespan (Weimer et al., 2014 ; Denzel et al., 2014), and it can be shunted through the HBP thereby increasing total GlcNAcylated protein levels (Harpur & Quastel, 1949; Brown, 1951; Masson, Wiernsperger, Lagarde & El Bawab, 2005), I upregulated the HBP and HexSP using genetic tools to see if I could observe a similar effect in *D. melanogaster.* Female virgin *Actin5C-Gal4/CyO* ; *Gal80^{ts}/TM3 Ser* flies were crossed at 18°C to one of *UAS-Ogt-cDNA, UAS-Oga-RNAi*, *UAS-Gfat1-cDNA* or *w^{1118},* which was used as a control. Tubulin driven *GAL80^{ts}* was used to inhibit the binding of the GAL4 transcription factor to the UAS as the flies developed at 18°C which became permitted after the flies eclosed and were shifted to 29°C. The average lifespan and log-rank scores and Kaplan-Meier survival analysis curve for the *UAS-Ogt-cDNA/Actin5C-Gal4* ; *+/Gal80^{ts}*, *UAS-Oga-RNAi/Actin5C-Gal4* ; *+/Gal80^{ts}*, and *UAS-Gfat1-cDNA/Actin5C-Gal4* ; *+/Gal80^{ts}* relative to *w^{1118} ; +/Actin5C-Gal4* ; *+/Gal80^{ts}* are represented in Figure 14. No significant changes were observed for

lifespan of the *UAS-Gfat1-cDNA/Actin5C-Gal4* ; *Gal80^{ts};* however, there were reductions in lifespan for the *UAS-Ogt-cDNA/Actin5C-Gal4* ; *+/Gal80^{ts}* and the *UAS-Oga-RNAi/Actin5C-Gal4* ; *+/Gal80^{ts}* line relative to the control (Figure 14).

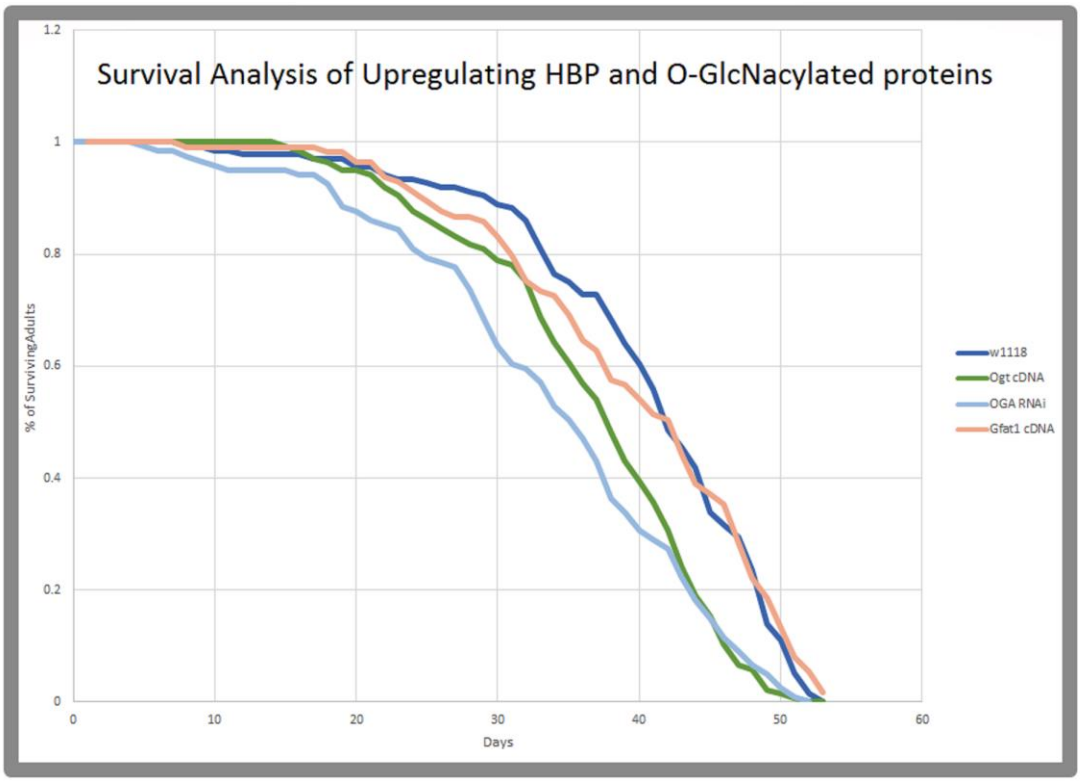

Figure 14 Kaplan-Meier survival analysis curve of w1118, Ogt cDNA, oga RNAi and Gfat1 cDNA driven with Actin5C-Gal4; Gal80^{ts}

w^{1118}; +/Actin5C-Gal4 ; *+/Gal80^{ts}* had an average lifespan of 39.81 days. *UAS-Ogt-cDNA/Actin5C-Gal4* ; *+/Gal80^{ts}* had an average lifespan 35.8 days and P-value of 0.000, chi-square value of 23.90. *UAS-Oga-RNAi/Actin5C-Gal4* ; *+/Gal80t^{s}* had an average lifespan of 34.1 days, a P-value of 0.000 and a chi-square value of 26.12. *UAS-Gfat1-cDNA/Actin5C- Gal4* ; *+/Gal80^{ts}* had an average lifespan of 39.0 days, a P-value of 0.1663, and a chi-square value of 1.92. All P and chi-square values were calculated using *w^{1118}; +/Actin5C-Gal4* ; *+/Gal80^{ts}* as the control group (Bonferonni adjustment 0.01)

3.6. Evolutionary analysis of *Gfat1* and *Gfat2* in six drosophilid species

3.6.1. Identifying *Gfat1* and *Gfat2* orthologues in five other drosophilid species and identifying neighbouring genes

Since previous work has highlighted major differences in gene architecture between orthologues in different chromatin environments (Schulze, et al., 2006), I decided to determine the chromatin environment of *Gfat1* and *Gfat2* in five other species of drosophilids. Using Flybase tBLASTn with the *D. melanogaster* GFAT1-PA and GFAT2-PA amino acid sequences (Appendix F), I successfully identified orthologues for each gene in all five of the species investigated which can be seen in Tables 4 and 5 and depictions of gene architecture can be seen in Figures 15 and 16. Each of the orthologues shared minimums of 96% and 91% amino acid identity for *Gfat1* and *Gfat2*, respectively (Table 1). Previously, Schaeffer et al. mapped the sequenced scaffolds of eleven *Drosophila* genus members to their respective Muller element and I used this work to identify that *Gfat1* and *Gfat2* are on element E in each of these species (Schaeffer et al., 2008). To see if any genetic rearrangements had occurred for *Gfat1* and *Gfat2* around their respective Muller's element, I also did tBLASTn searches for the flanking genes of *Gfat1* and *Gfat2*: *CG42402, CG40198, Moca-cyp,* and *larp,* to identify their position in each of the other five species.

In all five of the species, both *CG42402* and *CG40198* are 5' and 3', respectively, to *Gfat1* suggesting that no major chromosomal rearrangements had taken place around this locus (Table 4). With respect to *Gfat2*, *Moca-cyp* and *larp* are found 5' and 3', respectively, in all species except for *D. willistoni* in which *larp is* absent and found on scaffold scf1100000004921. The gene that is 3' to *larp* in melanogaster, *CG12156*, is not adjacent to it in *D. willistoni,* nor is it close to *Dwil/Gfat2,* suggesting the possibility of a major chromosomal rearrangement around this locus (Table 4).

Table 4 Architecture, homology, and neighbouring genes of *Gfat1* in six drosophilid species

Species	Annotation Symbol	Gene length (bp)	Largest number of introns in all isoforms	Number of Transcripts	Conserved Amino Acid Identities (%)	*CG42402* and *CG40198* 5' and 3' ?
D. melanogaster	*CG12449*	7362	10	9	100	Yes ; Yes
D. erecta	*GG12143*	6717	8	7	98	Yes ; Yes
D. ananassae	*GF23135*	8355	7	5	95	Yes ; Yes
D. pseudoobscura	*GA26267*	4861	9	8	97	Yes ; Yes
D. willistoni	*GK12920*	4610	8	5	96	Yes ; Yes
D. virilis	*GJ24380*	7611	9	6	96	Yes ; Yes
***Gfat1* in Euchromatin Average**	NA	5694	8.67	6.33	NA	NA
***Gfat1* in Heterochromatin Average**	NA	7468	8.33	7	NA	NA

Both *D. melanogaster* and *D. pseudoobscura* have annotated transcripts that would increase their gene sizes to 11,441 and 8911, respectively; however, these predictions are unlikely.

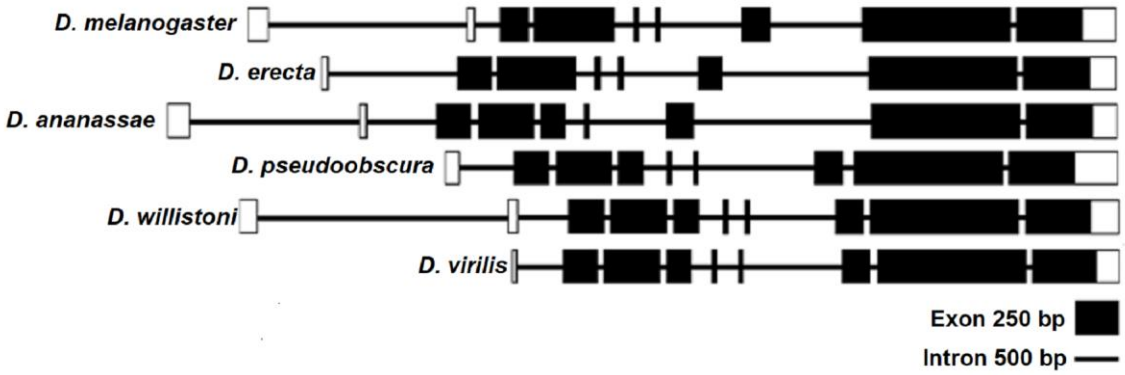

Figure 15 Architecture of Gfat1 in six drosophilid species

Translated exons are represented by black boxes. 5' and 3' UTRs are represented by white boxes. Introns are represented by black lines. The shorter versions of the gene models are depicted for *D. melanogaster* and *D. pseudoobscura.*

Table 5 Architecture, homology, and neighbouring genes of *Gfat2* in six drosophilid species

Species	Annotation Symbol	Gene length (bp)	Number of introns	Number of Transcripts	Conserved amino acid Identities (%)	*Moca-cyp* and *larp* 5' and 3' ?
D. melanogaster	*CG1345*	2747	1	1	100	Yes ; Yes
D. erecta	*GG12070*	2704	1	1	98	Yes ; Yes
D. ananassae	*GF16128*	2709	1	1	95	Yes ; Yes
D. pseudoobscura	*GA12297*	2587	0	1	92	Yes ; Yes
D. willistoni	*GK12142*	2287	0	1	92	Yes ; No
D. virilis	*GJ22773*	2327	0	1	91	Yes ; Yes
***Gfat2* Average**	NA	2560	0.5	1	NA	NA

The neighbouring genes in *D. melanogaster*, *Moca-cyp* and *larp* are adjacent to *Gfat2* in all six species except for *D. willistoni* which is lacking *larp* at its 3' end and is found on scaffold scf1100000004921.

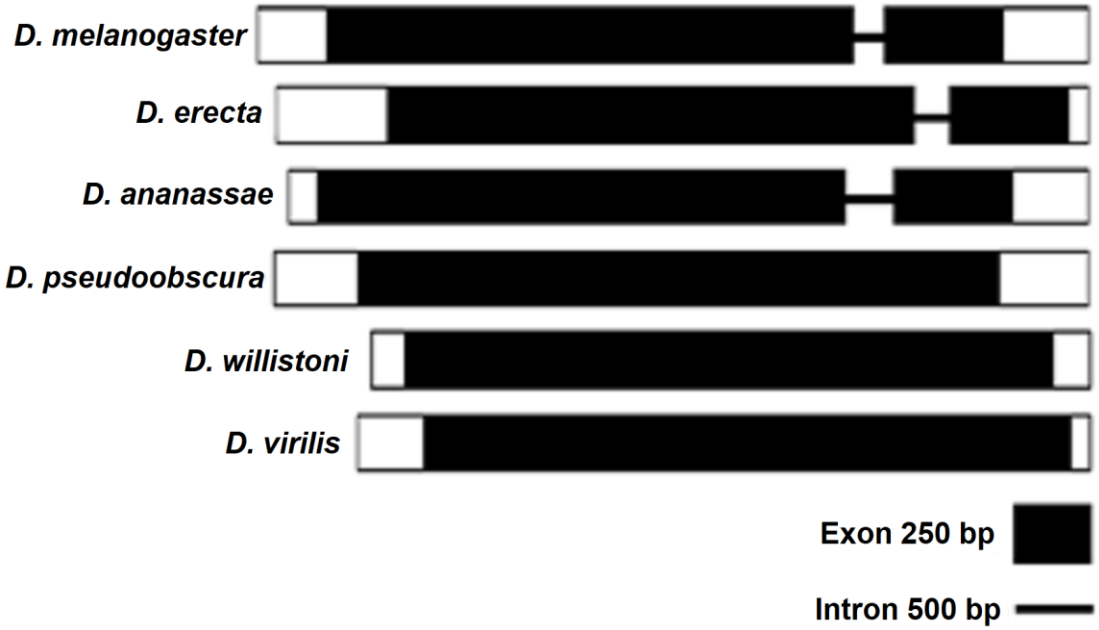

Figure 16 Gene architecture of Gfat2 in six drosophilid species.
Translated exons are represented by black boxes. 5' and 3' UTRs are represented by white boxes. Introns are represented by black lines

3.6.2. Development of probes for FISH of polytene chromosomes

Lisa Bell and I successfully generated fragments of each gene for each of these species, as well as *D. melanogaster*, using PCR and then ligated them into pJET1.2. The restriction analyses of each construct revealed the successful ligation of the gene of

interest (for an example, see Figure 17) which was confirmed by DNA sequencing by UBC NAPS.

Figure 17 Sample digestion of Gfat1 and Gfat2 probes in pJET 1.2 using EcoRI.

Expected fragment sizes of inserts: *Dana/Gfat1*: 593; *Dana/Gfat2*: 621; *Dere/Gfat1*: 644 & 281; *Dere/Gfat2*: 729. pJET 1.2 plasmid fragment ≈3 kb.

The constructs were sent to the Pimpinelli lab who performed the FISH on 3rd instar larval polytene chromosomes (Figure 18). All the *Gfat2* probes aligned with sequences along the chromosomal arm in every drosophilid species examined, suggesting a localization to euchromatin. The *Gfat1* probes also aligned along the chromosomal arm for *D. pseudoobscura, D. willistoni* and *D. virilis* additionally indicating their presence in euchromatin. However, the *Gfat1* probes aligned to the chromocenter for *D. melanogaster, D. erecta* and *D. ananassae* indicating a localization to pericentromeric heterochromatin which was confirmed by FISH on mitotic chromosomes for *D. erecta* and *D. ananassae* (Figure 18 insets).

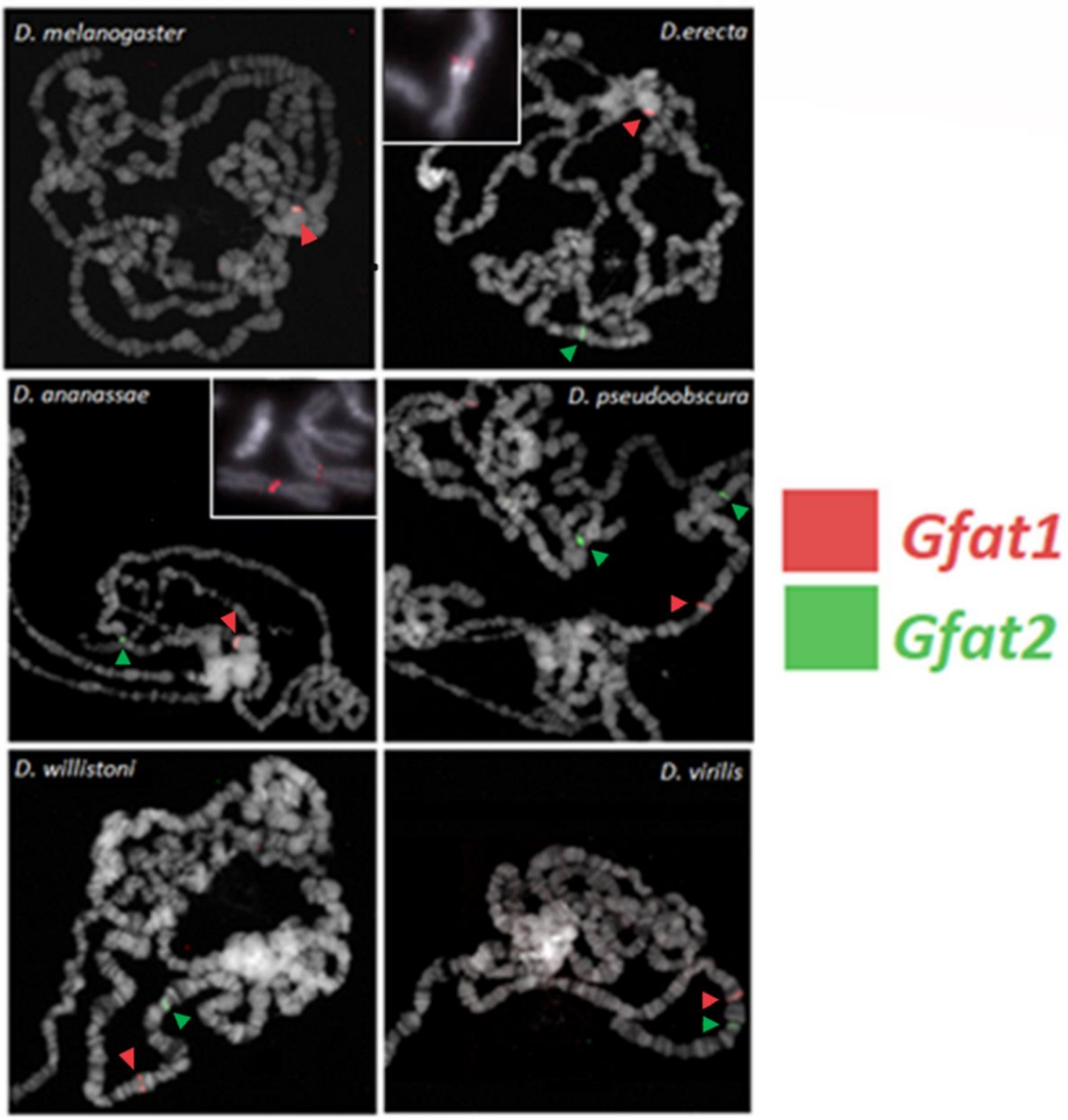

Figure 18 FISH localization of Gfat1 (red) and Gfat2 (green) probes in six drosophilid species.

Gfat1 is centromeric in *D. melanogaster*, *D. erecta* and *D. ananassae* suggesting a heterochromatic localization. This is confirmed in mitotic chromosomes for *D. erecta* and *D. ananassae*. *Gfat1* is euchromatic in *D. pseudoobscura*, *D. willistoni* and *D. virilis*. *Gfat2* is euchromatic in all species. Courtesy of the Pimpinelli lab.

3.6.3. Intron content analysis of *Gfat1* in twelve drosophilid species

Since the previous work has highlighted major differences in gene organization between heterochromatic and euchromatic genes i.e. gene length, intron length and intron number (Dimitri et al., 2003; Schulze et al., 2006), I tested for significant differences between the *Gfat1* orthologues based on their chromosomal localization. My

initial observation was that there was no significant difference in the number of introns between heterochromatic and euchromatic *Gfat1* genes (Pr T>t >0.20). I next decided to test for differences in gene length between these two categories; however, the genomic data of both the *D. melanogaster* and *D. pseudoobscura Gfat1* genes have 5' UTRs in certain transcripts which appear to be erroneously annotated. In the case of *D. melanogaster*, there are no cDNAs reported that contain the larger version of the 5' UTR observed in the *Gfat1-RH* and *Gfat1-RN* transcripts making its prediction unlikely (Flybase). In the case of *D. pseudoobscura*, the 5' UTR of the *GA26267-RF* transcript contains little sequence similarity with the 5' UTRs of *Gfat1* in the other drosophilid species, also making its prediction less likely (Flybase). In order to avoid problems that might be arising from misannotation, I determined the total intron content in the coding sequence of each *Gfat1* orthologue then used this as my basis for comparison for determining differences in "gene length" (Table 6). Using Welch's T-test revealed that a heterochromatic localization did significantly increase the amount of intron content for the *Gfat1* gene i.e. the heterochromatic versions of the gene contain ≈1.5x the intron content than the euchromatic versions (Pr T>t = 0.0671).

Table 6 Intron content within the coding sequence in *Gfat1* in twelve drosophilid species.

Species used in FISH	Known and Predicted Chromatin Localization	Annotation Symbol	Length (bp)	Distance between Genomic Start/Stop (bp)	Coding sequence in longest transcript length (bp)	Intron content between start and stop codon (bp)
D. melanogaster	Heterochromatin	*CG12449*	7362	4775	2085	2690
D. erecta	Heterochromatin	*GG12143*	6717	6495	2049	4446
D. ananassae	Heterochromatin	*GF23135*	8355	6107	2061	4046
D. pseudoobscura	Euchromatin	*GA26267*	4861	4861	2085	2776
D. willistoni	Euchromatin	*GK12920*	4610	4439	2085	2354
D. virilis	Euchromatin	*GJ24380*	7611	4385	2085	2300
Known Heterochromatin average	NA	NA	7478	5792	2065	3727
Known Euchromatin average	NA	NA	5694	4562	2085	2477
D. sechellia	(Heterochromatin)	*GM10731*	4344	4344	2085	2259
D. simulans	(Heterochromatin)	*GD28973*	6955	4444	2085	2359
D. yakuba	(Heterochromatin)	*GE25392*	11467	6430	2085	4345
D. persimilis	(Euchromatin)	*GL12297*	4840	4840	2058	2782
D. mojavensis	(Euchromatin)	*GI24373*	7826	4628	2085	2543
D. grimshawi	(Euchromatin)	*GH20131*	7903	4694	2085	2609
Total Heterochromatin Average	NA	NA	7533	5433	2075	3358
Total Euchromatin Average	NA	NA	6275	4641	2081	2561

Determining the amount of intron content in the translated region of *Gfat1* in six drosophilid species revealed that the orthologues tend to be larger when localized to heterochromatin (Pr T>t = 0.0671). The six other species of drosophilid which have been sequenced were included in the analysis and their chromatin environment was predicted to be the same as the most closely related species in which the chromatin environment is known based on FISH. These predictions are represented by the chromatin environment in brackets and including them improved the significance of the finding that the heterochromatic orthologues *Gfat1* tends to have more intron content than the euchromatic orthologues (Pr T>t = 0.0587).

I next extended this analysis to the six other drosophilid species with genomes that have been completely sequenced. Based on the assumption that the chromosomal localization of *Gfat1* in these six other species is the same as its closest relative, I included these species in the intron content analysis described above (Figure 19, Table 6). Though including these six species reduced the average intron content for the heterochromatic orthologues and increased it for the euchromatic orthologues, it did

improve the significance of the hypothesis that a localization to heterochromatin does correlate with an increase in total intron content (Pr T>t = 0.0587) (Table 6).

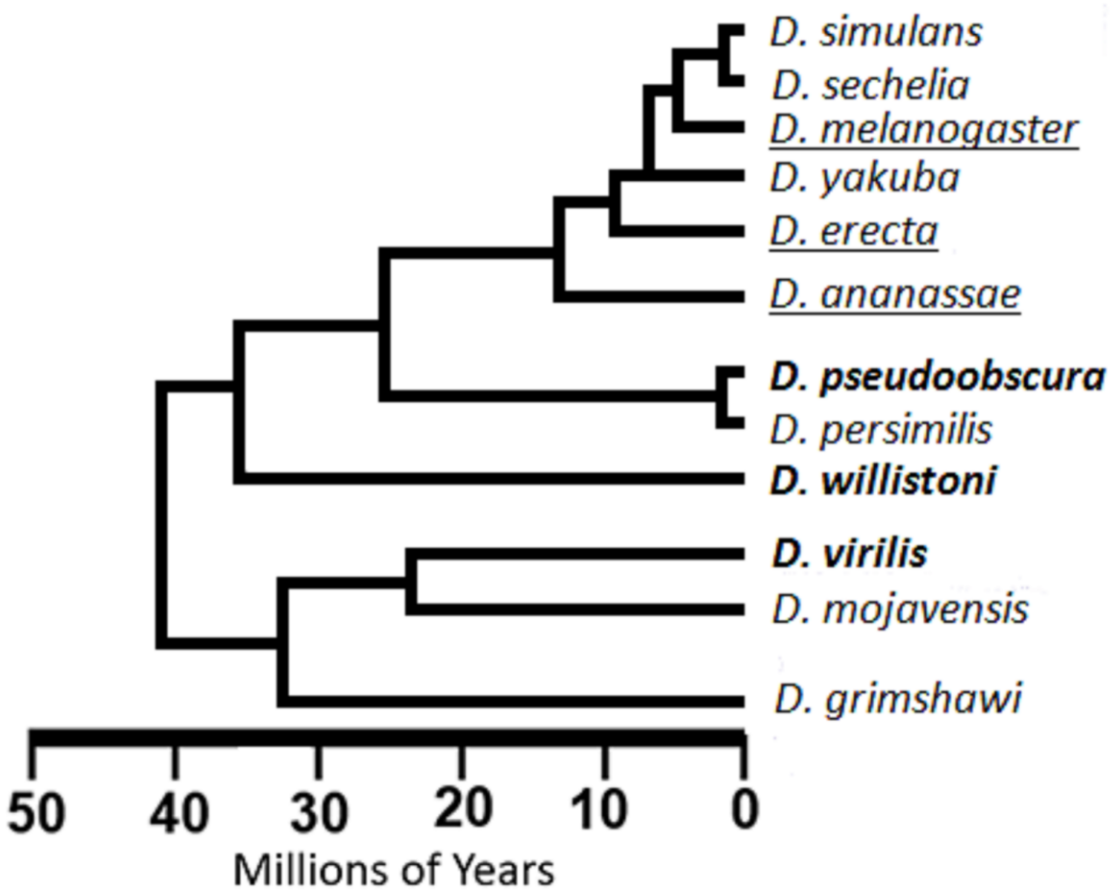

Figure 19 Depiction of Drosophila evolution over the last 50 million years. Species names are underlined for species in which *Gfat1* is known to reside in heterochromatin and are in bold when it is known to reside in euchromatin based on FISH. Each of the unknown species were grouped into heterochromatin v. euchromatin based on the most closely species with a known *Gfat1* localization. IE. *D. simulans, D. sechellia* and *D. yakuba* were considered to reside in heterochromatin, while *D. persimilis, D. mojavensis* and *D. grimshawi* were considered to reside in euchromatin for the analysis in Table 6.

Chapter 4. DISCUSSION

4.1. Overview

The isolation of 2 *Gfat2* mutants via P-element excision and their lethality in L1 larvae reveals that *Gfat2* is an essential gene in *Drosophila melanogaster*.

The *Gfat1 cDNA* and *Gfat2 cDNA* transgenic lines rescue both *Gfat1* and *Gfat2* mutants, thus providing convincing evidence that these genes encode enzymes that are functionally equivalent.

RT-qPCR revealed distinct patterns of expression for *Gfat1* and *Gfat2* during embryogenesis. While *Gfat1* is virtually absent during the earliest stages of embryogenesis prior to reaching a maximum in the 12 - 24 hour sample, *Gfat2* stays relatively consistent at fairly high levels.

Overexpression of *Gfat1* cDNA, which would likely result in increased generation of UDP-GlcNAc and total protein GlcNAcylation in *D. melanogaster* adults, showed no increases in lifespan. Furthermore, driving *Ogt cDNA* and *Oga RNAi* actually resulted in a reduced adult lifespan.

The development of probes for fluorescence *in situ* hybridization for L3 polytene and mitotic chromosomes in six drosophilid species has revealed that, most likely, a single relocation event placed *Gfat1* into heterochromatin after the *melanogaster* group split from the rest of *Drosophila* approximately 25 million years ago (Russo, Takazaki & Nae, 1995).

4.2. Analysis of the *Gfat2* mutants generated by P-element excision

The results from the sequencing reactions for $Gfat2^{10A\text{-}2}$ revealed a 1039 bp deletion starting at thymine 47 and deleting up to and including guanine 1085. This deletes the start codon and the entirety of GAAT2 domain which is necessary for the catalytic activity of the *GFAT* enzymes (Chou, 2004).

The results from the sequencing reactions for *Gfat2*$^{18A-14}$ revealed a 499 bp deletion starting at thymine 47 and removing up to and including cytosine 545. This deletes the start codon and the first 108 amino acids of the GFAT2 enzyme, which is just under a third of the GAAT2 domain.

Considering that the *Gfat2*$^{10A-2}$ has the entirety of the GAAT2 domain deleted, and that a substantial proportion of the *Gfat2*$^{18A-14}$ GAAT2 domain is also deleted, it is a safe assumption that both of these lines are null mutations because this domain is responsible for the binding of glutamine during catalysis (Chou, 2004).

The Gfat2-F sequencing reaction failed in both lines as this primer binds to a sequence in *Gfat2* that was excised in both the *Gfat2*$^{10A-2}$ and *Gfat2*$^{18A-14}$ mutants.

Of particular interest is the inclusion of the 5'- CATGATGAAATAA-3' sequence in both *Gfat2* mutants. Upon inspecting the sequence of the pP{EPgy2} used in the P-element excision, a molecular descendent of P{EPgy2}, it was discovered that this sequence is included twice in this 13668 bp transgene: at the very beginning of the 5' end, and at a position 10896bp from the 5' end (Flybase). Considering the nature of P-element excisions, this is most likely a remnant from the repeat element when said excision occurred and these P-element 'remnants' have been observed in other such experiments (Gloor, Moretti, Mouyal & Keeler, 2000).

4.3. Reciprocal genetic rescue of *Gfat1 and Gfat2* mutants using *Gfat1* and *Gfat2* cDNAs

I have demonstrated that the *D. melanogaster* copies of the *Gfat1* and *Gfat2* genes encode functionally equivalent enzymes via genetic rescue using transgenic cDNAs for both genes under the control of the constitutive driver *Actin5C-Gal4*.

Understanding how the GFAT enzymes are regulated post-translationally may provide insight into their ability to rescue one another. Perhaps the most substantial difference between the *Drosophila* GFAT enzymes and the human GFPT enzymes is that the *Drosophila* paralogues share a singular serine for regulation by PKA phosphorylation whereas in humans, GFPT1 has two such sites and GFPT2 only has 1 (Graack, Cinque & Kress, 2001). In part, this could serve as an explanation for their functional equivalency in *Drosophila*.

4.4. *Gfat1 and Gfat2* have unique expression profiles during embryogenesis

The data obtained from the RT-qPCR experiments demonstrate that *Gfat1* and *Gfat2* have considerably different expression patterns during embryogenesis. *Gfat1* is essentially absent in the early embryo, but increases in the 6 – 9 hour embryo sample and continues to increase in the older embryo samples. In contrast, *Gfat2* expression stays relatively constant, but can change up to 2-fold. These results are confirmed by Flybase RNA-seq data which show similar changes in expression (Graveley et al., 2011). These data offer some intriguing possibilities regarding the nature of the relationship between *Gfat1* and *Gfat2*, especially upon consideration of their functional equivalence. Perhaps foremost of these is that *Gfat1* appears to be expressed primarily in the 12 – 24 hour embryo sample which coincides with embryonic cuticle deposition (Hillman & Lesnik, 1970). The 'blimp*'* phenotype seen in *Gfat1* transheterozygous mutant embryos is characterized by a weakened cuticle and *Gfat1* expression appears to increase just before and during cuticle formation, suggesting that its expression has been adapted to produce an abundance of UDP-GlcNAc necessary for the synthesis of chitin during cuticle formation. This hypothesis is further supported by previous RNA *in situ* work which demonstrated that *Gfat1* is not significantly expressed until stages 16 and 17 in embryogenesis (Graack, Cinque & Kress, 2001). The RNA-seq data also demonstrate elevated levels of *Gfat1* mRNA in white pre-pupae, a stage right before *Drosophila* larvae form the pupal case which may also be adapted to generate enough UDP-GlcNAc for chitin synthesis (Graveley et al., 2011).

Equally interesting are the inferences made possible by the *Gfat2* expression pattern. Unlike *Gfat1*, *Gfat2* had a high-level of expression in the 0 - 1.5 hour embryo sample, and I hypothesize that this is the result of maternal deposition. This is supported by two observations: the first is that RNA-seq data have demonstrated that *Gfat2* is found to be moderately expressed in adult female ovaries (Flybase; Brown et al., 2014), whereas *Gfat1* is characterized as having the lowest expression detectable in the same tissues. The second observation is that *Gfat2* hemizygous mutants show only partial lethality in the embryo, whereas *Gfat1* transheterozygotes of the strongest mutant alleles show complete lethality characterized by the 'blimp' phenotype. That *Gfat2* hemizygous mutant embryos are able to molt to first instar larvae is likely due to the presence of sufficient maternally deposited *Gfat2* mRNA that is enabling them to develop beyond this

stage. Since *Gfat2* expression remains at a relatively elevated level throughout embryogenesis it is likely operating as a 'housekeeping gene' i.e. a gene that is constitutively active because it is necessary for the fundamental functions of the cell. That the final product of the HBP, UDP-GlcNAc, is used in so many different glycosylations as well as GlcNAcylation, would further support this hypothesis.

The RT-qPCR data of *Gfat1* and *Gfat2* are also supported by RNA *in situ* data made available by the Berkeley Drosophila Genome Project. With respect to *Gfat1* mRNA, expression is completely absent until stages 13-16 when it becomes expressed not just throughout the epidermis, presumably to meet the needs of chitin synthesis, but also in the embryonic salivary glands (Hammonds et al., 2013). With respect to *Gfat2* mRNA, expression is ubiquitous in the earliest stages of embryogenesis and then expressed in a wide variety of tissues throughout development including the endoderm, mesoderm, dorsal and ventral epidermis, and salivary gland body among many others (Hammonds et al., 2013). These data also support the notion that *Gfat2* is a housekeeping gene.

4.5. Survival analyses using genetic tools to drive HBP and O-GlcNAcylation demonstrated no increase in lifespan

Previously, Weimer et al. demonstrated that the lifespans of *C. elegans* and *M. musculus* can be extended by supplementing their diets with glucosamine (Weimer et al., 2014). Since glucosamine is known to drive activity of the HBP (Harpur & Quastel, 1949; Brown, 1951; Masson, Wiernsperger, Lagarde & El Bawab, 2005) and OGT activity correlates with HBP activity (Virkamaki, & Yki-Jarvinen, 1999; Hamiel, Pinto, Hau & Wischmeyer, 2009), I reasoned that increasing total GlcNAcylated protein levels might extend the lifespan in *D. melanogaster* by expressing *Gfat1* cDNA, *Ogt* cDNA and *Oga* RNAi with GAL4 under $GAL80^{ts}$ control in adult males. No extension of lifespan was seen in any of these groups; however, a significant reduction in life span for both *Ogt* cDNA and *Oga* RNAi was observed using a log-rank test for equality of survivors.

I am surprised that none of the transgenes I employed were able to extend the lifespans of *D. melanogaster,* despite Weimer et. al's explanation that mitochondrial respiration is responsible for the increased longevity in *C. elegans* and *M. musculus* upon glucosamine supplementation and Denzel et al.'s observation that *Gfat1* gof

mutants have an increased lifespan (Weimer et al., 2014 ; Denzel et al., 2014). I hypothesize that the genetic tools I used failed to duplicate the increases in lifespan seen by other researchers may have occurred due to three factors.

1: It is possible that supplementing the diets of worms and mice with glucosamine produces extensions in lifespan not by increasing the activity of OGT, but rather by another pathway that uses UDP-GlcNAc. Though this would explain why no lifespan increases were observed in the *Ogt cDNA* and *Oga RNAi* driven lines, it does not account for the absence of extended lifespan when driving *Gfat1 cDNA*.

2: It is also possible that the experimental conditions I employed were not sufficiently similar to those employed by Weimer et al., undermining the comparability of our findings. It is possible that, since I shifted the flies to 29°C within a few days of eclosing from their pupal cases, the flies were too young to show an effect. The mice under previous study were given glucosamine at 100 weeks of age, which is just over two thirds of the total lifespan of a mouse untreated with glucosamine, whereas the flies in my sample were shifted up immediately after they eclosed- a fraction of their normal lifespan. Also, a better negative control group, such as one that contained a UAS for a non-coding transcript that would have imposed a similar energetic burden as expressing the experimental transgenes, would have yielded more accurate data.

3: Finally, it is equally possible that the GAL4 induced expression of *Ogt* and *Gfat1* cDNA may have resulted in so much enzyme that it became detrimental to the well-being of the organisms. Other members of our lab have driven *Ogt* cDNAs in the past that have resulted in pharate adult lethality characterized by a rough eye phenotype. Whether this is a result of OGT activity or its conglomeration into protein aggregates is unknown and these transgenes will need to have the amount of *Ogt* and *Gfat1* mRNA quantified via RT-qPCR so that a more refined increase can be employed.

An ideal experiment using these genetic tools would involve first determining the degree of expression in the cDNA transgenes so that their induced expression can be modulated accordingly, employing a control that contained a non-coding transgene similar in length to the experimental cDNAs, and then shifting them up to 29°C at around 30 days of age, rather than immediately after eclosion.

4.6. *Gfat1* and *Gfat2* fluorescence *in situ* hybridization of polytene and mitotic chromosomes in six different drosophilid species reveals chromosomal localization

The probes Lisa Bell and I prepared were instrumental in visualizing the chromosomal localizations of *Gfat1* and *Gfat2* in *D. melanogaster, D. erecta, D. ananassae, D. pseudoobscura, D. willistoni*, and *D. virilis* when the Pimpinelli lab used them for FISH on 3rd instar larval polytene chromosomes. FISH using the *Gfat1* probes for mitotic chromosomes was also done on *D. erecta* and *D. ananassae*.

In all species, *Gfat2* is either mono- or bi-exonic and is located within euchromatin on Muller element E. In contrast, *Gfat1* is in heterochromatin on Muller element E for *D. melanogaster, D. erecta* and *D. ananassae* and in euchromatin on Muller element E for *D. pseudoobscura, D. willistoni*, and *D. virilis.* The most parsimonious explanation for this change in chromatin environment would be that *Gfat1* was in euchromatin in the last common ancestor for *Drosophila*, and relocated to heterochromatin when the *melanogaster* group, which includes *D. melanogaster, D. erecta and D. ananassae*, split from the rest of *Sophophora* 25 million years ago (Russo, Takazaki, & Nae, 1995) (Figure 20).

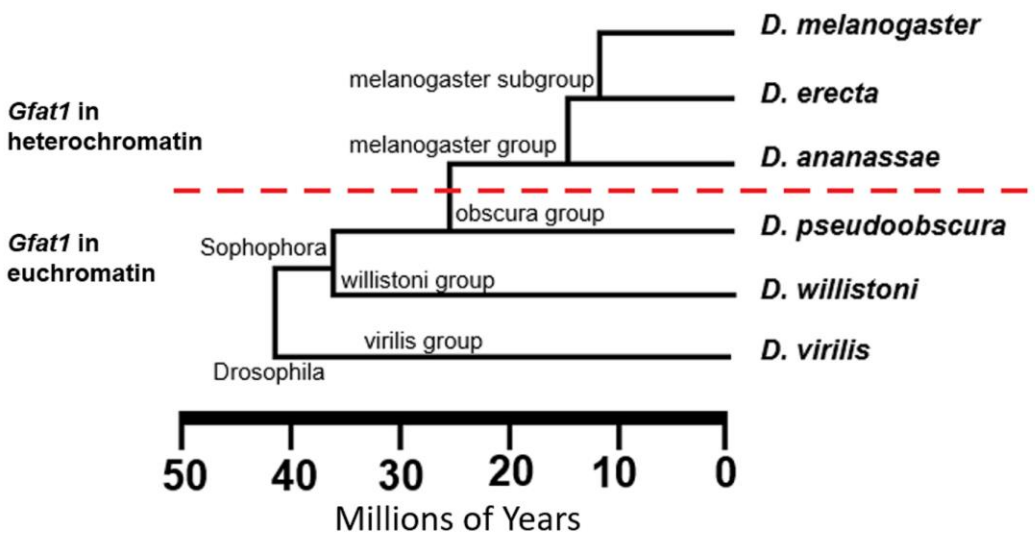

Figure 20 Depiction of predicted Gfat1 relocalization event
FISH on polytene and mitotic chromosomes revealed that *Gfat1* is in heterochromatin for all species of the *melanogaster group* and in euchromatin for the rest of the *Drosophila genus*.

It is possible that *Gfat1* was heterochromatic in the last common ancestor of the *Drosophila* genus, but this would necessitate at least three relocations of the gene when the *pseudoobscura, willistoni* and *virilis* group each diverged into their own clades. Although this hypothesis is less parsimonious, it is worth some consideration as *Gfat1* has a higher intron content in these species than the *D. melanogaster* average (Michael & Manyuan, 1999). It is therefore possible that the higher intron content observed for these species is a result of a previous heterochromatic localization and the architecture of the gene is in the process of being reconfigured to suit a euchromatic environment. This is also supported by the work of Schulze et al. who observed that *Dmel/Dbp80* had a much more dramatic heterochromatic character than the euchromatic *Dpse/Dbp80* and *Dvir/Dbp80* (Schulze et al., 2006).

Data from PEV experiments have demonstrated dramatic changes in expression when euchromatic genes enter a heterochromatic environment and it is possible that the *melanogaster* group's *Gfat1* relocation had a similar impact. Similar to *Gfat1*, the heterochromatic *spookier* and *Snap25* genes are also transcribed late in embryogenesis and not in maternal ovaries (Graveley et al., 2011; Brown et al., 2014; Flybase). It is interesting that for these three heterochromatin/euchromatin paralogue pairs, all of the heterochromatic copies share delayed transcription in the embryo and do not appear to be maternally deposited, while the inverse is true of the euchromatic copy (Vilinsky,

Stewart, Drummond, Robinson, & Deitcher, 2002; Ono H, 2002, Syrzycka, 2009, Graveley, 2011; Brown, 2014; Flybase). There is however, evidence of some heterochromatic genes, such as *Ogt*, being maternally deposited, and it is worth investigating the possibility of maternal deposition of *Gfat1* mRNA, as well as its expression during embryogenesis, in the *Drosophila* species in which it resides in euchromatin (Graveley et al., 2011; Brown et al., 2014; Flybase).

Interestingly, the increases in the average intron content for heterochromatic *Gfat1* are far less dramatic when compared to the difference seen between the heterochromatic *Dmel/Dbp80* and the euchromatic *Dpse/Dbp80*– the former being more than 7X greater (Schulze et al., 2006). Previous work in our lab has identified that *Gfat1* is less than 40kb from the heterochromatin/euchromatin boundary and it is possible that this is the reason why its gene architecture is not as "heterochromatinized" as *Dmel/Dbp80*. *D. sechellia* and *D. simulans*, the two species mostly closely related to *D. melanogaster*, have the lowest and third lowest intron content in their copies of *Gfat1* out of all the species examined. When all of the sequenced species are included in the statistical analyses, there was a significant increase in intron size for the *Gfat1* orthologues that were in heterochromatin; for this analysis, I assumed that *Dsec/Gfat1* and *Dsim/Gfat1* were in heterochromatin, but this may have been in error. It is possible, that since *Dmel/Gfat1* is so close to the heterochromatin/euchromatin boundary that it is actually in euchromatin for these two species

4.7. Concluding remarks

Unlike *Gfat1* transheterozygous mutants which are characterized by the 'blimp' phenotype, no clear phenotype was observed for *Gfat2* hemizygous mutants when we conducted embryonic cuticle preps (Data not shown). Flies with mutations in the *mummy* (*mmy*) gene, which encodes the UDP-N-acetylglucosamine-diphosphorylase downstream of the GFAT enzymes in the HBP, were found to develop a 'dorsal-open' phenotype during embryogenesis (Schimmelpfeng, Strunk, Stork, & Klämbt, 2006). Members of the Harden lab and I tested for this phenotype by first using *Gfat2* hemizygous mutants, then with *Gfat1, Gfat2* double mutants, but there was no significant number of dorsal closure failures observed in the embryos (Data not shown). This is may

be due to the high maternal deposition of *Gfat2*, allowing them to survive embryogenesis to the L1 stage. If further attempts at discovering this phenotype for *Gfat* mutants were undertaken, a cross that involves expressing *Gfat2* RNAi in the maternal ovaries of the *Gfat1, Gfat2* hemizygous mutants offers the most likely route to duplicating a dorsal-open phenotype. Additionally, Schimmelpfeng et al. found a variety of nervous system defects in *mmy* homozygous mutants including defasciculation of the embryonic central nervous system (Schimmelpfeng et al., 2006). It is possible that disruptions of the *Gfat* genes may also result in similar defects but the genetic difficulties in dealing with the high maternal contribution of *Gfat2*, and the potentially compensatory paralogue would also need to be overcome. However, there is a possibility that complete ablation of *Gfat* expression does not result in the phenotypes observed in *mmy* mutants. Of all the mutant alleles associated with genes encoding HBP enzymes, those in *mmy* appear to be best represented with these phenotypes despite evidence of its maternal deposition (Graveley et al., 2011; Brown et al., 2014; Flybase). This may be because it is the final enzyme of the HBP and as a result, cannot be bypassed by one of the salvage pathways (Figures 1 & 6). The GFAT enzymes, on the other hand, can be bypassed when either glucosamine or *N*-acetylglucosamine are phosphorylated by either HEXK or NAGK, respectively, to produce HBP intermediates and our inability to observe *mmy* phenotypes in our *Gfat* mutants may be a consequence of these salvage pathways (Harpur & Quastel, 1949; Brown, 1951; Hinderlich, Berger, Schwarzkopf, Effertz, & Reutter, 2000; Masson, Wiernsperger, Lagarde & El Bawab, 2005; Weihofen, Berger, Chen, Saenger, & Hinderlich, 2006; Ryczko, 2016).

Our collaborators in the Vocadlo lab have recently followed up on the regulatory impact of the Grh transcription factor and found that, not only does overexpressing it result in increased *Gfat1* and *Gfat2* expression, but increased expression of other genes encoding enzymes of the HBP. That Grh is a transcription factor responsible for controlling epithelial morphogenesis (Bray & Kafatos 1991; Mace, Pearson & McGinnis, 2005), is consistent with the ‘dorsal-open’ phenotype observed in *mmy* homozygous mutants (Schimmelpfeng, Strunk, Stork & Klämbt, 2006); additionally, *grh* alleles were identified in the screen for embryonic cuticle ‘blimp’ defects conducted by Ostrowski et al. (2002) Although it is still not known if Grh is upregulating the transcription of the members of the HBP directly or indirectly, the ChIP-seq data suggest a strong possibility of direct interaction (Nevil, Bondra, Schulz, Kaplan, & Harrison, 2017; Yao et al., 2017).

Recent work investigating the transcriptional regulation of two heterochromatic genes encoding ecdysteroidogenic enzymes, *neverland* and *spookier,* have identified the transcription factors Molting Defective, Séance, and Ouija board to be responsible for their expression- the first reported transcription factors to operate within heterochromatin (Uryu et al., 2018). As Grh is now also known to positively upregulate *Gfat1*, which is also in heterochromatin, the means of properly identifying the complement of interactors that are responsible for heterochromatic gene expression are beginning to emerge. How or if they interact with HP1 and related proteins provides a novel avenue into the research of heterochromatic gene expression.

Both the HBP and HexSP have been associated with numerous diseases in humans including diabetes, Alzheimer's, and cancer and *Drosophila melanogaster* has shown to be a suitable model organism for their study (Sekine, Love, Rubenstein, Hanover, 2010; Mhatre et al., 2014a; reviewed in Alvarez, Salceda, & Riesgo-Escovar, 2018; Parvy, Hodgson, & Cordero, 2018). For example, Na et al. have observed that raising flies on 0.1 M glucosamine diets leads to increased activity of the HBP, resulting in reduced heart contractility and knocking down *Gfat* transcription in the *D. melanogaster* heart can result in arrhythmia; both of which are signals of heart disease resulting from diabetic-like symptoms in *Drosophila* (Na et al., 2013). With respect to Alzheimer's, Mhatre et al. have found that expressing the Alzheimer's associated proteins APP (Amyloid Precursor Protein) and BACE (Beta Secratase) in the *Drosophila* nervous system resulted in defects in the larval neuromuscular junction (Mhatre et al., 2014b). Further understanding of the *Drosophila* GFAT enzymes should also be of considerable value into researching Alzheimer's since they are primarily responsible for generating the UDP-GlcNAc employed by OGT which has been shown to be an important enzyme in preventing the hyperphosphorylation of tau aggregates (Ksiezak-Reding, Liu & Yen, 1992; O'Donnell, Zachara, Hart & Marth, 2004; Yuzwa & Vocadlo, 2014). With respect to cancer, so far no studies examining the HBP or OGT have thus far been conducted in flies but the observation that *Gfpt2* expression is increased in human breast cancer cell lines gives oncologists an appealing starting point for conducting these types of studies in *Drosophila* (Simpson, Tryndyak, Beland, & Pogribny, 2012).

In summation: the *Gfat2* mutants that I characterized, the previously characterized *Gfat1* mutants, and the observations in this work regarding their functional

equivalence and transcriptional regulation will be valuable tools for the continued understanding of the impact of the HBP on human disease using *Drosophila melanogaster* as a model organism.

References

Alvarez-Rendon, J. P., Salceda, R., & Riesgo-Escovar, J. R. (2018). Drosophila melanogaster as a Model for Diabetes Type 2 Progression. *Biomed Res Int, 2018*, 1417528. doi:10.1155/2018/1417528

Baker, W. K. (1958). Crossing over in heterochromatin. *The American Naturalist, 92*(862), 59-60. doi:https://doi.org/10.1086/282010

Bauer, C., Gobel, K., Nagaraj, N., Colantuoni, C., Wang, M., Muller, U., . . . Leonhardt, H. (2015). Phosphorylation of TET proteins is regulated via O-GlcNAcylation by the O-linked N-acetylglucosamine transferase (OGT). *J Biol Chem, 290*(8), 4801-4812. doi:10.1074/jbc.M114.605881

Bellen, H. J., Levis, R. W., Liao, G., He, Y., Carlson, J. W., Tsang, G., . . . Spradling, A. C. (2004). The BDGP gene disruption project: single transposon insertions associated with 40% of Drosophila genes. *Genetics, 167*(2), 761-781. doi:10.1534/genetics.104.026427

Bray, S. J., & Kafatos, F. C. (1991). Developmental function of Elf-1: an essential transcription factor during embryogenesis in Drosophila. *Genes Dev, 5*(9), 1672-1683.

Brown, D. H. (1951). The phosphorylation of D (+) glucosamine by crystalline yeast hexokinase. *Biochim Biophys Acta, 7*(4), 487-493.

Brown, J. B., Boley, N., Eisman, R., May, G. E., Stoiber, M. H., Duff, M. O., . . . Celniker, S. E. (2014). Diversity and dynamics of the Drosophila transcriptome. *Nature, 512*(7515), 393-399. doi:10.1038/nature12962

Chang, Q., Su, K., Baker, J. R., Yang, X., Paterson, A. J., & Kudlow, J. E. (2000). Phosphorylation of human glutamine:fructose-6-phosphate amidotransferase by cAMP-dependent protein kinase at serine 205 blocks the enzyme activity. *J Biol Chem, 275*(29), 21981-21987. doi:10.1074/jbc.M001049200

Chiaradonna, F., Ricciardiello, F., & Palorini, R. (2018). The Nutrient-Sensing Hexosamine Biosynthetic Pathway as the Hub of Cancer Metabolic Rewiring. *Cells, 7*(6). doi:10.3390/cells7060053

Chou, K. C. (2004). Molecular therapeutic target for type-2 diabetes. *J Proteome Res, 3*(6), 1284-1288. doi:10.1021/pr049849v

Corradini, N., Rossi, F., Giordano, E., Caizzi, R., Verni, F., & Dimitri, P. (2007). Drosophila melanogaster as a model for studying protein-encoding genes that are resident in constitutive heterochromatin. *Heredity (Edinb), 98*(1), 3-12. doi:10.1038/sj.hdy.6800877

Denzel, M. S., & Antebi, A. (2015). Hexosamine pathway and (ER) protein quality control. *Curr Opin Cell Biol, 33*, 14-18. doi:10.1016/j.ceb.2014.10.001

Denzel, M. S., Storm, N. J., Gutschmidt, A., Baddi, R., Hinze, Y., Jarosch, E., . . . Antebi, A. (2014). Hexosamine pathway metabolites enhance protein quality control and prolong life. *Cell, 156*(6), 1167-1178. doi:10.1016/j.cell.2014.01.061

Dimitri, P., Corradini, N., Rossi, F., Verni, F., Cenci, G., Belloni, G., . . . Koryakov, D. E. (2003). Vital genes in the heterochromatin of chromosomes 2 and 3 of Drosophila melanogaster. *Genetica, 117*(2-3), 209-215.

Dietzl, G., Chen, D., Schnorrer, F., Su, K. C., Barinova, Y., Fellner, M., . . . Dickson, B. J. (2007). A genome-wide transgenic RNAi library for conditional gene inactivation in Drosophila. *Nature, 448*(7150), 151-156. doi:10.1038/nature05954

Eissenberg, J. C., & Reuter, G. (2009). Cellular mechanism for targeting heterochromatin formation in Drosophila. *Int Rev Cell Mol Biol, 273*, 1-47. doi:10.1016/s1937-6448(08)01801-7

Finke, M. D. (2007). Estimate of chitin in raw whole insects. *Zoo Biol, 26*(2), 105-115. doi:10.1002/zoo.20123

Fitzpatrick, K. A. (2005). *Genetic and molecular characterization of chromosome three heterochromatin in Drosophila melanogaster.* (Doctor of Philosophy), Simon Fraser University, Burnaby, BC.

Gloor, G. B., Moretti, J., Mouyal, J., & Keeler, K. J. (2000). Distinct P-element excision products in somatic and germline cells of Drosophila melanogaster. *Genetics, 155*(4), 1821-1830.

Graack, H. R., Cinque, U., & Kress, H. (2001). Functional regulation of glutamine:fructose-6-phosphate aminotransferase 1 (GFAT1) of Drosophila melanogaster in a UDP-N-acetylglucosamine and cAMP-dependent manner. *Biochemical Journal, 360*(Pt 2), 401-412.

Gramates, L. S., Marygold, S. J., dos Santos, G., Urbano, J.-M., Antonazzo, G., Matthews, B. B., . . . the FlyBase Consortium. (2017). FlyBase at 25: looking to the future. *Nucleic Acids Res, 45*(Database issue), D663-D671. doi:10.1093/nar/gkw1016

Graveley, B. R., Brooks, A. N., Carlson, J. W., Duff, M. O., Landolin, J. M., Yang, L., . . . Celniker, S. E. (2011). The developmental transcriptome of Drosophila melanogaster. *Nature, 471*(7339), 473-479. doi:10.1038/nature09715

Hallson, G. (2013). *The organization, regulation and functions of genes in the pericentric heterochromatin of the Drosophila melanogaster third chromosome.* (Doctor of Philosophy), Simon Fraser University, Burnaby, BC.

Hamiel, C. R., Pinto, S., Hau, A., & Wischmeyer, P. E. (2009). Glutamine enhances heat shock protein 70 expression via increased hexosamine biosynthetic pathway activity. *Am J Physiol Cell Physiol, 297*(6), C1509-1519. doi:10.1152/ajpcell.00240.2009

Hammonds, A. S., Bristow, C. A., Fisher, W. W., Weiszmann, R., Wu, S., Hartenstein, V., . . . Celniker, S. E. (2013). Spatial expression of transcription factors in Drosophila embryonic organ development. *Genome Biol, 14*(12), R140. doi:10.1186/gb-2013-14-12-r140

Hanover, J. A., Chen, W., & Bond, M. R. (2018). O-GlcNAc in cancer: An Oncometabolism-fueled vicious cycle. *J Bioenerg Biomembr, 50*(3), 155-173. doi:10.1007/s10863-018-9751-2

Hanover, J. A., Krause, M. W., & Love, D. C. (2010). The hexosamine signaling pathway: O-GlcNAc cycling in feast or famine. *Biochim Biophys Acta, 1800*(2), 80-95. doi:10.1016/j.bbagen.2009.07.017

Harpur, R. P., & Quastel, J. H. (1949). Phosphorylation of d-Glucosamine by Brain Extracts. *Nature, 164*, 693. doi:10.1038/164693a0

Hart, G. W., Housley, M. P., & Slawson, C. (2007). Cycling of O-linked beta-N-acetylglucosamine on nucleocytoplasmic proteins. *Nature, 446*(7139), 1017-1022. doi:10.1038/nature05815

Hillman, R., & Lesnik, L. H. (1970). Cuticle formation in the embryo of Drosophila melanogaster. *Journal of Morphology, 131*(4), 383-395. doi:10.1002/jmor.1051310403

Hinderlich, S., Berger, M., Schwarzkopf, M., Effertz, K., & Reutter, W. (2000). Molecular cloning and characterization of murine and human N-acetylglucosamine kinase. *Eur J Biochem, 267*(11), 3301-3308.

Irion, U., & Leptin, M. (1999). Developmental and cell biological functions of the Drosophila DEAD-box protein abstrakt. *Curr Biol, 9*(23), 1373-1381.

Ito, K., Awano, W., Suzuki, K., Hiromi, Y., & Yamamoto, D. (1997). The Drosophila mushroom body is a quadruple structure of clonal units each of which contains a virtually identical set of neurones and glial cells. *Development, 124*(4), 761-771.

Jackson, C. (2007). *Gfat1/zeppelin is an essential heterochromatic gene involved in cuticle formation of D. Melanogaster.* (Masters of science), Simon Fraser University, Burnaby, BC.

Kaasik, K., Kivimae, S., Allen, J. J., Chalkley, R. J., Huang, Y., Baer, K., . . . Fu, Y. H. (2013). Glucose sensor O-GlcNAcylation coordinates with phosphorylation to regulate circadian clock. *Cell Metab, 17*(2), 291-302. doi:10.1016/j.cmet.2012.12.017

Koundakjian, E. J., Cowan, D. M., Hardy, R. W., & Becker, A. H. (2004). The Zuker collection: a resource for the analysis of autosomal gene function in Drosophila melanogaster. *Genetics, 167*(1), 203-206.

Kress, H. (1993). The salivary gland chromosomes of Drosophila virilis: a cytological map, pattern of transcription and aspects of chromosome evolution. *Chromosoma, 102*, 734-742.

Letsou, A., Alexander, S., Orth, K., & Wasserman, S. A. (1991). Genetic and molecular characterization of tube, a Drosophila gene maternally required for embryonic dorsoventral polarity. *Proc Natl Acad Sci U S A, 88*(3), 810-814.

Lewis, E. B. (1951). Additions and corrections to the cytology for rearrangements. . *Drosophila Information Service, 25*, 108-190.

Lindsley, D. L., Sandler, L., Baker, B. S., Carpenter, A. T., Denell, R. E., Hall, J. C., . . . Gould-Somero, M. (1972). Segmental aneuploidy and the genetic gross structure of the Drosophila genome. *Genetics, 71*(1), 157-184.

Mace, K. A., Pearson, J. C., & McGinnis, W. (2005). An epidermal barrier wound repair pathway in Drosophila is mediated by grainy head. *Science, 308*(5720), 381-385. doi:10.1126/science.1107573

Marshall, S., Bacote, V., & Traxinger, R. R. (1991). Discovery of a metabolic pathway mediating glucose-induced desensitization of the glucose transport system. Role of hexosamine biosynthesis in the induction of insulin resistance. *J Biol Chem, 266*(8), 4706-4712.

Masson, E., Wiernsperger, N., Lagarde, M., & Bawab, Samer E. (2005). Glucosamine induces cell-cycle arrest and hypertrophy of mesangial cells: implication of gangliosides. *Biochemical Journal, 388*(Pt 2), 537-544. doi:10.1042/BJ20041506

McKnight, G. L., Mudri, S. L., Mathewes, S. L., Traxinger, R. R., Marshall, S., Sheppard, P. O., & O'Hara, P. J. (1992). Molecular cloning, cDNA sequence, and bacterial expression of human glutamine:fructose-6-phosphate amidotransferase. *J Biol Chem, 267*(35), 25208-25212.

Mhatre, S. D., Michelson, S. J., Gomes, J., Tabb, L. P., Saunders, A. J., & Marenda, D. R. (2014). Development and characterization of an aged onset model of Alzheimer's disease in Drosophila melanogaster. *Exp Neurol, 261*, 772-781. doi:10.1016/j.expneurol.2014.08.021

Mhatre, S. D., Satyasi, V., Killen, M., Paddock, B. E., Moir, R. D., Saunders, A. J., & Marenda, D. R. (2014). Synaptic abnormalities in a Drosophila model of Alzheimer's disease. *Dis Model Mech, 7*(3), 373-385. doi:10.1242/dmm.012104

Michael, D., & Manyuan, L. (1999). Intron—exon structures of eukaryotic model organisms. *Nucleic Acids Res, 27*(15), 3219-3228. doi:10.1093/nar/27.15.3219

Moussian, B., Tång, E., Tonning, A., Helms, S., Schwarz, H., Nüsslein-Volhard, C., & Uv, A. E. (2006).;Drosophila Knickkopf and Retroactive are needed for epithelial tube growth and cuticle differentiation through their specific requirement for chitin filament organization. *Development, 133*(1), 163.

Muller, H. J. (1940). *Bearings of the 'Drosophila' work on systematics, pp. 185–268 in* Oxford, UK: Oxford University Press.

Na, J., Musselman, L. P., Pendse, J., Baranski, T. J., Bodmer, R., Ocorr, K., & Cagan, R. (2013). A Drosophila model of high sugar diet-induced cardiomyopathy. *PLoS Genet, 9*(1), e1003175. doi:10.1371/journal.pgen.1003175

Nevil, M., Bondra, E. R., Schulz, K. N., Kaplan, T., & Harrison, M. M. (2017). Stable Binding of the Conserved Transcription Factor Grainy Head to its Target Genes Throughout Drosophila melanogaster Development. *Genetics, 205*(2), 605-620. doi:10.1534/genetics.116.195685

O'Donnell, N., Zachara, N. E., Hart, G. W., & Marth, J. D. (2004). Ogt-dependent X-chromosome-linked protein glycosylation is a requisite modification in somatic cell function and embryo viability. *Mol Cell Biol, 24*(4), 1680-1690.

Ono, H., Rewitz, K. F., Shinoda, T., Itoyama, K., Petryk, A., Rybczynski, R., . . . O'Connor, M. B. (2006). Spook and Spookier code for stage-specific components of the ecdysone biosynthetic pathway in Diptera. *Dev Biol, 298*(2), 555-570. doi:10.1016/j.ydbio.2006.07.023

Ostrowski, S., Dierick, H. A., & Bejsovec, A. (2002). Genetic control of cuticle formation during embryonic development of Drosophila melanogaster. *Genetics, 161*(1), 171-182.

Parvy, J. P., Hodgson, J. A., & Cordero, J. B. (2018). Drosophila as a Model System to Study Nonautonomous Mechanisms Affecting Tumour Growth and Cell Death. *Biomed Res Int, 2018*, 7152962. doi:10.1155/2018/7152962

Pfaffl, M. W. (2001). A new mathematical model for relative quantification in real-time RT-PCR. *Nucleic Acids Res, 29*(9), e45.

Pimpinelli, S. B. S. F. L. G. M. (2000). Preparation and analysis of Drosophila mitotic chromosomes In M. A. a. R. S. H. W. Sullivan (Ed.), *Drosophila Protocols* (pp. 3-23). Cold spring Harbor, NY: Cold Spring Harbor Laboratory Press.

Qin, C. X., Sleaby, R., Davidoff, A. J., Bell, J. R., De Blasio, M. J., Delbridge, L. M., . . . Ritchie, R. H. (2017). Insights into the role of maladaptive hexosamine biosynthesis and O-GlcNAcylation in development of diabetic cardiac complications. *Pharmacol Res, 116*, 45-56. doi:10.1016/j.phrs.2016.12.016

Radermacher, P. T., Myachina, F., Bosshardt, F., Pandey, R., Mariappa, D., Muller, H. A., & Lehner, C. F. (2014). O-GlcNAc reports ambient temperature and confers heat resistance on ectotherm development. *Proc Natl Acad Sci U S A, 111*(15), 5592-5597. doi:10.1073/pnas.1322396111

Rahman, M. M., Stuchlick, O., El-Karim, E. G., Stuart, R., Kipreos, E. T., & Wells, L. (2010). Intracellular protein glycosylation modulates insulin mediated lifespan in C.elegans. *Aging (Albany NY), 2*(10), 678-690. doi:10.18632/aging.100208

Russo, C. A., Takezaki, N., & Nei, M. (1995). Molecular phylogeny and divergence times of drosophilid species. *Mol Biol Evol, 12*(3), 391-404. doi:10.1093/oxfordjournals.molbev.a040214

Ryczko, M. C., Pawling, J., Chen, R., Abdel Rahman, A. M., Yau, K., Copeland, J. K., . . . Dennis, J. W. (2016). Metabolic Reprogramming by Hexosamine Biosynthetic and Golgi N-Glycan Branching Pathways. *Scientific reports, 6*, 23043. doi:10.1038/srep23043

Schaeffer, S. W., Bhutkar, A., McAllister, B. F., Matsuda, M., Matzkin, L. M., O'Grady, P. M., . . . Kaufman, T. C. (2008). Polytene chromosomal maps of 11 Drosophila species: the order of genomic scaffolds inferred from genetic and physical maps. *Genetics, 179*(3), 1601-1655. doi:10.1534/genetics.107.086074

Schimmelpfeng, K., Strunk, M., Stork, T., & Klambt, C. (2006). Mummy encodes an UDP-N-acetylglucosamine-dipohosphorylase and is required during Drosophila dorsal closure and nervous system development. *Mech Dev, 123*(6), 487-499. doi:10.1016/j.mod.2006.03.004

Schulze, S. R., McAllister, B. F., Sinclair, D. A. R., Fitzpatrick, K. A., Marchetti, M., Pimpinelli, S., & Honda, B. M. (2006). Heterochromatic Genes in Drosophila: A Comparative Analysis of Two Genes. *Genetics, 173*(3), 1433-1445. doi:10.1534/genetics.106.056069

Sekine, O., Love, D. C., Rubenstein, D. S., & Hanover, J. A. (2010). Blocking O-linked GlcNAc cycling in Drosophila insulin-producing cells perturbs glucose-insulin homeostasis. *J Biol Chem, 285*(49), 38684-38691. doi:10.1074/jbc.M110.155192

Senderek, J., Müller, J. S., Dusl, M., Strom, T. M., Guergueltcheva, V., Diepolder, I., . . . Lochmüller, H. (2011). Hexosamine Biosynthetic Pathway Mutations Cause Neuromuscular Transmission Defect. *American Journal of Human Genetics, 88*(2), 162-172. doi:10.1016/j.ajhg.2011.01.008

Simpson, N. E., Tryndyak, V. P., Beland, F. A., & Pogribny, I. P. (2012). An in vitro investigation of metabolically sensitive biomarkers in breast cancer progression. *Breast Cancer Res Treat, 133*(3), 959-968. doi:10.1007/s10549-011-1871-x

Sinclair, D., Syrzycka, M., Macauley, M., Rastgardani, T., Komljenovic, I., J Vocadlo, D., . . . M Honda, B. (2009). *Drosophila O-GlcNAc transferase (OGT) is encoded by the Polycomb group (PcG) gene, super sex combs (sxc)* (Vol. 106).

Srinivasan, V., Sandhya, N., Sampathkumar, R., Farooq, S., Mohan, V., & Balasubramanyam, M. (2007). Glutamine fructose-6-phosphate amidotransferase (GFAT) gene expression and activity in patients with type 2 diabetes: inter-relationships with hyperglycaemia and oxidative stress. *Clin Biochem, 40*(13-14), 952-957. doi:10.1016/j.clinbiochem.2007.05.002

Syrzycka, M. (2009). *Genetic and molecular characterization of essential heterochromatic genes in Drosophila melanogaster*. Doctor of Philosophy Thesis. Molecular Biology and Biochemistry. Simon Fraser University. Burnaby British Columbia.

T., J. (1986). Preparation of nucleic acids. In D. B. Roberts (Ed.), *Drosophila: a practical approach* (pp. 275-286). Oxford England: IRL Press.

Thibault, S. T., Singer, M. A., Miyazaki, W. Y., Milash, B., Dompe, N. A., Singh, C. M., . . . Margolis, J. (2004). A complementary transposon tool kit for Drosophila melanogaster using P and piggyBac. *Nat Genet, 36*(3), 283-287. doi:10.1038/ng1314

Traxinger, R. R., & Marshall, S. (1991). Coordinated regulation of glutamine:fructose-6-phosphate amidotransferase activity by insulin, glucose, and glutamine. Role of hexosamine biosynthesis in enzyme regulation. *J Biol Chem, 266*(16), 10148-10154.

Uryu, O., Ou, Q., Komura-Kawa, T., Kamiyama, T., Iga, M., Syrzycka, M., . . . Niwa, R. (2018). Cooperative Control of Ecdysone Biosynthesis in Drosophila by Transcription Factors Seance, Ouija Board, and Molting Defective. *Genetics, 208*(2), 605-622. doi:10.1534/genetics.117.300268

Vaidyanathan, K., & Wells, L. (2014). Multiple tissue-specific roles for the O-GlcNAc post-translational modification in the induction of and complications arising from type II diabetes. *J Biol Chem, 289*(50), 34466-34471. doi:10.1074/jbc.R114.591560

Vermaak, D., & Malik, H. S. (2009). Multiple roles for heterochromatin protein 1 genes in Drosophila. *Annu Rev Genet, 43*, 467-492. doi:10.1146/annurev-genet-102108-134802

Vilinsky, I., Stewart, B. A., Drummond, J., Robinson, I., & Deitcher, D. L. (2002). A Drosophila SNAP-25 null mutant reveals context-dependent redundancy with SNAP-24 in neurotransmission. *Genetics, 162*(1), 259-271.

Virkamaki, A., & Yki-Jarvinen, H. (1999). Allosteric regulation of glycogen synthase and hexokinase by glucosamine-6-phosphate during glucosamine-induced insulin resistance in skeletal muscle and heart. *Diabetes, 48*(5), 1101-1107.

Weihofen, W. A., Berger, M., Chen, H., Saenger, W., & Hinderlich, S. (2006). Structures of human N-Acetylglucosamine kinase in two complexes with N-Acetylglucosamine and with ADP/glucose: insights into substrate specificity and regulation. *J Mol Biol, 364*(3), 388-399. doi:10.1016/j.jmb.2006.08.085

Weimer, S., Priebs, J., Kuhlow, D., Groth, M., Priebe, S., Mansfeld, J., . . . Ristow, M. (2014). D-Glucosamine supplementation extends life span of nematodes and of ageing mice. *Nature Communications, 5*, 3563. doi:10.1038/ncomms4563

Willems, A. P., van Engelen, B. G., & Lefeber, D. J. (2016). Genetic defects in the hexosamine and sialic acid biosynthesis pathway. *Biochim Biophys Acta, 1860*(8), 1640-1654. doi:10.1016/j.bbagen.2015.12.017

Yao, L., Wang, S., Westholm, J. O., Dai, Q., Matsuda, R., Hosono, C., . . . Samakovlis, C. (2017). Genome-wide identification of Grainy head targets in Drosophila reveals regulatory interactions with the POU domain transcription factor Vvl. *Development, 144*(17), 3145-3155. doi:10.1242/dev.143297

Yki-Jarvinen, H., Daniels, M. C., Virkamaki, A., Makimattila, S., DeFronzo, R. A., & McClain, D. (1996). Increased glutamine:fructose-6-phosphate amidotransferase activity in skeletal muscle of patients with NIDDM. *Diabetes, 45*(3), 302-307.

Yuzwa, S. A., & Vocadlo, D. J. (2014). O-GlcNAc and neurodegeneration: biochemical mechanisms and potential roles in Alzheimer's disease and beyond. *Chem Soc Rev, 43*(19), 6839-6858. doi:10.1039/c4cs00038b

Appendix A. Interproscan results

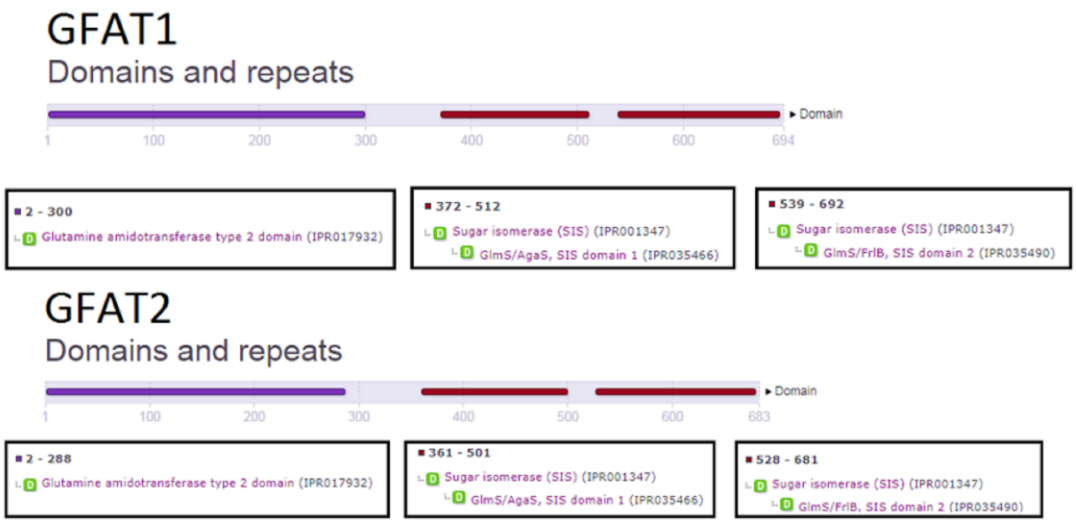

Figure A1. **Interproscan results delineating the extent of the GAAT2 and SIS domains for the Drosophila GFAT enzymes.**

Appendix B. Fly lines used in this study

Table B1. List of Drosophila melanogaster mutants and defieciency

Mutant name	Mutagen	Gene/Chromosome affected	Source/Reference
$Gfat2^{18A-14}$	P-element Excision	Gfat2	URP*
$Gfat2^{10A-2}$	P-element Excision	Gfat2	URP*
$Gfat2^{3A-3}$	P-element Excision	Gfat2	URP*
$Gfat2^{11A-1}$	P-element Excision	Gfat2	URP*
$Gfat2^{19A-1}$	P-element Excision	Gfat2	URP*
$Gfat2^{14A-10}$	P-element Excision	Gfat2	URP*
$Gfat2^{9A-16}$	P-element Excision	Gfat2	URP*
$Gfat2^{1C-25}$	P-element Excision	Gfat2	URP*
$Gfat2^{13A-4}$	P-element Excision	Gfat2	URP*
$Gfat1^{l400\#8}$	EMS	Gfat1	Irion and Leptin, 1999
$Gfat1^{8740\#20}$	P-element Excision	Gfat1	Fitzpatrick, 2005
$Gfat1^{z-1904}$	EMS	Gfat1	Koundakjian, 2004
Df(3R)BSC460	FLP-Recombinase	3R deficiency 98B6;98D2	Thibault, 2004
Df(3R)BSC567	FLP-Recombinase	3R deficiency 98B6;98E5	Thibault, 2004
Df(3R)XM3	X-ray mutagenesis	3R deficiency (82A3-6; 82B)	Letsou, 1991

*URP refers to the undergraduate research project that used the P{EPgy2}Gfat2[EY21762] for the P-element excision

Table B2. List of transgenic *Drosophila melanogaster* lines

Name of Transgenic Line	Inserted Chromosome	Nature of transgene	Source/Reference
UAS-3632-2-3M-CH3-(pUAST-Ogt-cDNA)	3	UAS Ogt cDNA	Sinclair, 2009
UAS-4145-1-1M-(pUAST-Gfat1-cDNA)	2	UAS *Gfat1* cDNA	Jackson, 2007
UAS-Oga-RNAi 23-5	3	UAS Oga RNAi	Stefanelli, 2014
pUAS-attp-Gfat2-cDNA	2	UAS Gfat2 cDNA	Nicoli, 2016
BL#22502 y[1] w[67c23]; P{w[+mC] y[+mDint2]=EPgy2}Gfat2[EY21762]	3	P-element in *Gfat2*	Bellen, 2004
BL# 7017 w[*]; P{w[+mC]=tubP-GAL80[ts]}2/TM2	3	Temperature sensitive Gal80 under tubulin promoter control	McGuire, 2003

BL refers to Bloomington Drosophila Stock Center

Table B3. Stocks used for generating strains used in genetic rescue

Genotype/Reference	In this study	Stock #	Chromosome	Feature	Source/Reference
w[*]; T(2;3)ap[Xa], ap[Xa]/CyO; TM3, Sb[1];	Ap^{Xa}/CyO ; TM3 Sb	BL# 2475	2, 3	Double Balanced; Chromosomal Fusion	Sturtevant, 1934
y[1] w[*]; P{w[+mC]=Act5C-GAL4}25FO1/CyO, y[+]	Actin5C-Gal4	BL# 4414	2	Gal4 cDNA driven by Actin5C promoter	Ito, 1997

w[*] ; CyRoi/sxc^3; tub-Gal4/TM3 ser	CyRoi/sxc^3; tub-Gal4*/TM3 ser	NA	2,3	Double balanced Stock	Sinclair, 2009
w[*] ; Sco/CyO ; hipk-RNAi / TM6 B Hu Tb	Sco/CyO ; hipk-RNAi* / TM6 B	VDRC# 108254	2, 3	Double Balanced Stock	Dieztl, 2007

BL refers to Bloomington Drosophila Stock Center. VDRC refers to Vienna Drosophila Resource Center. *is the original stock from VDRC 108254 that was rebalanced in experiments unrelated to this work.

Appendix C. Lists of PCR primers used in this study

Table C1. Primers used for identifying *Gfat2* P-element excision mutants

Gene	Forward Primer Name	Forward Primer Sequence	Reverse Primer Name	Reverse Primer Sequence	Amplicon Length (bp)
Grip84	Grip84Fwd	GCAGCCGACGATGTG GGTGATGCA	Grip84Rev	GGTCCACGATCAC GCCCTTCTGGA	225
e-GFP	eGFPfwd	CAAGTCCGCCATGCC CGAAG	eGFPrev	CACGGGGCCGTCG CCGATGG	328
Moca-cyp	Mocacypfwd	AGTTCTGAGTAGAGC TGGCAACGCC	Mocacyprev	AACAGCAGCACACA CACACAAGCG	471
Gfat2	Gfat2Complete GeneFwd2	GCGCCGTTCACTTGT CTTGTCAAT	Gfat2Complet eGeneRev	TCACACCCTTGTAC TGCAGCTTCT	4298

Table C2. **Primers used to sequence *Gfat2***

Primer Name	Primer Sequence
Gfat2CompleteGene2fwd	GCGCCGTTCACTTGTCTTGTCAAT
Gfat2CompleteGene1fwd	AAGTAGTGGGTCCACAACACAAAGGGTCAG
Gfat2fwd135	GCTCATGAAGCGTGGGACAAACATAATA
Gfat2fwd206	GGTAGGATGTGCCGCACGCAATTA
Gfat2-R	TGGAGGCCACGCACTCGC
Gfat2CompleteGene2rev	TCACACCCTTGTACTGCAGCTTCT
Gfat2CompleteGene1rev	CACCATTGATTACTCTCAGCAACC
Gfat2-F	CATCGATGCGCTGAACTCTGG
Gfat2rev227	CGCGAGATCATCACGCTGA
Gfat2rev151	GGAGGGCGCACTGGTAATCCATTT

Table C3. Primers used for RT-qPCR using Taqman method

Gene	Primer and Probe Mix name	Forward Primer Sequence	Reverse Primer sequence	Probe Sequence	Probe Length(bp)
Gfat1	Gfat1qpcr	ACCTATACCAAC ACAAGTCGC	CTTCAATTCACC GGCCATG	56FAM/TGCCTAGAA/Z EN/GGTGCATTGAAAG TCAAAGAG/3IABkFQ	131
Gfat2	Gfat2qpcr	TTGCCAAGGAG TTGTACGAG	TCCGTGTTTCA GTTCTCCAG	56-FAM/ AGTTGAAGC /ZEN/ CCCTGCCCATAATGA /3IABkFQ/-3	146
RpL32	RpL32qpcr	GTCGGATCGAT ATGCTAAGCTG	CAGATACTGTC CCTTGAAGCG	56-FAM/ TCGATATGC /ZEN/ TAAGCTGTCGGCACA AA /3IABkFqQ	91

Table C4. Primers used for probe generation of FISH in six different drosophild species

Species	Gene	Flybase Accession Number	Forward Primer	Reverse Primer	Probe Length (bp)
D. melanogaster	*Gfat1*	CG12449	GTACAGAATTGGAATG TGGTCTGT	CGGGCTTGAAGAGATTG GAATAC	628
D. melanogaster	*Gfat2*	CG1345	AAAGTCAAGGAGCTGA CGTA	TAGTGGGTCCACAACAC AAA	601
D. erecta	*Gfat1*	GG12143	GCGGAGGAGAATACAG CG	CTTGAGGTTTTCCAGAGT CTGTAT	907
D. erecta	*Gfat2*	GG12070	GCATATTCGCGTACCT AAATTACT	GCAATACTTGATAGGCCT GC	711
D. ananassae	*Gfat1*	G23135	CGCCAAATCGCGACAG	GCATCGGGCAAACTTAC CA	674
D. ananassae	*Gfat2*	GF16128	GCAATGGGGATCCTCT CC	GCATATTCGCTTACCTGA ACTAC	603
D. pseudoobscura	*Gfat1*	GA26267	GCCAGACGAGTCTTTG TCTTG	TGCCATCGATTCACCGG A	657
D. pseudoobscura	*Gfat2*	12297	CGACATCCTTCTGGTG AAACG	CGTATATGCGGATCGTC CGA	756
D. virilis	*Gfat1*	GJ24380	GCTGGTGACAGGCTTG AA	CGGAGTCGGCATCTAGA CAGACG	1247
D. virilis	*Gfat2*	GJ22773	GCTGAGAGTTCCATCC CGCTT	GCTATGATCAGCCCGTG GACAT	653
D. willistoni	*Gfat1*	GK12920	GTCTGGTAGCCACTGC AC	TTTGCCCCGTTCGGAC	501
D. willistoni	*Gfat2*	GK12142	GCAAGGTTAAGATACT GGAGGATG	CCGAGGATGATTTGTTCA AACGA	726

Appendix D. Relevant sequencing results for *Gfat2* putative mutants

Gfat2^{10A-2}:

Primer: Gfat2fwd206 raw annotated sequencing data:

CGCTTGATCTCCGGTATGTACTCCTTGATGCCNCCCAGAACCACGGTCTGCGTATC
GAACCTCATCCTGCCgCGCATGGTGTTGACCACGGATTCCGGCTGCTCGAAGATCT
CCTTCAGCATAAAGTAGTCGTAGTTGCCCTTCATGATCTGCTGGATCTCCATTTTCA
GCGTGATGATCTCGCGGGCGTGCGGATCATCGGATGATTTGTTTAGGCGATGAAT
GCTGAGCGTG[1086]*TTATTTCATCATG*A[46]ACCAACCCAATTATTTGCTTTTTCGGCGA
AAAGAACACGTCTTCGCCCTGCTCTCCCGCTCGCACGCACNCACGCGCCGCTCTT
GCGCTCTCGCTCACGCACACAGCTACAGCCACACGCGAGCTGCCATGTAAACATT
GGCTTTGTGTGACCGTATTGCAGCCAGGGATGGAACGGTAATTTAATAAATTATTTT
TTTACTATGTATTGAATAATATAATAAACTTTTAAAGCTATATACAAAGATGTTAACTG
TGTAAATTGTCTGAAAAAGCTTAATATAATATGACCATAAAGGCCAGATCTCATTTCA
TAGTTGGTTTAAACGACATTCTGTTTTTCCCNNNATATGANCATTGAAGATAATATTT
TCAACCCATGTTCTAAAGGNTTTGGAAGTTATACCAAAAAGCATAAAATGATTATTG
GTTGCTGANAGTAATCAATGGTGTATTTTGACTATATATAGCTCAAAGTTTACCGTTT
ATTTGAGCGTACATATGTATGTATTAACAAATTTAANAAAATATATATATTAAAATTAA
TATATCGATACCCGAAAATATGCTAAGCATATTGCANNTCNATATTTCTAACTGTATG
TTTTTGACATCCCTAGTNNTGANTANAGCTGGCAACNCCNANNTGTGCACTCGAAA
CGGC

5’ of P-element Excision

3’ of P-element Excision

Remaining fragment of P-element from excision “CATGATGAAATAA”

Missing 1039 bp from excision

Primer: Gfat2CG1rev raw annotated sequencing data:

CTTTTTGGTANACTTCCANACCTTTAGAACATGGGTTGAAAATATTATCTTCAATGCT
CATATTTTTGGGAAAAACAGAATGTCGTTTAAACCAACTATGAAATGAGATCTGGCC
TTTATGGTCATATTATATTAAGCTTTTTCAGACAATTTACACAGTTAACATCTTTGTAT
ATAGCTTTAAAAGTTTATTATATTATTCAATACATAGTAAAAAAATAATTTATTAAATTA
CCGTTCCATCCCTGGCTGCAATACGGTCACACAAAGCCAATGTTTACATGGCAGCT
CGCGTGTGGCTGTAGCTGTGTGCGTGAGCGAGAGCGCAAGAGCGGCGCGTGTGT
GCGTGCGAGCGGGAGAGCAGGGCGAAGACGTGTTCTTTTCGCCGAAAAAGCAAAT
AATTGGGTTGGT[46]*CATGATGAAATAA*C[1086]ACGCTCAACATTCATCGCCTAAACAAA
TCATCCGATGATCCGCACGCCCGCGAGATCATCACGCTGAAAATGGAGATCCAGC
ANATCATGAANGGCAACTACGACTACTTTATGCTGAAGGAGATCTTCNAGCAGCCG
GAATCCGTGGTCAACACCATGCGCGGCAGGATGAGGTTCGATACNCANACCGTGG
TTCTGGGTGGCATCAAGGAGTACATACCGGANATCAAGCGCTGCCGCCGCTTGAT
GCTGATTGCGTGCGGCACATCCTACCACAGTGCGGTGGCCACCANGCANCTGCTG
GAGGAACTGACCGAACTGCCCGTTATGGTGGAACTGGCCTCCNATTTTCTGGACAG
AAACACGCCCATTTTCCNGGACNACNTGTGCTTCTTCATCTCCCAATCNGGCGAGA
CAGCNNACACCCTGATGGCGCTCNNATACTGCAAGCANNNAGGAGCGCTCATCGT
GGGCGTTACCAACACNGTGGGCAGCANCNTCTGNCGCGAGTCGNACTGNGCG

5’ of P-element Excision

3’ of P-element Excision

Remaining fragment of P-element from excision “CATGATGAAATAA”

Missing 1039 bp from excision

Gfat2$^{18A\text{-}14}$:

Primer: Gfat2fwd206 raw annotated sequencing data:

CGCTTGATCTCCGGTATGTACTCCTTGATGCCNCCCAGAACCACGGTCTGCGTATC
GAACCTCATCCTGCCGCGCATGGTGTTGACCACGGATTCCGGCTGCTCGAAGATC
TCCTTCAGCATAAAGTAGTCGTAGTTGCCCTTCATGATCTGCTGGATCTCCATTTTC
AGCGTGATGATCTCGCGGGCGTGCGGATCATCGGATGATTTGTTTAGGCGATGAAT
GCTGAGCGTGCCATCGCTCTTGACGGCGGCCACGTCGTCATCTTCCAGGTAAATC
ACCCGATTTGTGTGCTCTATAACGGCCGATGCGTCCGAGGCGAAGAAGTACTCCAC
TTCCTTGCGCTCCAGCGGTTGAAACTCGGCGTTGCAATCGCCGGGCGGCAATAGT
TGATAGGCCTGCTGCTGCGGCTGACCATGTGGCCGATGGGCCTTGGCGTACAGGA
TGGGTATGTGATCGGTGGCCAGCTTGGTCTTGGCCTTGATGCCCACCAGAAGCGG
TGAGCCTCGCCTGGAGGCCACGCACTCGCCCGGGAAGTGCTTCGACTTGAAGGC
GATGGCGAAGGCGCCCTCCAGCTGCTGAATGGCCTGCTCCACGAGCTCGCCGAAA
GTGTAGCCAGGATGCTGCTGCCACAGGTGGTGTACCAGCTTGGCAATCACCTCCG
TGTCCGTGTCGGACTCAAATACATATCCGCGCTTCTCCAGCAGCGTCTTCACATCC
TTGTAGTTGGTTATAATGCCATTGTGCACCACCACAAAGCTATTATCCTCATCG^{546}*T
TATTTCATCATG*A^{46}ACCAACCCAATTATTTGCTTTTTCGGCGAAAAGAACACGTCTT
CGCCCTGCTCTCCCGCTCGCACGCACACACGCGCCGCTCTTGCGCTCTCGCTCAC
GCACACAGCTACAGCCACACGCGAGCTGCCATGTAAACATTGGCTTTGTGTGACCG
TATTGCAGCCAGGGATGGAACGGTAATTTAATAAA

5’ of P-element excision

3’ of P-element excision

Remaining fragment of P-element from excision “CATGATGAAATAA”

Missing 499 bp from excision

Primer: Gfat2-R: raw annotated sequencing data:

GCGCCCTCCAGCTGCTGAATGGCCTGCTCCACGAGCTCGCCGAAAGTGTAGCCAG
GAAGCTGCTGCCACAGGTGGTGTACCAGCTTGGCAATCACCTCCGTGTCCGTGTC
GGACTCAAATACATATCCGCGCTTCTCCAGCAGCGTCTTCACATCCTTGTAGTTGGT
TATAATGCCATTGTGCACCACCACAAAGCTATTATCCTCATCG[546]*TTATTTCATCATG
*A[46]ACCAACCCAATTATTTGCTTTTTCGGCGAAAAGAACACGTCTTCGCCCTGCTCT
CCCGCTCGCACGCACACACGCGCCGCTCTTGCGCTCTCGCTCACGCACACAGCTA
CAGCCACACGCGAGCTGCCATGTAAACATTGGCTTTGTGTGACCGTATTGCAGCCA
GGGATGGAACGGTAATTTAATAAATTATTTTTTTACTATGTATTGAATAATATAATAAA
CTTTTAAAGCTATATACAAAGATGTTAACTGTGTAAATTGTCTGAAAAAGCTTAATAT
AATATGACCATAAAGGCCAGATCTCATTTCATAGTTGGTTTAAACGACATTCTGTTTT
TCCCAAAAATATGAGCATTGAAGATAATATTTTCAACCCATGTTCTAAAGGTTTTGGA
AGTTATACCAAAAAGCATAAAATGATTATTGGTTGCTGAGAGTAATCAATGGTGTATT
TTGACTATATATAGCTCAAAGTTTACCGTTTATTTGAGCGTACATATGTATGTATTAA
CAAATTTAAGAAAATATATATATTAAAATTAATATATCGATACCCGAAAATATGCTAAG
CATATTGCACATCGATATTTCTAACTGTATGTTTTTGACATCCCTAGTTCTGAGTAGA
GCTGGCAACGCCGACATTGTGCAACTCGAAAACGGCGTGAAATACGTATTAAACAG
CATTTATTGGNANAATCGGCGCATA

5’ of P-element excision

3’ of P-element excision

Remaining fragment of P-element from excision “CATGATGAAATAA”

Missing 499 bp from excision

Primer: Gfat2CG1rev raw annotated sequencing data:

GCTTTTTGGTATACTTCNAAACCTTTAGAACATGGGTTGAAAATATTATCTTCAATGC
TCATATTTTTGGGAAAAACAGAATGTCGTTTAAACCAACTATGAAATGAGATCTGGC
CTTTATGGTCATATTATATTAAGCTTTTTCAGACAATTTACACAGTTAACATCTTTGTA
TATAGCTTTAAAAGTTTATTATATTATTCAATACATAGTAAAAAAATAATTTATTAAATT
ACCGTTCCATCCCTGGCTGCAATACGGTCACACAAAGCCAATGTTTACATGGCAGC
TCGCGTGTGGCTGTAGCTGTGTGCGTGAGCGAGAGCGCAAGAGCGGCGCGTGTG
TGCGTGCGAGCGGGAGAGCAGGGCGAAGACGTGTTCTTTTCGCCGAAAAAGCAAA
TAATTGGGTTGGTT[46]*CATGATGAAATAA*C[546]GATGAGGATAATAGCTTTGTGGTGG
TGCACAATGGCATTATAACCAACTACAAGGATGTGAAGACGCTGCTGGAGAAGCGC
GGATATGTATTTGAGTCCGACACGGACACGGAGGTGATTGCCAAGCTGGTACACCA
CCTGTGGCAGCAGCATCCTGGCTACACTTTCGGCGAGCTCGTGGAGCAGGCCATT
CAGCAGCTGGAGGGCGCCTTCGCCATCGCCTTCAAGTCGAAGCACTTCCCGGGCG
AGTGCGTGGCCTCCAGGCGAGGCTCACCGCTTCTGGTGGGCATCAAGGCCAAGAC
CAAGCTGGCCACCGATCACATACCCATCCTGTACGCCAAGGCCCATCGGCCACAT
GGTCAGCCGCAGCAGCACGCCTATCAACTATTGCCGCCCGGCGATTGCAACGCCG
AGTTTCAACCGCTGGAGCGCAAGGAAGTGGAGTACTTCTTCGCCTCGGACGCATC
GGCCGTTATAGAGCACACAAATCGGNGATTTACCTGGANATGACGACGTGNNGCC
GTCAGAGCGATGGCACGCTCAGCATTCATCGCCTAAACAAATCATCCGATGATCCG
CACGNCCNGCNAGATCATCACGCTGAAATGNNATCCAGCNNATCATGNNNNAACTA
CNACTANTTTATGCTG

5’ of P-element excision

3’ of P-element excision

Remaining fragment of P-element from excision “CATGATGAAATAA”

Missing 499 bp from excision

Appendix E. Genetic crosses

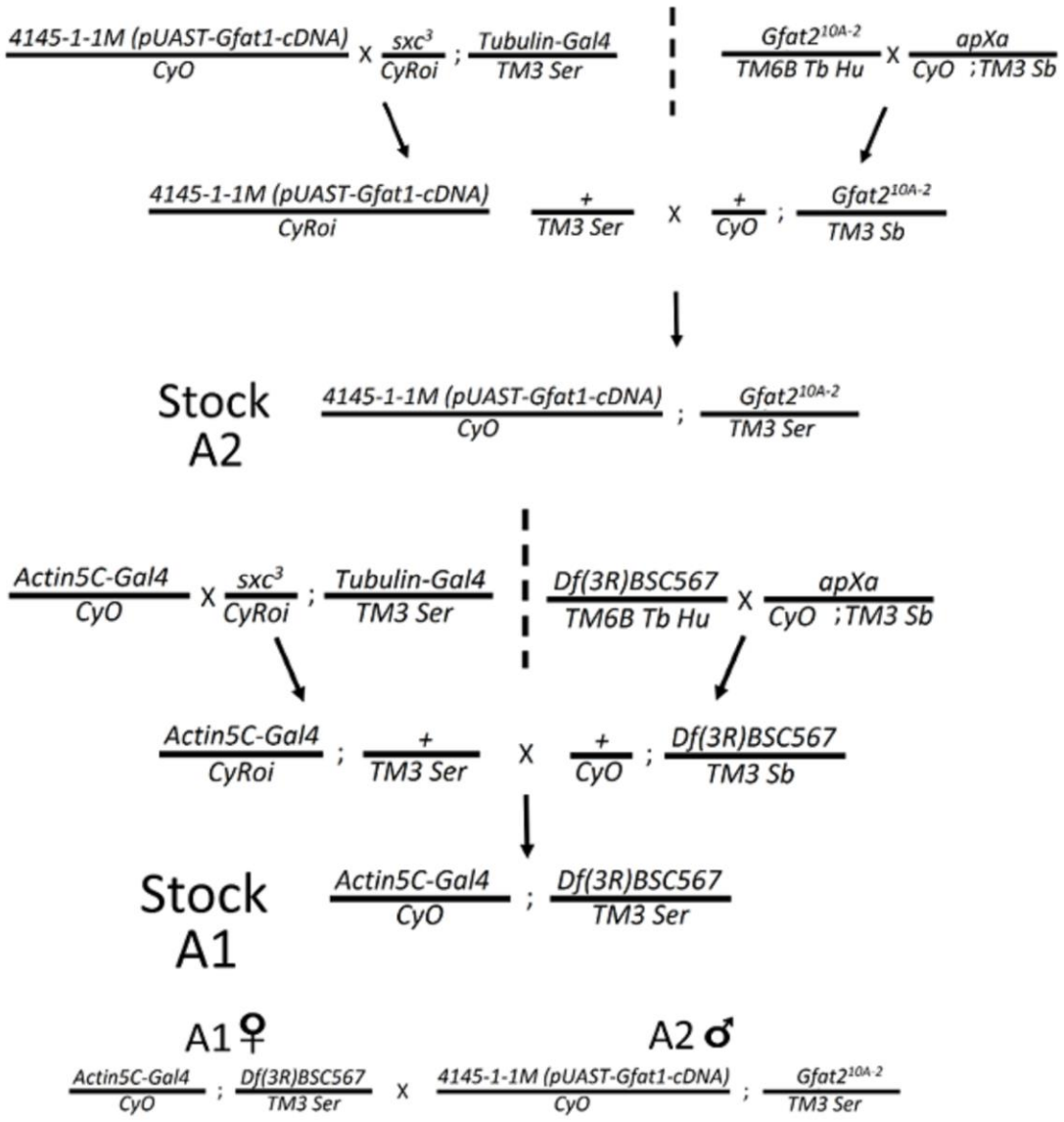

Figure E1. Stock generation and genetic rescue of Gfat2 hemizygotes by constitutively expressed Gfat1 cDNA.

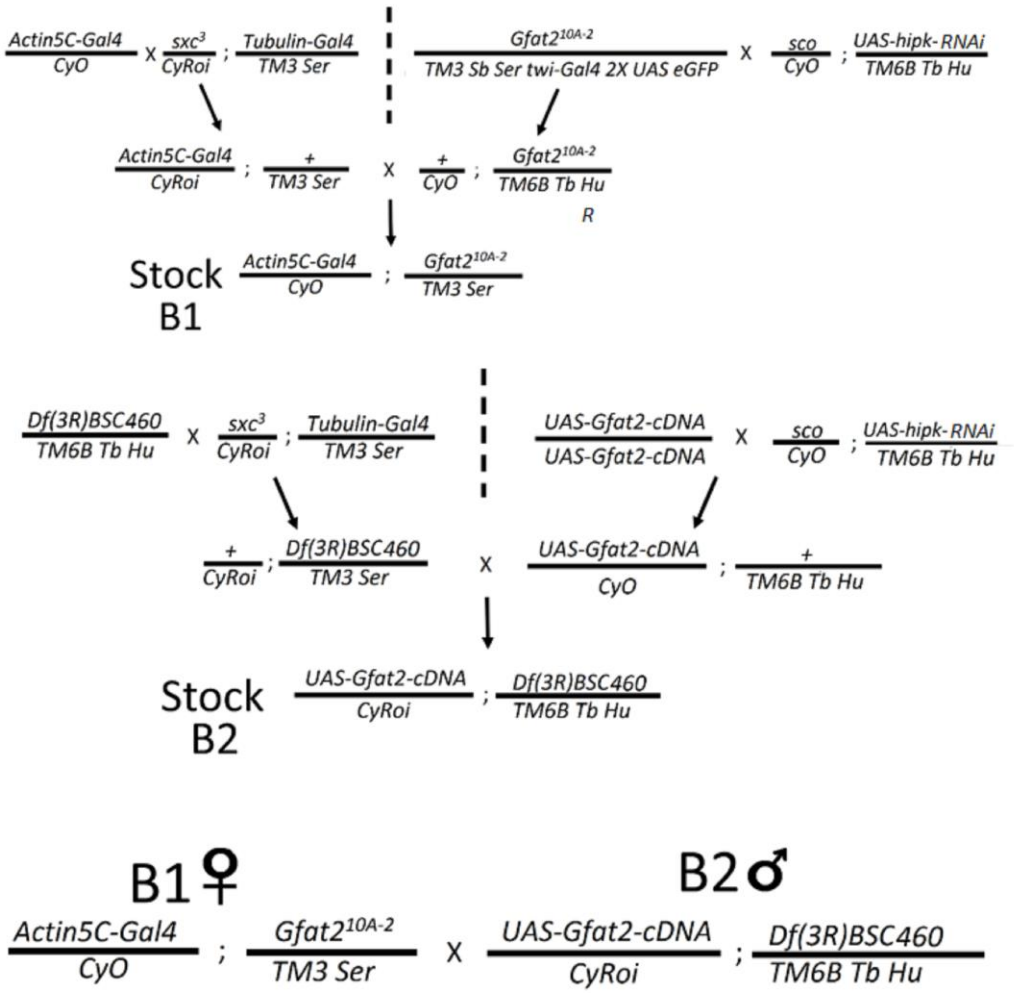

Figure E2. Stock generation and genetic rescue of Gfat2 hemizygotes by constitutively expressed Gfat2 cDNA.

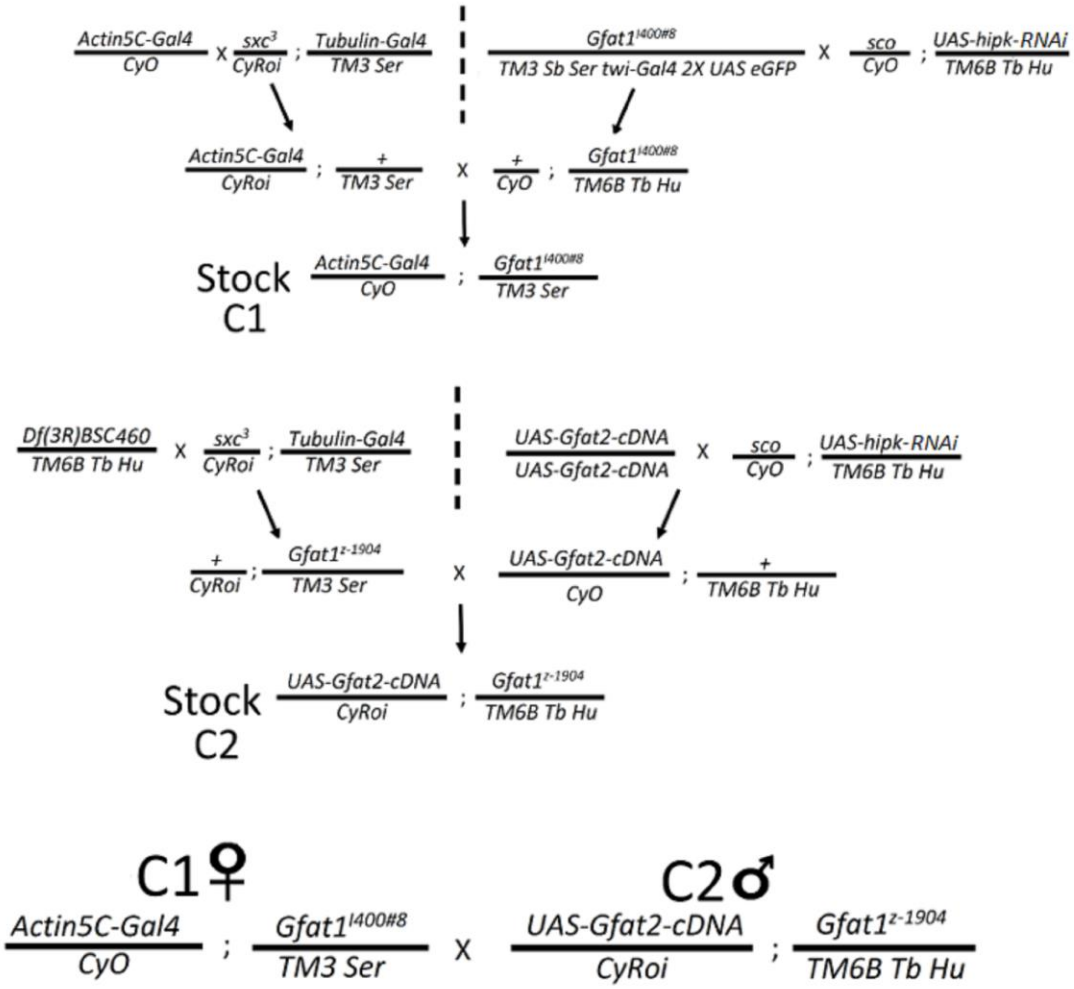

Figure E3. Stock generation and genetic rescue of Gfat1 transheterozygous mutants by constitutively expressed Gfat2 cDNA.

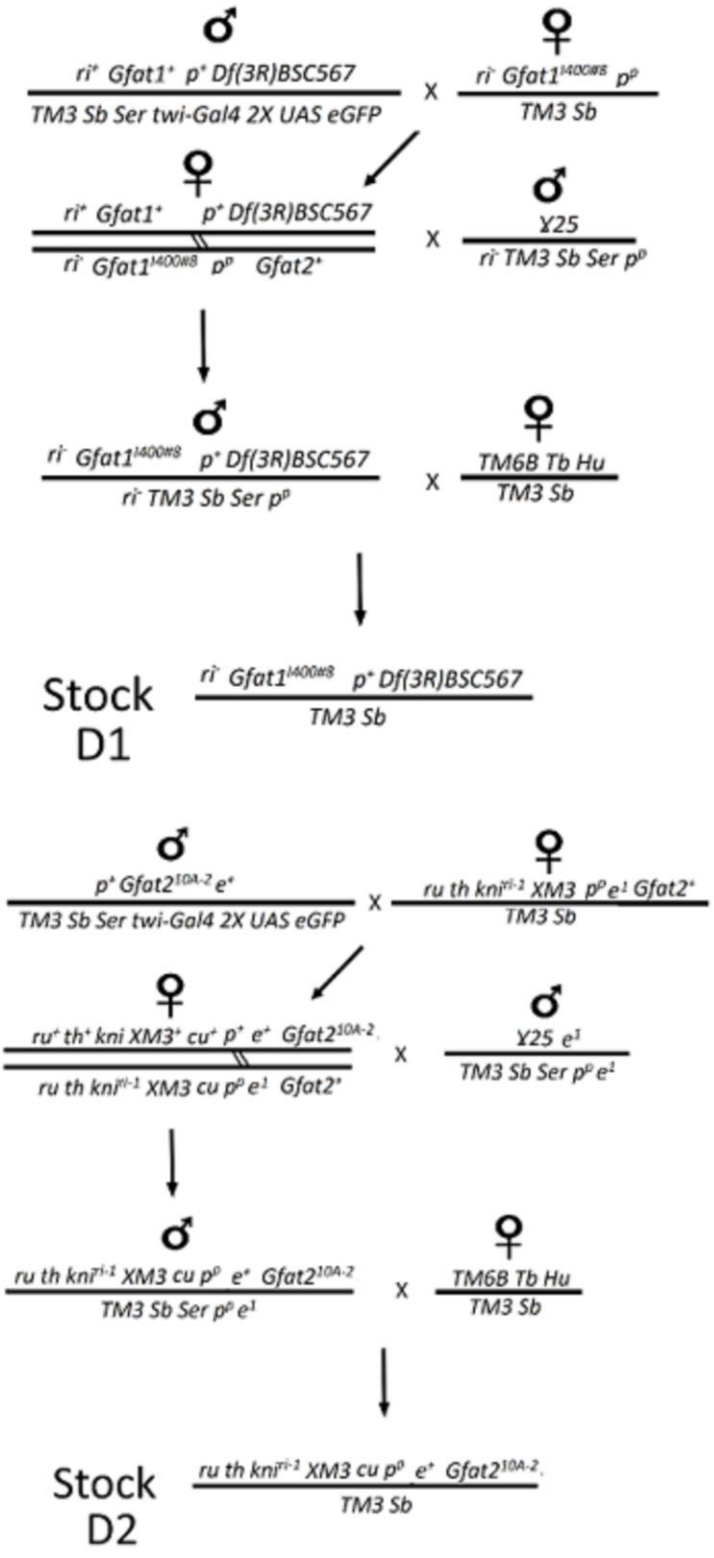

Figure E4. Generation of Gfat1, Gfat2 double mutant stocks

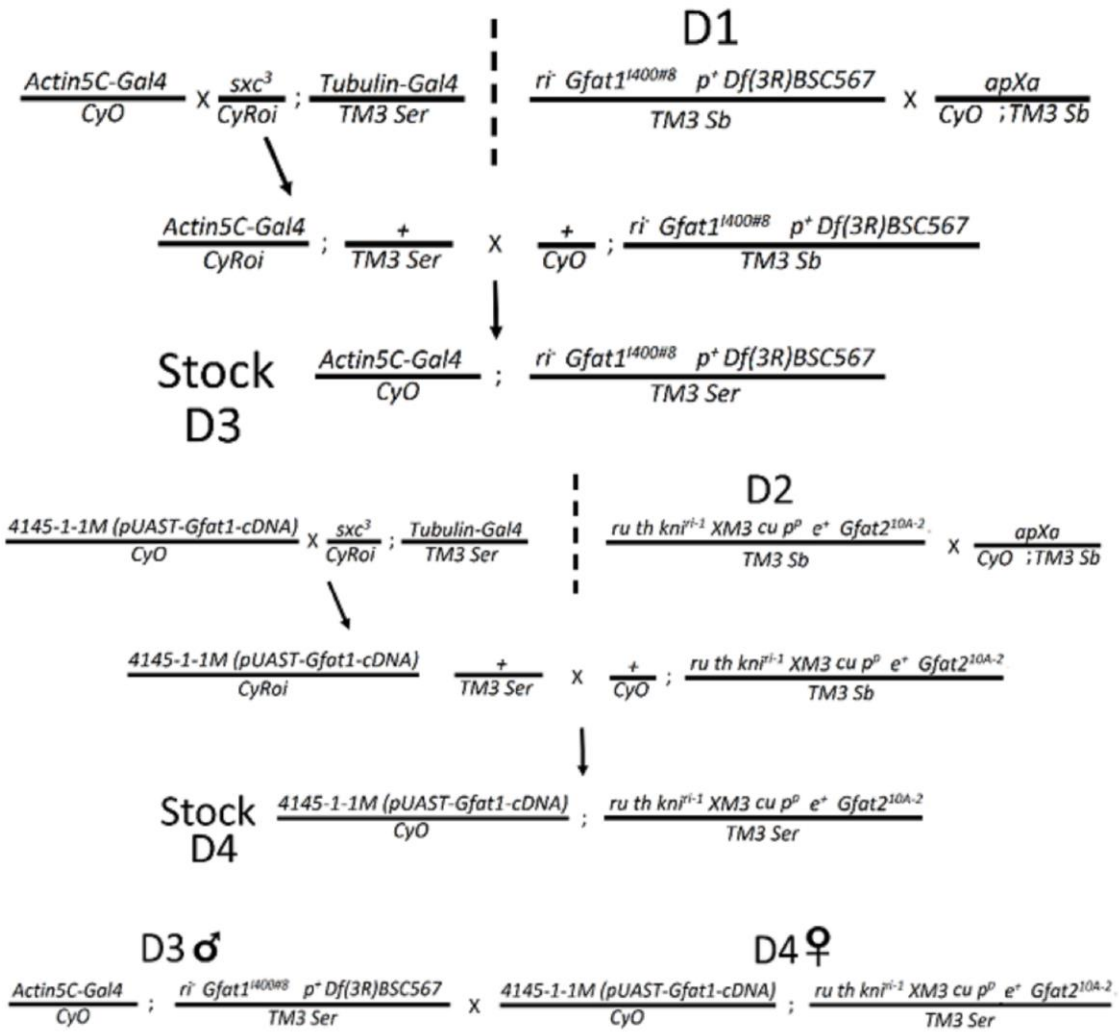

Figure E5. Stock generation and genetic rescue of Gfat1, Gfat2 double mutant rescue by constitutively expressed Gfat1 cDNA.

Appendix F. Amino Acid sequences of *Gfat1* and *Gfat2* used to identify orthologues in 11 other drosophilids

Gfat1-PA:

MCGIFAYLNYLTPKSRQEVLDLLVTGLKRLEYRGYDSTGVAIDSPDNKNIVMVKRTGKV
KVLEEAIQEHFSGREYSEPVLTHVGIAHTRWATHGVPCEKNSHPHRSDDENGFVVVHN
GIITNYNDVKTFLSKRGYEFESDTDTEVFAKLVHHLWKTHPTYSFRELVEQAILQVEGAF
AIAVKSKYFPGECVASRRSSPLLVGIKTKTRLATDHIPILYGKDDKKLCTDQDADSGKPQ
DIRPHGQSRELPVLPRSESTSEFMPLEEKEVEYFFASDASAVIEHTNRVIYLEDDDVAAV
RDGTLSIHRLKKSLDDPHAREITTLKMEIQQIMKGNYDYFMQKEIFEQPDSVVNTMRGR
VRFDGNAIVLGGIKDYIPEIKRCRRLMLIGCGTSYHSAVATRQLLEELTELPVMVELASDF
LDRNTPIFRDDVCFFISQSGETADTLMALRYCKQRGALIVGITNTVGSSICRESHCGVHI
NAGPEIGVASTKAYTSQFISLVMFALVMSEDRLSLQQRRLEILQALSKLADQIRDVLQLD
SKVKELAKDLYQHKSLLIMGRGYNFATCLEGALKVKELTYMHSEGIMAGELKHGPLALV
DDSMPVLMIVLRDPVYVKCMNALQQVTSRKGCPIIICEEGDEETKAFSSRHLEIPRTVDC
LQGILTVIPMQLLSYHIAVLRGCDVDCPRNLAKSVTVE

Gfat2-PA:

MCGIFAYLNYLTPKSRQEVLDLLLQGLKRLEYRGYDSTGIAIDALNSGEAQSIMLVKRTG
KVKVLEDAVAEVCRGQDYSLPIDTHIGIAHTRWATHGVPSEVNSHPQRSDEDNSFVVV
HNGIITNYKDVKTLLEKRGYVFESDTDTEVIAKLVHHLWQQHPGYTFGELVEQAIQQLE
GAFAIAFKSKHFPGECVASRRGSPLLVGIKAKTKLATDHIPILYAKAHRPHGQPQQQAY
QLLPPGDCNAEFQPLERKEVEYFFASDASAVIEHTNRVIYLEDDDVAAVKSDGTLSIHRL
NKSSDDPHAREIITLKMEIQQIMKGNYDYFMLKEIFEQPESVVNTMRGRMRFDTQTVVL
GGIKEYIPEIKRCRRLMLIACGTSYHSAVATRQLLEELTELPVMVELASDFLDRNTPIFRD
DVCFFISQSGETADTLMALRYCKQRGALIVGVTNTVGSSICRESHCGVHINAGPEIGVA
STKAYTSQFISLVMFALVMSEDRLSLQQRRLEIIDGLSQLDEHIRTVLKLNSQVQQLAKE
LYEHKSLLIMGRGFNFATCLEGALKVKELTYMHSEGILAGELKHGPLALVDKEMPVLMIV
LRDPVYTKCMNALQQVTSRKGRPILICEEGDNETMSFSTRSLQIPRTVDCLQGVLTVIPL
QLLSYHIAVLRGCDVDCPRNLAKSVTVE

Appendix G. Fluorescence *in situ* hybridization protocol for polytene and mitotic chromosomes

Polytene chromosome were of *D. melanogaster, D. erecta, D. ananassae, D. pseudoobscura, D. willistoni,* and *D. virilis* were squashed and mounted as described by Kress (1993). Mitotic chromosomes from neuroblasts of *D. erecta* and *D. ananassae* were prepared according to Pimpinelli (2000).

Probes were generated using nick translation to incorporate either digoxigenin- or biotin-coupled dUTP. Probes were hybridized to polytene squashes and washed three times in 2X SSC and visualized with fluorescein-avidin and antidigoxigenin-rhodamine antibody then counterstained with DAPI.